Investigating the Biological Effects of Rosemary (*Rosmarinus officinalis L.)* Extract on Skeletal Muscle Glucose Uptake

Madina Naimi, BSc (Honours)

Submitted in partial fulfillment of the requirements for the degree of

Master of Science in Applied Health Sciences

(Health Sciences)

Under the supervision of Dr. Evangelia Tsiani

Faculty of Applied Health Sciences

Brock University

St. Catharines, Ontario

Abstract

Skeletal muscle (SKM) is the most important tissue in maintaining glucose homeostasis and impairments in this tissue leads to insulin resistance (IR). Activation of 5' AMP-activated kinase (AMPK) is viewed as a targeted approach to counteract IR. Rosemary extract (RE) has been reported to decrease blood glucose levels but its effects on SKM are not known. We hypothesized that RE acts directly on SKM to increase glucose uptake (GU). We found an increase in GU (184±5.07% of control, $p<0.001$) in L6 myotubes by RE to levels similar to insulin and metformin. Carnosic acid (CA) and rosmarinic acid (RA), major polyphenols found in RE, increased GU. RE, CA, and RA significantly increased AMPK phosphorylation and their effects on GU was reduced by an AMPK inhibitor. Our study is the first to show a direct effect of RE, CA and RA on SKM GU by a mechanism that involves AMPK activation.

Acknowledgements

First of all, I would like to thank my supervisor Dr. Evangelia Tsiani for her guidance, help, support and patience through this entire journey. Her support and encouragement significantly affected the quality of this thesis.

I would like to thank the internal committee members, Dr. Huidi Wang and Dr. Ana Sanchez for their valuable comments and suggestions. Their advice was invaluable in all the stages of my thesis.

Finally, a special thanks goes to my family and friends for their continuous support, and encouragement, without whom I would not have made it this far.

Table of Contents

List of Figures

List of Tables

List of Abbreviations

ACC: acetyl CoA carboxylase

AICAR: 5-Aminoimidazole-4-carboxamide ribonucleotide

5’ AMP: adenosine monophosphate

AMPKK: AMPK kinase

AMPK: AMP-activated kinase

CA: Carnosic acid

CaMKK: Ca^{2+}/calmodulin kinase kinase

CAT: catalase

Cbl: “Casitas B-lineage Lymphoma” E3 ubiquitin-protein ligase

COOH-: carboxyl terminal

C-peptide: connecting peptide

DAG: diacylglycerol

EGP: endogenous glucose production

ELISA: enzyme-linked immunoassorbant assay

ER: Endoplasmic reticulum

FFA: free fatty acid

FOXO1: forkhead box 1

G6Pase: glucose-6-phosphatase

Gab-1: GRB2-associated-binding protein 1

GDM: gestational diabetes mellitus

GLUTs: glucose transporters

GPx: glutathione peroxidase

GSK3: glycogen synthase kinase 3

GU: Glucose uptake

HFF: high fat fed

HFR: high fructose fed

HGP: hepatic glucose production

HNF: hepatocyte nuclear factor

Hs-CRP: high sensitivity C-reactive protein

HSL: hormone sensitive lipase

IAPP: islet amyloid polypeptide

ICAM-1: intercellular adhesion molecule

IGF-1,-2: insulin-like growth factors-1, -2

IGT: impaired glucose tolerance

IKK: inhibitor Iκβ Kinase

IL-6: interleukin-6

INF-γ: interferon-γ

IPF-1: insulin promoter factor-1

IR: insulin resistance

IRS: insulin receptor substrate

JNK: c-Jun-N-terminal kinase

LCACoAs: long chain fatty acyl CoAs

LKB1: liver kinase B1

MAPK: mitogen activated protein kinase

MCP-1: monocyte chemoattractant protein-1

MDA: malonadialdehyde

MEFs: mouse embryonic fibroblasts

MIP-1β: macrophage inflammatory protein-1β

mTOR: mammalian target of rapamycin

N-: amino terminal

NFκβ: nuclear factor κβ

NeuroD: neurogenic differentiation 1

NMR: nuclear magnetic resonance

NOS: nitric oxide synthase

p70S6K: p70S6 ribosomal protein kinase

PAI-1: plasminogen activator inhibitor-1

PDK1: 3-phosphoinositide dependent protein kinase-1

PEPCK: phosphophenolphyruvate carboxykinase

PH: pleckstrin homology

PI3K: phosphatidylinositol-4,5-bisphosphate-3-kinase

PIP2: Phosphatidylinositol 4,5-bisphosphate

PIP_3: Phosphatidylinositol (3,4,5)-triphosphate

PKA: protein kinase B (Akt)

PKC: protein kinase C

PGC-1: Peroxisome proliferator-activated receptor-gamma coactivator-1

PL: pancreatic lipase

PP1: protein phosphatase 1

PPARγ: peroxisome proliferator-activated receptors (PPARs)

RE: rosemary extract

siRNA: small interference RNA technique

SH_2: Src homology 2

SKM: skeletal muscle

SOD: superoxide dismutase

STZ: streptozotocin

T1DM: type 1 diabetes mellitus

T2DM: type 2 diabetes mellitus

TCF7L2: transcription factor 7-like 2

TSC1/2: tuberous sclerosis complex 1/2

Chapter 1: Introduction

Skeletal muscle tissue accounts for approximately 80% of insulin-mediated glucose uptake in the post-prandial state and therefore plays a predominant role in maintaining glucose homeostasis. The facilitative glucose transporters (GLUTs) enable glucose entry into skeletal muscle cells and represent the rate-limiting step in restoration of post-prandial euglycemia. Insulin increases skeletal muscle glucose uptake by increasing translocation of intracellular stored GLUT4 glucose transporters to the plasma membrane through the phosphatidylinositol-3 kinase (PI3K) and Akt signaling pathway. Impaired PI3K-Akt signaling causes insulin resistance (IR) and combined with impaired pancreatic beta-cell function leads to Type 2 diabetes mellitus (T2DM), which accounts for 90-95% of all diabetes cases.

The AMP-activated protein kinase (AMPK) is a heterotrimeric serine/threonine kinase that functions as a cellular energy sensor. Importantly, skeletal muscle AMPK is activated by exercise/contraction and various compounds including metformin, thiazolidineones, and the polyphenols resveratrol and naringenin leading to stimulation of glucose uptake. In recent years, AMPK has become an attractive pharmacological target for the treatment of insulin resistance (IR) and T2DM. Therefore, the study of novel compounds that activate AMPK and increase skeletal muscle glucose uptake is of major importance and could lead to broadening the treatment options for insulin resistance (IR) and T2DM.

Rosemary (*Rosmarinus officinalis L.)* Extract

Rosemary (*Rosmarinus officinalis Lamiaceae*) is an aromatic evergreen shrub/plant indigenous to the Mediterranean region and South America reported to have anti-microbial, anti-cancer, and antioxidant properties. Additionally, effects on lipid metabolism and plasma glucose levels have been reported. *In vitro* studies have shown that rosemary extract (RE) has an insulin-like effect to inhibit gluconeogenesis in hepatocytes. In *in vivo* studies, RE administration decreased plasma glucose levels in streptozotocin (STZ)-induced diabetic rats, alloxan-induced diabetic rabbits, genetic and dietary animal models of obesity and insulin resistance (IR). Direct effects of RE on skeletal muscle glucose transport have not been examined previously and its mechanism of action is not known.

In the present thesis, the effects of RE on glucose transport in L6 rat skeletal muscle cells were examined. RE increased glucose uptake in L6 myotubes and increased AMPK phosphorylation. The effects of RE on skeletal muscle cell glucose uptake are similar to that seen with metformin and the polyphenol resveratrol and its mechanisms of action deserves further study.

1.1 Glucose Transporters

Glucose is a major energy source and is an important substrate for both protein and lipid synthesis in mammalian cells (1). It provides energy in the form of ATP through glycolysis and the citric acid cycle. It is also used in the synthesis of glycerol for triglyceride production and provides intermediates for synthesis of non-essential amino acids. Virtually all mammalian cells possess one or more transport systems to allow

glucose movement through the plasma membrane (2).The plasma membrane of cells is composed of a lipid bilayer impermeable to carbohydrates. Therefore, glucose does not freely travel across the plasma membrane and requires membrane- associated carrier proteins for transport. There are two main groups of glucose transporters, the sodium-glucose cotransporters (SGLTs) and the facilitated diffusion glucose transporters (GLUTs). The SGLTs are predominantly found in the intestinal epithelial and renal tubular cells where they are responsible for sodium-dependent secondary active transport of glucose. In the presence of sodium, these transporters have increased affinity for glucose and transport glucose against its concentration gradient (2).

Cells take up glucose from interstitial fluid by a passive, facilitative transport process, driven by the downward glucose concentration gradient across the plasma membrane (1). The passive facilitative transport process is mediated by the family of facilitative glucose transporters [gene symbol, SLC2A (solute carrier family 2, facilitated glucose transporter), protein symbol GLUT] (3). Thirteen members of this family have been identified, GLUT1-12 and H+/myoinositol transporter (HMIT) with a tertiary structure of 12 transmembrane domains containing cytoplasmic carboxyl (C)- and amino (N)- terminals (1,2). These proteins are structurally conserved specifically in the putative transmembrane (TM) regions and are more divergent in the loops between the TM and in the C- and N- terminal regions (2). The GLUT proteins have distinct substrate specificities, kinetic properties and tissue distributions that dictate their functional roles (3). The characteristics of GLUT1 to GLUT4, the most extensively studied transporters, are shown in Table 1.

Table 1: Characteristics of the Major Facilitated Glucose Transporters

Transporter	Approximate K_m for Glucose (mM)	Tissue Distribution	Characteristics
GLUT1	20	Widely expressed: high expression in brain, erythrocytes, and endothelial cells	Constitutive glucose transporter
GLUT2	42	Kidney, small intestine epithelia, liver, pancreatic β-cells.	Low-affinity; role as glucose sensor in β-cells
GLUT3	10	Neurons, placenta	High affinity glucose transporter
GLUT4	2-10	Skeletal & cardiac muscle; adipose tissue	Insulin-responsive glucose transporter

The GLUT1 transporter is characterized as the basal glucose transporter. GLUT1 (46kDa) is ubiquitously expressed with high concentrations in human erythrocytes and in endothelial cells lining blood vessels in the brain (1,3) (Table 1). GLUT1 has a high affinity (K_m=20 mM) for glucose. GLUT2 is a low affinity transporter (K_m = 42mM) found in the liver, intestine, kidney, and pancreatic β cells. This transporter plays a role in the glucose sensory system in pancreatic β cells and functions in the basolateral transport of intestinal epithelial cells. GLUT3 (45 kDa, K_m = 10mM) is expressed in fetal embryonic tissues like placenta and neurons allowing glucose to cross the blood brain barrier (3) GLUT4 (48 kDa, K_m = 2- 10mM) is an insulin-responsive glucose transporter present in skeletal muscle, cardiac muscle, and adipose tissue (Table.1).

While GLUT1 appears to be largely responsible for glucose transport under basal conditions (2), it cannot compensate for postprandial blood glucose elevations. The restoration of blood glucose levels following an exogenous glucose load is largely

achieved by increased availability of the insulin sensitive-GLUT4 transporter on the plasma membrane of skeletal muscle, cardiac muscle and adipose tissue. GLUT4 exhibits the unique characteristic of mostly being intracellularly localized in the unstimulated state whereas insulin or other stimuli can acutely redistribute these transporters to the plasma membrane (1). During the basal state, GLUT4 containing intracellular vesicles continually cycle between the plasma membrane and several intracellular compartments, where the majority of the transporters are located inside the cell (~90%) (2). It is believed that the unique sequences in GLUT4's COOH- and N- terminal cytoplasmic domains direct its characteristic membrane trafficking capacity (2). Both insulin stimulation and exercise acutely increases the recruitment of GLUT4 to the cell surface of adipose and muscle tissue through different intracellular pathways (2). Insulin stimulation increases the rate of GLUT4-vesicle exocytosis and reduces the rate of endocytosis in adipocytes only thus resulting in an increased number of GLUT4 transporters at the plasma membrane. Indeed, rapid translocation of GLUT4 from an internal pool to the plasma membrane was demonstrated to occur in response to acute insulin stimulation in both fat cells and muscle fibres (3).

Theoretically, mutations in GLUT4 could lead to impaired insulin action, termed insulin resistance. Polymorphisms in the GLUT4 gene, however, are extremely rare in insulin resistant, type 2 diabetic individuals, and have the same prevalence among nondiabetics (4,5). GLUT4 concentrations are reduced in adipocytes derived from obese insulin resistant individuals or type 2 diabetes mellitus (T2DM) but these findings are not reflected in skeletal muscle of obese subjects, type 1 or type 2 or gestational diabetic

individuals or insulin resistant relatives of persons with T2DM indicating that reduction in GLUT4 production is not a prime cause of impaired glucose transport and handling (3). On the other hand, reduction in insulin-stimulated glucose uptake in skeletal muscle in obese and diabetic individuals appears to be associated with an impairment in insulin-stimulated translocation of GLUT4 from intracellular vesicles to the plasma membrane either involving defects in the insulin signaling pathway that regulate GLUT4 translocation or in the molecular machinery directly involved in the recruitment of GLUT4-containing vesicles to the plasma membrane, their docking, and their fusion with the membrane (6).

Heterozygous GLUT4 knockout mice that display decreased GLUT4 protein in muscle and adipose tissue show insulin resistance and propensity towards diabetes (7). Overexpression of GLUT4 in skeletal muscle of heterozygous GLUT4 knockout mice normalized insulin sensitivity and glucose tolerance (8). Mice with tissue-specific GLUT4 deficiency exhibited insulin resistance in adipose tissue, liver (9) and muscle tissue (10). Levels of insulin-induced GLUT4 translocation in the skeletal muscle of type 2 diabetic patients are typically reduced by approximately 90% (11). These abovementioned studies underscore the importance of GLUT4 in the regulation of glucose homeostasis.

There is evidence of at least two distinct intracellular pools of recruitable GLUT4 in muscle and at least one of the pools can respond to stimuli other than insulin in subjects with insulin resistance (3). Stimuli such as muscle contraction and hypoxia activate pools distinct from that activated by insulin, and the glucose uptake response to exercise and hypoxia is normal in muscle from obese subjects and those with diabetes. Food

components that potentially target this latter, distinct pool of GLUT4 may prove to be beneficial in alleviation of tissue insulin resistance.

1.2 Insulin

Insulin, a protein hormone first discovered in 1922 by Banting and Best, is primarly involved in glucose homeostasis and is responsible for decreasing postprandial blood glucose elevations by promoting tissue uptake of glucose from the circulation and inhibiting endogenous glucose production (EGP) by the liver (12). It is produced by the β-cells in the islets of Langerhans of the pancreas. Insulin has a half-life of approximately five minutes and it is cleared by receptor-mediated endocytosis and degraded by lysosomal insulinase. Once insulin binds to its receptor in target tissues/cells, it activates several signaling pathways that result in the hormone's effects.

Insulin plays a key role in maintaining blood glucose homeostasis, which is needed for proper energy metabolism. Figure 1 shows that following ingestion of a meal, there is a rise in blood glucose levels which is sensed by the endocrine portion of the pancreas specifically the β cells of the islets of Langerhans. In reponse to elevated blood glucose levels, the β cells release insulin into the circulation which binds to its receptors located on skeletal muscle, adipose tissue and liver, its main target tissues and collectively restore physiological blood glucose levels. Insulin promotes glucose uptake and utilization by skeletal muscle as well as storage of glucose as glycogen in this tissue. In adipose tissue, insulin stimulates glucose uptake and storage as triglycerides (13,14).

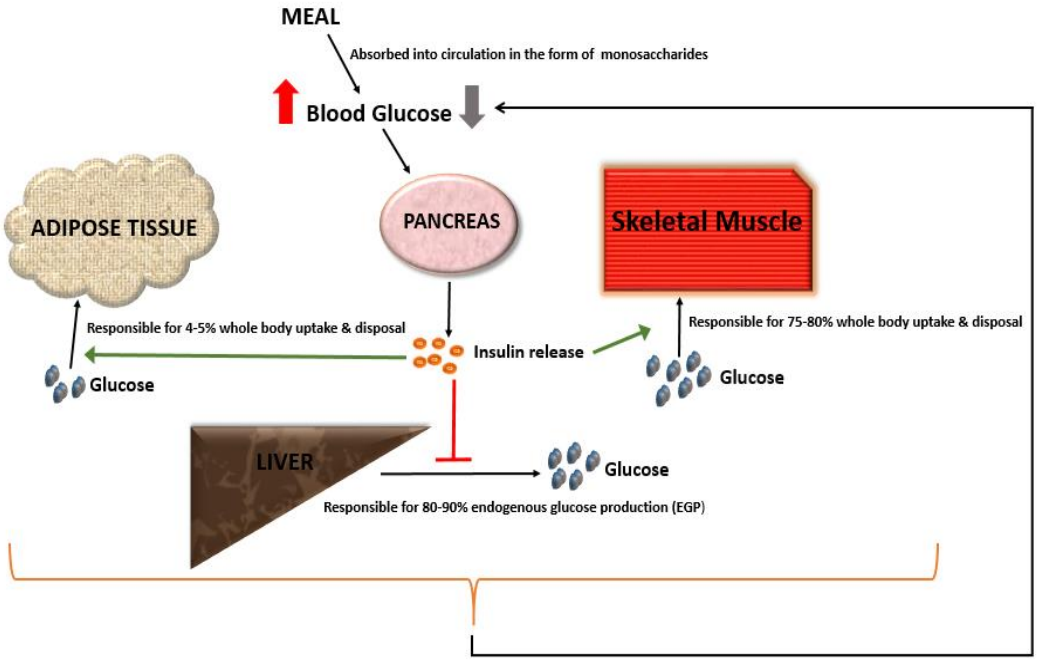

Figure 1: Role of Insulin in Glucose Homeostasis

In the liver, insulin inhibits glucose production by inhibiting gluconeogenesis and glycogenolysis. The end result of these actions of insulin is to restore and maintain plasma glucose levels within a physiological range of four to seven millimolar (80-115 mg/dL).

1.3 Insulin Resistance

Insulin resistance (IR) is a condition in which major insulin target tissues such as skeletal muscle, fat and liver display diminished responsiveness to normal circulating levels of insulin. In other words, IR is the failure to respond to physiological plasma concentrations of insulin and this state is commonly associated with obesity, aging, sedentary lifestyle as well as a genetic predisposition (15). In skeletal muscle, insulin's stimulation of glucose uptake, utilization for energy production and storage as muscle

glycogen is compromised in insulin-resistant state (16). Insulin's action on adipose tissue to promote glucose uptake and storage as lipids as well as suppressing lipolysis via the inhibition of hormone sensitive lipase (HSL) is compromised when this tissue becomes insulin-resistant. Additionally, the suppression of glucose production and release by inhibiting gluconeogenesis and glycogenolysis in liver is compromised in an insulin-resistant state. As a result of tissue (skeletal muscle, adipose tissue and liver) insulin resistance, there is chronic elevation of plasma glucose levels (hyperglycemia). Chronic hyperglycemia can lead to short-term complications including diabetic ketoacidosis; as well as long-term complications including macrovascular/microvascular damage, cardiovascular disease, retinopathy, neuropathy and nephropathy (16,17). Moreover, chronic hyperglycemia not only exacerbates target tissue IR but dramatically contributes to pancreatic β cell exhaustion and loss of function (discussed in section 1.8).

1.3.1 Skeletal Muscle Insulin Resistance

Skeletal muscle is quantitatively the most important tissue in glucose homeostasis, accounting for 75 to 80% of postprandial glucose uptake and disposal (13) and therefore skeletal muscle insulin resistance (IR) will lead to major imbalances in blood glucose levels instigating hyperglycemia, impaired glucose tolerance (IGT) and T2DM. It has been consistently demonstrated that T2DM individuals are severely resistant to insulin compared to age-, weight- and sex-matched controls (18-20) and 85-90% of the impairment in total body glucose disposal has been demonstrated to be a result of muscle IR (21). In addition, there is evidence to indicate that skeletal muscle IR precedes hepatic IR and dysfunctional pancreatic islet-induced insulin deficiency by decades (22).

About 75-80% of insulin stimulated glucose disposal is converted to glycogen, whereas the remaining 20-25% is oxidized to carbon dioxide ($C0_2$) and water (H_20) (23). Previous studies have demonstrated that in the state of T2DM, impaired glycogen synthesis secondary to reduced glycogen synthase activity is the earliest metabolic defect (24,25). In muscle tissue, glucose enters myocytes through the facilitated GLUTs through mass action. Once inside the cell, glucose is converted to glucose-6-phosphate by hexokinase followed by isomerization to glucose-1-phosphate, activation to uridine 5-diphosphate glucose and turned into glycogen by glycogen synthase. Insulin modulates glycogen accumulation through a coordinated increase in glucose transport and glycogen synthesis. The hormone increases muscle glucose uptake by causing increased translocation of GLUT4 to the plasma membrane as well as inducing GLUT4 protein synthesis thereby increasing the number and overall plasma membrane availability of GLUT4 transporters. The hormone activates glycogen synthase by dephosphorylation through inhibition of kinases such as protein kinase A (PKA) and glycogen synthase kinase 3 (GSK3) (26) and activation of protein phosphatase 1 (PP1) (27). In terms of muscle IR, emerging evidence indicates that decreased glycogen content is mainly attributable to impairments in insulin-stimulated glucose transport and to a much lesser extent to decreased phosphorylation activity (22). Glucose transport is the rate-limiting step in non-oxidative and oxidative muscle glucose utilization and storage as glycogen; and therefore aberrations in the signaling pathway underlying glucose uptake are a primary cellular explanation of muscle IR (signaling pathway discussed in section 1.4).

1.3.2 Adipose Tissue Insulin Resistance

As mentioned before, insulin acts on adipose tissue to promote glucose uptake and storage as lipids and inhibits lipolysis. Adipose tissue accounts for 4-5% of whole body glucose disposal in the postprandial state, therefore from a quantitative standpoint; lack of insulin action on this tissue may seemingly appear to be irrelevant for glucose homeostasis. On the contrary, deranged adipocyte metabolism plays a very important role in the pathogenesis of T2DM (28). Lack of insulin action on adipose tissue to exhibit antilipolytic effects by inhibiting HSL leads to increased plasma free fatty acid (FFA) levels (29-31). Elevated FFA levels have been consistently implicated in skeletal muscle and liver IR (32,33). Chronically elevated FFA levels have various effects in terms of glucose homeostasis including inhibition of muscle glucose transport and glucose utilization; inhibition of muscle and liver glycogen synthase; increased expression and activity of phosphophenolpyruvate carboxykinase (PEPCK) and pyruvate carboxylase, the rate-limiting enzymes involved in gluconeogenesis (34). Therefore, elevated FFA levels secondary to insulin resistant adipose tissue counteracts the effects of insulin on muscle and liver instigating and exacerbating muscle and hepatic IR.

1.3.3 Liver Insulin Resistance

In the fasting state, the liver is the main source of endogenous glucose production (EGP) especially for the brain (13). The liver is responsible for 80-90% of EGP while the kidney generates the remaining 10-20%. It is evident from various epidemiological studies that individuals with T2DM have increased basal EGP compared to healthy counterparts with concomitant higher fasting plasma insulin levels suggesting that this tissue is resistant to

the action of insulin (13,28). The increased hepatic glucose production (HGP) in the state of hepatic IR is primarily caused by a deregulation of insulin-induced inhibition of hepatic gluconeogenesis and glycogenolysis.

Thus, insulin resistance occurs in skeletal muscle, adipose tissue and liver and these tissues collectively impair glucose homeostasis. Chronically elevated plasma glucose levels (hyperglycemia) trigger pancreatic β cell-induced elevations of plasma insulin levels (hyperinsulinemia), a condition that further desensitizes tissues to insulin, which is followed by reduced insulin secretion as a result of β cell exhaustion. Therefore it is evident that there is a vicious cycle of impaired insulin action and insulin secretion that collectively lead to T2DM. Although, there is ongoing research trying to determine whether the initial defect in the natural history of T2DM is insulin resistance or pancreatic β-cell dysfunction, it still remains unclear (discussed in section 1.8).

1.4 Insulin Signaling Cascade

The insulin receptor is a plasma membrane intrinsic tyrosine kinase receptor belonging to a subfamily of receptor tyrosine kinases which also includes the insulin-like growth factor (IGF)-1 receptor and the insulin receptor-related receptor (IRR) (13). The receptor is a heterotetramer composed of two α and two β subunits linked by a disulfide bond. The α subunits are localized in the extracellular fluid and contain the insulin-binding domain while the β subunits extent from the extracellular fluid into the cytosolic surface where the tyrosine kinase domain is located. The action of insulin on its target tissues is initiated by insulin binding to its receptor and increasing the receptor's tyrosine kinase activity towards intracellular substrates (35,36) (Figure 2). When insulin binds to the α

subunits of the receptor, it leads to a conformational change that allows autophosphorylation of the β subunits resulting in increased activity of the intrinsic tyrosine kinase domain of the receptor. Once activated, the insulin receptor phosphorylates a number of intracellular substrates on tyrosine including members of the insulin receptor substrate family (IRS1/2/3/4) and the Shc adaptor proteins, Gab-1 and Cbl. Tyrosine phosphorylation of these proteins creates recognition sites for additional effector molecules containing Src Homology 2 (SH_2) domains such as p85, the regulatory subunit of phosphatidylinositol 3-kinase (PI3K). Binding of the p85 regulatory subunit of PI3K to IRS activates its catalytic subunit, p110. Activated PI3K generates the lipid phosphatidylinositol 3,4,5-trisphosphate (PIP3) and increased levels of this intermediate bind PKB/Akt and phosphatidylinositol-3,4,5-phosphate-dependent kinase-1 (PDK-1) by their pleckstrin homologous (PH) domains (15). PKB/Akt and PDK-1 colocalize to the plasma membrane and this allows phosphorylation of PKB/Akt on threonine308 by PDK-1. PKB/Akt mediates many of insulin's actions in its target cells such as glucose uptake, glycolysis, glycogen synthesis as well as protein synthesis (37). As shown in Figure 2, activation of the PI3K-Akt signaling cascade by insulin leads to GLUT4 glucose transporter translocation and increased glucose uptake.

Akt (PKB) substrates that have been well established include glycogen synthase kinase-3; the Rab GTPase activating protein AS160/TBC1D4 responsible for regulating glucose transport; the Rheb GTPase activating complex, tumor suppressor tuberous sclerosis complex 1/2 (TSC1/2) responsible for regulating mammalian target of

rapamycin (mTOR) and protein synthesis; and forkhead box protein (FOXO) transcription factors regulating expression of gluconeogenic and other genes (38,39).

Insulin-stimulated phosphorylation of the Akt (PKB) substrate, AS160/TBC1D4 leads to inhibition of its Rab-GTPase activating protein (Rab-GAP) activity and has emerged as a key component of regulation of GLUT4 trafficking, although its site of action is uncertain (40,41). Insulin stimulation dramatically increases the translocation rate of GLUT4-containing intracellular vesicles to the plasma membrane via exocytosis and also has effects on decreasing the rate of GLUT4 internalization (42). Therefore, the end result of this signaling pathway is to increase plasma membrane GLUT4 number and activity (Figure 2). Increased plasma membrane availability of GLUT4 provides a route for glucose entry into skeletal muscle and adipose cells driven by a concentration gradient that is maintained by hexokinase (phosphorylates glucose and traps it inside cell). Phosphorylated glucose can either enter the pathway that leads to glycogen synthesis (anabolic) or glucose metabolism (catabolic) which is ultimately determined by the energy needs of cell.

Another well-established insulin signaling pathway is the Ras-MAPK pathway , not discussed in this thesis since it mainly mediates insulin's growth, and proliferation and not metabolic/glucose transport effects.

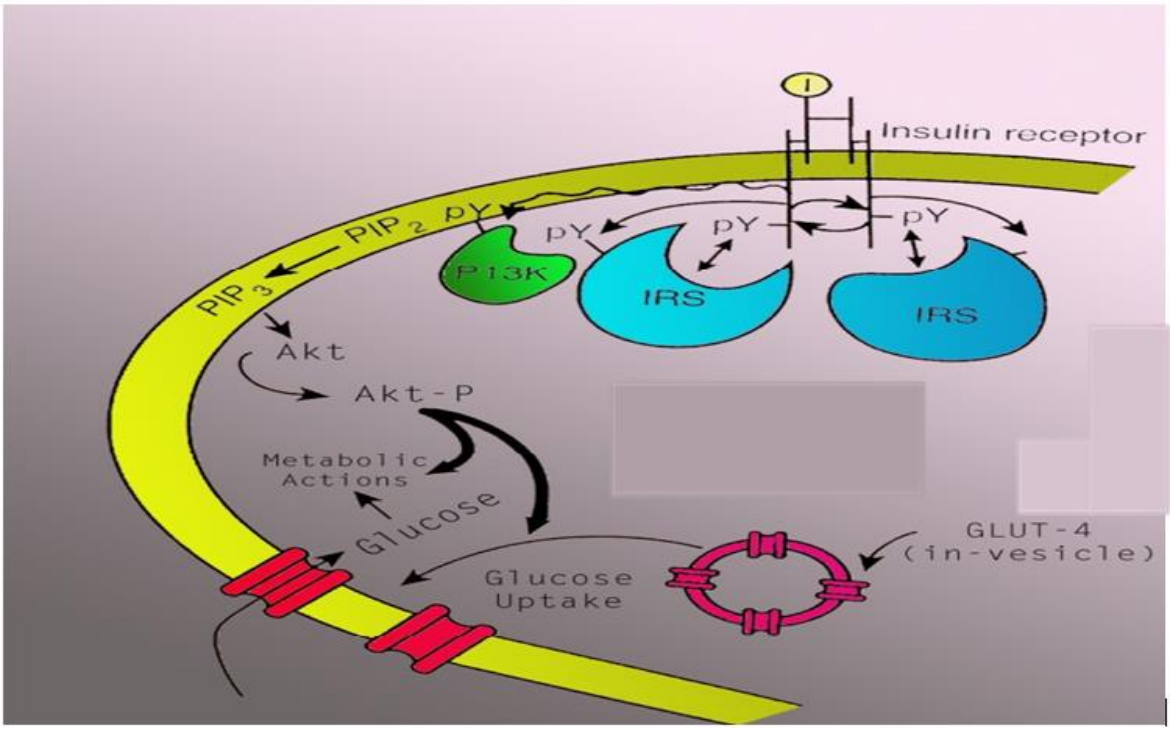

Figure 2: Insulin stimulates the PI3K-Akt signaling cascade in skeletal muscle leading to increased glucose uptake. IRS, Insulin receptor substrate; PI3K, phosphatidylinositol-3-kinase; Akt (PKB), protein kinase B; GLUT4, glucose transporter; pY, phosphorylated tyrosine residues.

1.4.1 Importance of Insulin Receptor Substrate in Insulin Signaling

The insulin receptor substrate (IRS) family of proteins consists of at least four isoforms (IRS-1 to -4) which differ in their tissue distribution, cellular localization and function. IRS-1 (180kDa) mainly regulates metabolic processes including involvement in protein synthesis and glucose transport in skeletal muscle and adipose tissue, while IRS-2 (185kDa), expressed in liver, adipose and muscle tissue performs a broad range of cellular activity. IRS-3 and IRS-4 are predominantly expressed in adipose and neuroendocrine tissue and suggested to exert a negative regulation on IRS-1 and IRS-2 (15). Intact IRS signaling is crucial for insulin action and aberrations in IRS activity results in functional disturbances. Overexpression of human recombinant IRS-1 in L6 skeletal

muscle cells increased basal and insulin-stimulated glucose uptake, and increased plasma membrane content of GLUT4 indicating its role in this signaling pathway (43). Moreover, insulin-stimulated IRS-1 associated PI3K activity was increased in cells overexpressing recombinant IRS-1 compared to control cells (43). In L6 myotubes, small interfering RNA (siRNA)-induced IRS-1 gene silencing caused a marked reduction in insulin-induced glucose uptake and GLUT4 translocation (44). In primary skeletal muscle cells derived from patients with impaired glucose tolerance (prediabetes), the level of insulin-induced glucose uptake was reduced by 30-50% compared to that of control (45). This decrease in glucose uptake was associated with reduced IRS-2 tyrosine phosphorylation and impaired IRS-2 activation of PI3K in response to insulin. Moreover, skeletal muscle biopsies from type 2 diabetic subjects displayed impaired insulin action on IRS-1 and PI3K without these defects being associated with reduced protein expression of the insulin receptor, IRS-1 or the p85 subunit of PI3K (46).

IRS-1/2 knockout mice developed peripheral IR and T2DM (47,48) indicating the importance of IRS in the insulin signaling pathway *in vivo*.

Insulin-stimulated 2-deoxyglucose uptake was 53% lower in intact muscle strips from obese subjects compared to control subjects (49). Furthermore, insulin-stimulated IRS-1 phosphorylation and PI3K activity was reduced in obese subjects compared to control subjects (49). In lean type 2 diabetic subjects, insulin-stimulated IRS-1 phosphorylation and PI3K activity was significantly decreased compared to healthy individuals (50). The reduced IRS-1 phosphorylation in lean type 2 diabetic individuals was not related to changes in IRS-1 protein content which was similar between the

groups (50). Insulin-stimulated muscle disposal was decreased in normoglycemic relatives of type 2 diabetic patients compared to those without family history of diabetes (51). Moreover, there was decreased insulin-stimulated IRS-1 phosphorylation and association of PI3K activity with IRS-1 in skeletal muscle of normoglycemic subjects with history of diabetes compared to control group (51) providing stronger support for the importance of IRS in the insulin signaling pathway. Therefore, obese and T2DM individuals display reductions in IRS phosphorylation and IRS-associated PI3K activity which results in comparable reductions in insulin-stimulated glucose uptake in muscle tissue.

Thus, *in vitro* studies in different cell lines, and *in vivo* studies in different animal models and in humans support the critical importance of insulin substrate receptor (IRS) in the insulin signaling pathway.

1.4.2 Importance of Phosphatidylinositiol-3-kinase in Insulin Signaling

Phosphatidylinositol-3-kinase (PI3K) is composed of a p110 catalytic subunit and a p85 regulatory subunit that has two SH_2 domains which interact with specific phosphotyrosine-containing motifs, pYMXM and pYXXM, in the IRS proteins (15). This family of proteins consists of 14 members divided into four classes where class I, II, and III are lipid kinases and class IV are related protein kinases (15). Importantly, only the heterodimeric p85/p110 PI3K of the class I family of proteins is responsive to insulin (13,37). Class I is further subdivided into class 1A which encompasses the p110α and p110β catalytic subunits whereas class 1B contains the p110γ subunit. There are various isoforms of the regulatory p85 subunit including p85α, p55α, p85β, and p55γ (37).

Treatment of 3T3-L1 adipocytes with LY294002, a potent inhibitor of PI3K, blocked insulin-stimulated glucose uptake by inhibiting translocation of GLUT4 to the plasma membrane (52). Treatment of rat adipocytes with wortmannin, another inhibitor of PI3K, abolished insulin-stimulated PI3K activation and subsequent insulin-stimulated 2-deoxyglucose uptake (53). Many other studies with PI3K inhibitors including LY29002, and wortmannin, showed similar abolishment of insulin-stimulated glucose uptake in skeletal muscle cells indicating the importance of PI3K in this action of insulin (54).

The expression of a constitutively activated mutant of PI3K catalytic subunit p110 in 3T3-L1 adipocytes caused plasma membrane translocation of GLUT4 which was abolished with co-treatment with wortmannin (55). Overexpression of p110α in 3T3-L1 cells caused a 1.4 fold increase in basal glucose transport rate compared to control cells which was associated with increased plasma membrane translocation of GLUT4 (56). These studies demonstrate that PI3K, specifically the catalytic p110 subunit, is crucial for GLUT4 translocation *in vitro*.

Mice with double heterozygous loss of p110α +/- p110β+/- had an observed 40% reduction in insulin-induced IRS-1 associated PI3K activity and 50% reduction in PI3K activity in muscle tissue and displayed mild glucose tolerance and hyperinsulinemia compared to wild-type mice (57). Similarly, it was demonstrated that mice deficient in p85α and p85β regulatory subunits of PI3K had impaired PI3K signaling in muscle and exhibited muscle insulin resistance and whole-body glucose intolerance (prediabetes) (58).

Furthermore, human skeletal muscle cells isolated from type 2 diabetic subjects had decreased IRS-1 tyrosine phosphorylation, decreased association of PI3K with IRS-1 and decreased PI3K activity in response to insulin compared to control cells from healthy subjects (59). These *in vivo* studies not only underscore the important role of the p110 subunit of PI3K in the context of glucose transport in muscle but also demonstrate that the regulatory p85 subunit is crucial for the overall activity of PI3K. Altogether the abovementioned *in vitro* and *in vivo* studies clearly indicate the importance of PI3K in basal- and insulin-stimulated glucose uptake. Thus, PI3K activity is crucial for intact insulin signaling.

1.4.3 Importance of Protein Kinase B (Akt /PKB) in Insulin Signaling

Protein Kinase B (PKB/Akt) is a serine/threonine kinase with three mammalian isoforms identified including Akt1, Akt2, and Akt3. Akt1 is ubiquitously expressed in mammalian tissue while Akt2 is also expressed in the majority of tissues albeit at lower levels than the former isoform. Importantly, Akt2 is predominantly found in insulin-reponsive tissues including skeletal muscle, liver and adipose tissue. Lastly, Akt3 displays a low level expression in mammalian tissue excluding the testes and brain (1). Akt requires phosphorylation of two of its residues including threonine residue (Thr308) and serine residue (Ser473) for full activation (15). While under basal conditions, the majority of Akt is localized in the cytosol, upon PI3K activation, Akt translocates to the plasma membrane and becomes activated by PI3K. Activated Akt will detach from the plasma membrane and migrate through the cytosol and into the nucleus (15). The expression of constitutively active PKB/Akt in 3T3-L1 adipocytes induced glucose uptake in the

absence of insulin by stimulating translocation of GLUT4 to the plasma membrane (60). Katome et al. used a small interference RNA (siRNA) approach to investigate the role of PKB/Akt in insulin-stimulated glucose uptake. It was shown that constitutively active PKBα/Akt1 stimulates glucose uptake in both Chinese hamster ovary and 3T3-L1 cells overexpressing GLUT4, whereas inhibition of PKB/Akt function by siRNA markedly reduces insulin-stimulated glucose uptake (61). Akt2-null adipocytes derived from immortalized mouse embryo fibroblasts (MEFs) displayed significantly reduced insulin-stimulated hexose uptake, and plasma membrane GLUT4 translocation which was restored with re-expression of Akt2 (62). Many studies in muscle cells also showed similar abolishment of insulin-stimulated glucose uptake indicating the importance of Akt in this action (17,38).

Mice with homozygous deletion of Akt2 presented with fasting hyperglycemia and insulin-stimulated 2-deoxyglucose uptake was impaired in muscle tissue *in vitro* (63). Similarly, Akt2-null mice exhibited impaired insulin-stimulated muscle glucose uptake which was accompanied by elevated plasma glucose levels (hyperglycemia) (64).

Insulin-induced glucose uptake was reduced by 60% in adipocytes from type 2 diabetic patients compared to healthy controls (65). Moreover, adipocytes isolated from type 2 diabetic patients had decreased insulin-induced total serine phosphorylation and activation of Akt (PKB) (65). A recent study in humans detected a missense mutation in the kinase domain of PKBβ (AKT2) in a family of severely insulin resistant patients (66).

Thus, it can be seen from the abovementioned studies that Akt plays a crucial role in insulin-induced GLUT4-plasma membrane translocation and loss of Akt function leads to insulin resistance and type 2 diabetes mellitus (discussed in section 1.8).

It is well established from *in vitro* and *in vivo* studies that IRS, PI3K, and Akt are important proteins involved in insulin's actions on glucose homeostasis and manipulating the levels of these proteins in different experimental models have proven to significantly alter insulin-stimulated glucose uptake. More importantly, there is unequivocal evidence to show that IRS, PI3K, and Akt activity is reduced in the insulin-resistant state both *in vitro* and *in vivo*. In terms of changes in the protein expression of IRS, PI3K, and Akt in the insulin resistant state, there is conflicting results from different studies. In the next section, the underlying mechanisms involved in reduced IRS, PI3K and Akt activity will be discussed.

1.5 Mechanisms Underlying Insulin Resistance

Although, there is evidence from genetic studies that indicate certain mutations in the insulin receptor can invariably cause IR, the majority of IR cases arise from post-receptor changes (3). As seen from the previous discussion, the insulin receptor is a tyrosine kinase and its activation lead to activation of the serine/threonine kinase Akt. Certain tyrosine kinase phosphatases have been implicated in insulin resistance. Glucose transport in insulin resistant muscle is activated normally by inhibitors of tyrosine phosphatases (vanadate) (3). Vanadate stimulates glucose transport by increasing translocation of GLUT1 and 4 in muscle and fat cells. Several organo-vanadium compounds have been found to improve insulin sensitivity in both muscle and liver in

type 2 diabetic subjects and to reduce insulin requirements in those with type 1 diabetes (3). Studies have shown that the insulin signal is attenuated through the activation of particular serine/threonine kinases. Under physiological conditions, there is a negative feedback mechanism that uncouples IRS-1 protein from its upstream and downstream effector molecules and abrogates insulin signal transduction. Chronic hyperinsulinemia in skeletal muscle cells and adipocytes was shown to induce serine phosphorylation of IRS-1 (22). Thus, the inhibitory serine phosphorylation of IRS-1 may be one of the ways the cell attempts to nullify insulin's signal transduction after steady state plasma glucose levels are achieved. However, over-stimulation of pathways that lead to serine phosphorylation of IRS-1 in pathological conditions has been shown to cause insulin resistance. Several signaling molecules including glycogen synthase kinase 3 (GSK3), mammalian target of rapamycin (mTOR), p70S6K, c-Jun N-terminal kinase (JNK), protein kinase C (PKC), and inhibitor of κBα (IκBα) kinase (IKK) have been implicated in causing tissue IR (Figure 3). The abovementioned enzymes cause IR by phosphorylating IRS-1 protein on specific serine residues which consequently inhibits tyrosine phosphorylation of IRS-1 and leads to decreased insulin-stimulated glucose uptake in skeletal muscle and adipose tissue. Serine phosphorylation of IRS-1 renders it a worse substrate for the insulin receptor thereby intervening IRS-1 tyrosine phosphorylation by the insulin receptor and subsequent association with its downstream effector PI3K. Specific serine residues of IRS-1 have been implicated in insulin resistance including Ser307, Ser612, Ser636/639, Ser1101 which are differentially phosphorylated by the abovementioned serine/threonine kinases (15).

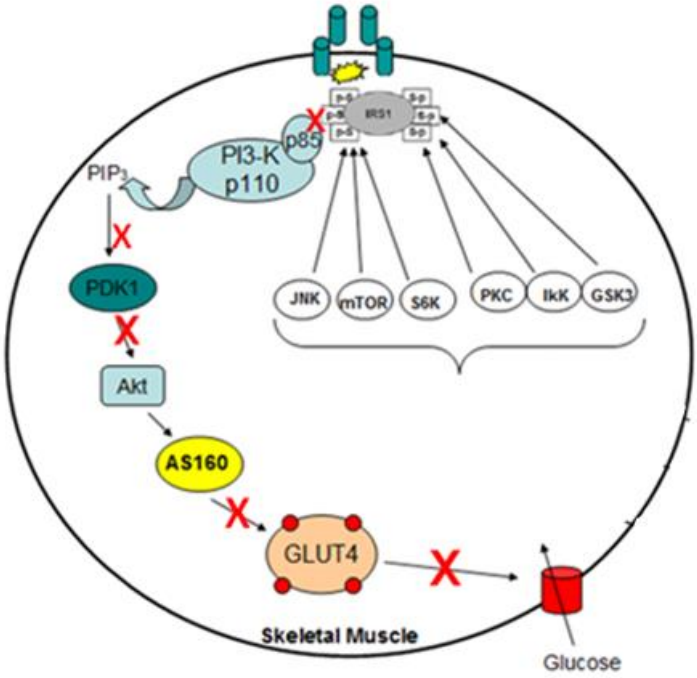

Figure 3: Mechanism of insulin resistance in skeletal muscle. Akt, protein kinase B; AS160, Akt substrate of 160 kDa; GLUT4, glucose transporter 4; GSK3, glycogen synthase kinase 3; IKK, inhibitor of IκB; IRS-1, insulin receptor substrate-1; JNK, c-Jun-N-terminal kinase; mTOR, mammalian target of rapamycin; PDK-1, phosphoinositide-dependent kinase-1; PI3K, phosphatidylinositol-3-kinase; PIP3, phosphatidylinositol (3,4,5)-triphosphate; PKC, protein kinase C; S6K, ribosomal protein S6 kinase.

Factors such as nonesterified free fatty acids (FFA), and its metabolic derivatives, as well as certain inflammatory cytokines phosphorylate and activate the abovementioned serine/threonine kinases. More importantly, elevated FFA levels, and inflammatory cytokines are strongly associated with tissue IR. In section 1.7.4, the role of FFAs and inflammatory cytokines will be discussed briefly.

Although the insulin signaling pathway is compromised in IR primarily through the action of various serine/threonine kinases, there is an insulin-independent pathway that regulates glucose and lipid metabolism and more importantly has been shown to

play a role in cellular glucose transport (Figure. 4, refer to page 27). This pathway involves 5`-adenosine monosphosphate activated protein kinase (AMPK) which will be discussed below.

1.6 5'-Adenosine Monophosphate Activated Protein Kinase

5'-adenosine monosphosphate activated protein kinase (AMPK), a heterotrimeric protein, acts as a sensor of cellular fluctuations in energy status (67). It participates in the regulation of cellular metabolic processes, integration of nutritional and hormonal activity in peripheral tissues and the hypothalamus, as well as modulation of adipokines' effects on glucose and lipid metabolism. In general terms, activated AMPK at the cellular level inhibits anabolic pathways (ATP-consuming) and promotes catabolic pathways (ATP generating) through combined effects on enzymatic activity and expression (38). Various stimuli such as heat shock, ischemia, hypoxia, glucose deprivation, hypoglycemia, metabolic inhibitors such as arsenate & oligomycin, exercise, muscle contraction, and hyperosmotic stress have been shown to activate AMPK albeit in different mechanistic ways (67). AMPK is comprised of three subunits including a catalytic α, and regulatory β and γ subunits. There are two mammalian α subunit isoforms weighing 63 kDA (α1 and α2), two β subunits weighing 30 kDa (β1 and β2), and three γ subunits ranging between 37-63 kDa (γ1, γ2, γ3), which give rise to atleast 12 possible isoform combinations (68). The α subunit of AMPK contains the serine/threonine kinase catalytic domain. Although, AMPK has several residues that can be phosphorylated including Thr172, Thr258, and Ser485 (α1)/491 (α2), phosphorylation of the Thr172 residue located on the activation loop of the catalytic domain, by

upstream kinases is mandatory for activation of this enzyme (67). The β subunit contains a glycogen-binding domain, a COOH-terminus required for complex formation with the other two subunits, and multiple phosphorylation sites while the γ subunit has variable N-terminal regions followed by cystathionine-β-synthase (CBS) domains which act in pairs to form the Bateman domain, a binding site for 5`-adenosine monophosphate (5'-AMP). Although AMPK expression is found in most mammalian cells, there is a pattern of isoform expression that is tissue-specific with the α1, β1 and γ1 isoforms being the predominant form of AMPK in most cell types and α2, β2, γ2, γ3 highly expressed in cardiac and skeletal muscle cells (67).

The activation of AMPK occurs through binding of 5'-AMP as well as phosphorylation of threonine 172 (Thr172) residue on the catalytic α subunit catalyzed by upstream AMPK kinase (AMPKK) and inhibition of dephosphorylation of Thr172 by protein phosphatases. Cellular 5'-AMP levels rise under conditions that lead to depletion of ATP levels resulting in an increased ADP to ATP ratio. The majority of AMP is produced by the adenylate kinase reaction (2ADP <--> ATP + AMP) when the cell under energy stress is attempting to recover ATP from anaerobic processes. Binding of AMP to AMPK renders it a better substrate for upstream AMPKK and a worse substrate for protein phosphatases especially protein phosphatase-2C. AMP also causes allosteric activation of the upstream kinase AMPKK. The combined effect of these mechanisms allows for more than a 200 fold activation of AMPK. At least two protein kinases (AMPKK) have been implicated in Thr172 phosphorylation of AMPK *in vivo* including liver kinase B1 (LKB1) and Ca^{2+}/calmodulin-dependent kinase kinase (CaMKK) (67).

Downstream effectors of AMPK include acetyl CoA carboxylase (ACC), and peroxisome proliferator-activated receptor coactivator-1 (PGC-1) (69). The Akt substrate, Akt substrate of 160 kDa (AS160) is a novel Rab GTPase that is phosphorylated by Akt upon insulin stimulation (70). In L6 muscle cells, AS160 plays a key role in insulin-stimulated GLUT4 translocation (71). It has been recently reported that muscle contraction and 5-aminoimidazole-4-carboxamide ribonucleotide (AICAR), an 5`-AMP analog, increased AS160 phosphorylation in muscle (41,72-74). Similarly in C_2C_{12} myotubes, AICAR treatment acted synergistically with insulin to stimulate glucose transport (75). This synergistic effect was abolished upon co-treatment with compound C, an AMPK inhibitor (75). These abovementioned studies provide strong evidence for AS160 being a downstream target of AMPK. Moreover, AS160 has been suggested to be the point of convergence mediating GLUT4 trafficking by Akt, PKC and AMPK (71). The idea of a shared substrate by Akt and AMPK would not be a new finding since both molecules appear to have similar substrate motifs and have previously been shown to phosphorylate 6-phosphofructo-2-kinase/fructo-2,6-bisphosphatase on Ser466 (76).

Various stimuli (exercise, muscle contraction, metformin) that lead to activation of AMPK are associated with increased glucose transport under normal conditions and enhanced glucose transport under insulin-resistant states *in vitro* and *in vivo*.

Perfusion of isolated rat hindlimb AICAR caused a twofold increase in insulin-stimulated glucose uptake (77). Electrical stimulation-induced contraction and AICAR treatment of isolated rat muscles significantly increased AMPK activity which was associated with increased glucose transport (78). Furthermore, wortmannin, a specific

inhibitor of PI3K, inhibited insulin-stimulated transport without having effects on AICAR- or contraction-stimulated transport. While, the combination of AICAR and insulin had additive effects on glucose transport, the combination of AICAR and contraction did not (78).

Regular exercise improves muscle insulin sensitivity, glucose uptake and utilization and overall glycemic control in insulin resistant (79) and type 2 diabetic patients (80). This improvement in skeletal muscle glucose homeostasis in response to exercise is insulin-independent and partly involves AMPK activation (78,80). Indeed, AMPK activity is increased in response to both physical exercise (68) and electrical stimulation to produce muscle contractions *in situ* (81). Together, these findings suggest that exercise-induced improvement in muscle glucose uptake is in part mediated by AMPK activation. Therefore, exercise and simulated exercise conditions in experimental animal models improve plasma glucose levels by increasing skeletal muscle glucose uptake in an AMPK-dependent manner (Figure 4).

In obese, insulin-resistant Zucker rats, AICAR increased AMPK activity more than fivefold and increased glucose transport activity by approximately 2.4 fold while insulin did not have any effects on glucose transport activity in these insulin-resistant rats (82). In obese, insulin-resistant mice, AICAR administration improved hyperglycemia, glucose tolerance and increased GLUT4 expression in skeletal muscle (83). While insulin-stimulated glucose transport was reduced in isolated muscle from obese, insulin-resistant mice, AICAR-stimulated glucose transport was comparable to lean controls (83). Furthermore, high-fat fed (HFF) skeletal muscle-AMPKα2 knockout mice had

exacerbated glucose intolerance and insulin resistance compared to HFF control mice (84). Thus, these studies indicate that artificially increased AMPK activity in genetic and dietary animal models of IR lead to enhanced glucose handling and therefore activation of this kinase may provide a cellular pathway to counteract IR.

A hypoglycemic drug used to treat insulin resistance, metformin and the polyphenol resveratrol found in red wine have been demonstrated to mediate their glucose lowering effects through AMPK activation (Figure 4). In isolated rat skeletal muscle, metformin activated AMPK and concomitantly stimulated glucose uptake (85). Metformin treatment increased skeletal muscle AMPK activity in subjects with type 2 diabetes which was associated with improved glucose disposal rates (glucose uptake and utilization) (86).

Resveratrol, a natural polyphenolic compound found in grapes and red wine increased AMPK and ACC phosphorylation comparable to metformin in HepG2 hepatocytes (87). Resveratrol induced glucose uptake in rat L6 myotubes comparable to insulin (88). This effect of resveratrol was abolished by AMPK inhibition (88). Additionally, co-incubation of L6 myotubes, C_2C_{12} myotubes and primary human myotubes with resveratrol prevented prolonged TNF-α and insulin-induced insulin resistance in these cells with attenuated serine phosphorylation of IRS1/2 (89). These *in vitro* findings indicate that the ability of resveratrol to behave as an insulin-mimetic requires AMPK activation (89).

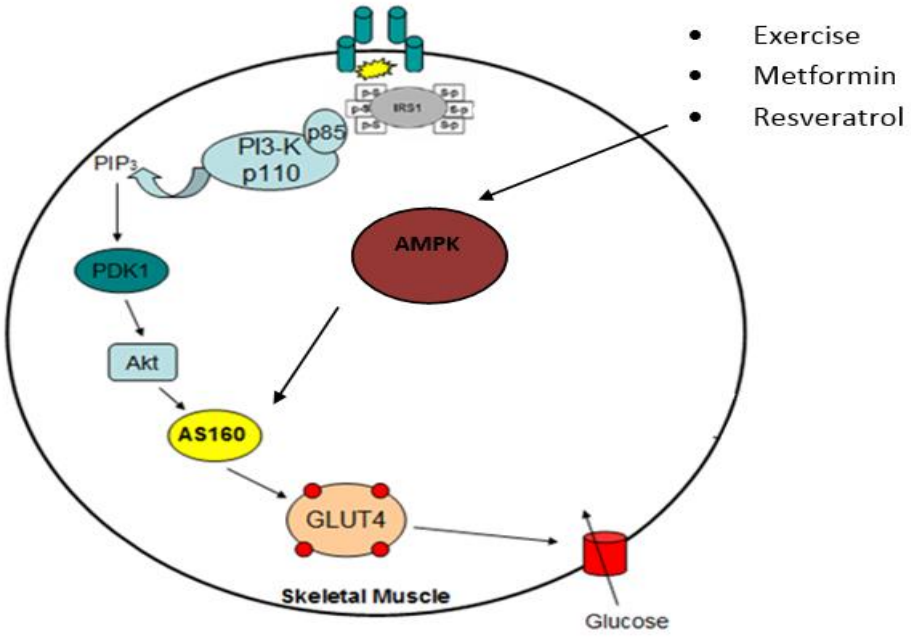

Figure 4: Role of AMPK in skeletal muscle glucose uptake in response to exercise, metformin & resveratrol. Akt (PKB), protein kinase B; AMPK, AMP-activated Kinase (heterotrimer αβγ subunits); AS160, Akt substrate of 160 kDa; GLUT4, glucose transporter; IRS, Insulin receptor substrate; PDK; phosphoinositide-dependent kinase-1; PI3K, phosphatidylinositol-3-kinase; PIP_3, phosphatidylinositol (3,4,5)-trisphosphate.

Resveratrol significantly improved insulin sensitivity in high-calorie diet-fed mice with concomitant increase in AMPK activity (90). In agreement, HFF mice deficient in the catalytic subunit of AMPKα1/2, resveratrol supplementation failed to increase insulin sensitivity and glucose tolerance in contrast to an improved insulin sensitivity seen in wildtype mice (91). In a randomized double-blind cross-over study involving healthy, obese men, 30 days of 150 mg/day of resveratrol treatment activated AMPK in muscle tissue and significantly decreased plasma glucose and insulin levels, (92). Therefore, resveratrol exerts its *in vivo* glucose lowering effects in an AMPK-dependent manner.

Accumulating evidence indicates that AMPK activation by external stimuli in insulin resistant tissues *in vitro* and *in vivo* can improve parameters compromised in this state such as tissue glucose transport. It has been demonstrated that AMPK, an intracellular energy sensor, mediates exercise-, metformin, and polyphenol (resveratrol)-induced elevations in tissue glucose uptake leading to improvements in overall glucose homeostasis (Figure 4). Since the PI3K-Akt pathway and AMPK activation have been shown to converge on AS160 and regulate GLUT4 translocation *in vitro* and *in vivo*, activation of AMPK may prove to be a valuable therapeutic target in increasing glucose uptake in insulin-resistant states. Moreover, AMPK may play a role in alleviating tissue insulin resistance through inhibition of the mTOR/p70S6K pathway which is involved in downregulation of the insulin signaling pathway. Indeed, AMPKα null mice have impaired insulin sensitivity (76). Since AMPK has been shown to inhibit the mTOR/p70S6K pathway by directly phoshorylating these enzymes as well as indirectly inhibiting this pathway by activation of tuberous sclerosis complex proteins 1/2 (TSC) which increases the Rheb-GDP levels, the removal of AMPK activity will lead to increased mTOR/p70S6K activity which is implicated in inhibitory serine phosphorylation of IRS and interference in the insulin signaling pathway. As mentioned above, resveratrol is a polyphenol found in grapes and red wine that activates AMPK, a molecule shown by many studies to be an excellent therapeutic target in regulating glucose homesotais. It is possible that other polyphenols found in various food components including herbs may act as activators of AMPK and have positive effects on glucose homeostasis.

1.7 Role of Obesity in Insulin Resistance and Type 2 Diabetes Mellitus

Obesity, and particularly intra-abdominal adiposity, is considered to be amongst the most important acquired risk factors for type 2 diabetes with over 80% of people with type 2 diabetes being obese (93). Obesity is also associated with reductions in insulin responsiveness of target tissues (reduced insulin sensitivity) (22,94). Prospective epidemiological studies have suggested that elevated plasma FFA levels, as seen in obesity, is an independent predictor of progression to T2DM (95) in Caucasians and Pima Indians (96). Therefore, the link between obesity and T2DM appears to be elevated fasting plasma FFA concentrations which are commonly seen in obese individuals and in individuals with T2DM (95).

In streptozotocin (STZ)-induced diabetic rats exposed to nicotinic acid and phenylisopropyladenosine, potent antilipolytic agents, there was a reduction in plasma FFA levels which was accompanied by a significant decrease in plasma glucose concentrations secondary to both increased basal and insulin-stimulated glucose uptake as demonstrated in isolated adipocytes *in vitro* (97). Lipodystrophic (fatless) mice, which are characterized as severely insulin resistant, had a twofold increase in myocellular lipid content paralled by reduced insulin-stimulated IRS-1 and PI3K activity in muscle tissue (98). Upon transplantation of normal adipose tissue in these mice, intracellular lipid content and insulin signaling were concurrently restored to normal levels (98). Similarly, transgenic mice with muscle-specific overexpression of plasma membrane associated lipoprotein lipase (a member of the lipase gene family responsible for hydrolyzing triglycerides in lipoproteins into FFAs and glycerol) had a threefold increase in muscle

triglyceride content and were insulin resistant due to decreases in insulin-stimulated skeletal muscle glucose transport (99). Furthermore, attenuation of insulin-stimulated IRS-1 associated PI3K activity was attributed to intramyocellular derivatives of triglyceride lipolysis including diacylglycerol (DAG) and fatty acyl coenzyme A content (99). Therefore, the abovementioned *in vivo* animal models of chemically-induced and genetic obesity demonstrate the temporally causative relationship of elevated FFA levels and reduced activity of the insulin signaling pathway (reduced glucose transport).

In obese diabetic and non-diabetic subjects, overnight administration of Acipimox, a long-acting nicotinic acid analogue, decreased fasting plasma FFA levels by 60-70% which was accompanied by a twofold increase in insulin-stimulated glucose uptake (assessed by euglycemic-hyperinsulinemic clamp) in the obese, non-diabetic and a partial improvement in the obese, diabetic subgroups (100). Lean offspring of type 2 diabetic parents who were characterized as insulin-resistant had increased intramyocellular triglyceride content compared to healthy controls as assessed by nuclear magnetic resonance spectroscopy (NMR) (101). Similarly, lipid and heparin infusion-induced increase in plasma FFA levels in healthy volunteers was associated with a proportionate increase in intramyocellular triglyceride content and a significant increase in muscle tissue insulin resistance (95). Thus, the findings of the close relationship of FFAs and tissue insulin resistance are corroborated in human studies.

1.7.1 Role of Free Fatty Acids in Skeletal Muscle Insulin Resistance

Triglycerides in muscle are in a constant state of turnover and its metabolites from lipolysis including FFA, fatty acyl coenzymes A, ceramides, and diacylglyercol (DAG)

impair insulin action in this tissue (23,102). Lipid infusion into normal rats for five hours caused a 40-50% reduction in muscle glucose oxidation and glycogen synthesis through impairment of glucose transport and this was accompanied by a fall in insulin-mediated tyrosine phosphorylation of IRS-1, and 50% reduction in IRS-1 associated PI3K activity (103). Both obese Zucker rats (104) and insulin resistant obese humans (with or without diabetes) (105) showed reduced levels of insulin-stimulated IRS-1 tyrosine phosphorylation and PI3K activity in muscle tissue. Elevated plasma FFA in humans abolished insulin induced IRS-1 associated PI3K activity (106). Additionally, increased long chain fatty acyl CoAs' (LCACoAs) have been implicated in the compromised insulin signaling pathway in muscle tissue through direction inhibition of hexokinase, the enzyme involved in converting glucose to glucose-6-phosphate which can subsequently undergo glycolysis and/or glycogenesis (107). In conclusion, both animal and human studies have demonstrated a strong negative correlation between increased intramuscular lipid levels including triglycerides (108,109), DAG (110,111) and LCACoAs (112) and insulin-stimulated glucose metabolism.

1.7.2 Role of Free Fatty Acids in Liver Insulin Resistance

FFA-induced IR is not limited to the muscle tissue but also affects the liver. The relationship between elevated plasma FFA, FFA oxidation and hepatic glucose production (HGP) are as follows: 1) increased plasma FFA by mass action enhance hepatocyte FFA uptake leading to increased lipid oxidation and accumulation of acetyl CoA. An increase in acetyl CoA causes activation of pyruvate carboxylase and phosphophenolpyruvate carboxykinase (PEPCK), the rate limiting enzymes in

gluconeogenesis (113) as well as glucose-6-phosphatase, the rate controlling enzyme for glucose release from hepatocytes (114). Therefore, the cumulative effects of increased FFA influx in hepatocytes lead to increased glucose production and release into the circulation. Additionally, increased FFA oxidation provides a source of energy (glycerol) and reduced NADH to drive gluconeogenesis (42).

The single gateway hypothesis introduced by Bergman & coworkers outlines that hepatic glucose output is indirectly associated with the hormonal regulation of lipolysis in adipocytes (115). Visceral fats which are inherently less sensitive to insulin action and specifically its antilipolytic effects, release FFAs into the portal vein which drains into the liver. Hepatocyte FFA accumulation causes hepatic glucose production and hepatic insulin resistance (IR). Normally, insulin acts on hepatocytes to decrease the transcription of genes encoding gluconeogenic enzymes such as phosphophenolpyruvate carboxykinase (PEPCK), fructose 1,6-bisphosphate and glucose-6-phosphatase (G6Pase) while increasing transcription of glycolytic enzymes including glucokinase; and lipogenic enzymes such as fatty acid synthase and acetyl CoA carboxylase. The cumulative actions of insulin on the liver are to decrease hepatic gluconeogenesis and increase hepatic lipogenesis. Elevated FFA levels cause liver IR by activating certain serine/threonine kinases that interfere with the insulin signaling pathway thereby compromising insulin's anti-gluconeogenic and anti-glycogenolytic effects in this tissue. Moreover, FFA by upregulating gluconeogenic enzymes (PEPCK, G6Pase) cause increased hepatic glucose production.

1.7.3 Mechanism of Free Fatty Acid-Induced Insulin Resistance in Skeletal Muscle

Long chain fatty acyl CoAs (LCACoAs) and diacylglycerol (DAG) activate protein kinase C-Θ (PKC-Θ) which increases serine phosphorylation of IRS-1 (116,117). Additionally, a direct, negative effect of LCACoAs on glucose transport, glucose phoshorylation, and glycogen synthase have been demonstrated in muscle (107,118). In HFF rats, the level of triglycerides and DAG were elevated four- and twofold in muscle tissue respectively accompanied by chronic activation of the protein kinase C (PKC) isozymes, PKCΘ and PKCε compared to control animals (119). In addition, transgenic mice with inactivation of PKCΘ were demonstrated to be protected from lipid-induced defects in insulin action and signaling in skeletal muscle (99,120). Similarly, PKCΘ knockout mice escaped lipid infusion-induced decrease in insulin-stimulated skeletal muscle glucose uptake and also escaped the decrease in insulin-stimulated tyrosine phosphorylation of IRS-1 and IRS-1 associated PI3K activity (120).

Intramuscular ceramide concentrations are elevated in skeletal muscle obtained from insulin resistant rats (121) and humans (122). In rat L6 myotubes, exposure to palmitate, a saturated FFA, abrogated insulin-stimulated glucose transport which was accompanied by suppression of insulin-induced plasma membrane recruitment and phosphorylation of PKB/Akt (123). This inhibition of PKB/Akt was attributable to elevation of intracellular synthesis of ceramide from palmitate and a concomitant activation of PKCζ. Indeed, co-incubation with inhibitors of serine palmitoyl transferase (enzyme that synthesizes ceramide from palmitate) prevented PKCζ activation and

reversed the observed effects. Similarly, co-incubation with a PKCζ inhibitor, Ro31.8220, also restored normal insulin-signaling and response in myocytes (123). In addition, activation of serine kinase PKC-ε as a result of intracellular accumulation of lipid metabolites was associated with reduced tyrosine phosphorylation of IRS-2 in liver (124,125). Taken together, these studies indicate that elevated FFA and its metabolic derivatives potently activate PKC which may underlie the development of insulin resistance in muscle, liver and adipose tissue.

In insulin resistant 3T3-L1 adipocytes, pretreatment with rapamycin, an inhibitor of mTOR, enhanced insulin stimulated 2-[^{3}H]-deoxy-D-glucose uptake indicating that mTOR is implicated in downregulating the insulin signaling pathway (126). More importantly, palmitate was demonstrated to increase phosphorylation of mTOR which was associated with hyperphosphorylation of IRS-1 at serine residues 632/639 in rat hepatocytes (127) showing that FFA may cause insulin resistance through activation of this particular serine/threonine kinase. Similar findings have been substantiated in skeletal muscle cells and adipocytes (128). An *in vitro* study indicated that abolishment of p70S6K, a downstream target of mTOR, by siRNA approach significantly increased insulin-stimulated Akt phosphorylation and increased insulin sensitivity in mouse embryonic fibroblasts (128).

HFF rats exhibited increased mTOR and its downstream target, p70 S6K activity in liver and skeletal muscle tissue suggestive of the importance of this pathway in the induction of insulin resistance *in vivo* (129). In accordance, rapamycin (mTOR inhibitor)

administration in mice decreased serine phosphorylation of IRS-1 and prolonged insulin-stimulated PI3K activity in skeletal muscle (129). Additionally, p70S6K knocknout mice administered a HFF exhibited decreased IRS-1 phosphorylation on ser307 and ser636/639 residues compared to their wild-type counterparts (130). Therefore *in vitro* and *in vivo* studies provide evidence for the involvement of mTOR, and p70 S6K in FFA-induced insulin resistance.

c-Jun-N-terminal kinase (JNK), a serine/threonine kinase belonging to the MAPK family, is activated by elevated FFA, cytokines (including TNF-α) and other stress stimuli leading to subsequent Ser307 phosphorylation of IRS-1 in muscle and adipose tissue causing impairment of insulin action (131,132). Both TNF-α, and FFA are potent activators of JNK (133). In murine models of dietary and genetic obesity, total JNK activity was increased in muscle, liver and adipose tissue (134). In these mice, there was also increased serine-307 residue phosphorylation of IRS-1 and subsequent reduced tyrosine phosphorylation upon insulin stimulation. Moreover, in JNK-1 deficient mice, obesity-related ser-307 phosphorylation of IRS-1 and insulin resistance was significantly reduced (134). Collectively, these studies implicate the abovementioned serine/threonine kinases in tissue insulin resistance and T2DM.

1.7.4 Role of Obesity-Induced Inflammation in Insulin Resistance

Obesity is a state of chronic, low-grade inflammation particularly in white adipose tissue (133). Obesity-derived inflammation is implicated in insulin resistance (IR) through disturbances in the insulin signaling pathway mediated by increased inflammatory pathways (29). The primary mechanism underlying obesity-derived inflammation in

muscle includes elevated levels of intracellular FFA levels' and adipocyte-derived hormones' and adipocytokines' reduction of tyrosine phosphorylation by preferential phosphorylation of serine residues of IRS (135,136) and reduction of IRS to associate with the insulin receptor (131,136,137).

Obesity is associated with increased activation of inflammatory pathways with tumor necrosis factor-α (TNF-α), an inflammatory cytokine, initially identified to be a link between obesity and inflammation (133). Indeed, TNF-α was demonstrated to be overexpressed in adipose tissue of obese rodents (138,139). Infusion of lipids, to mimic the increased FFA levels seen in obesity, and TNF-α in nonobese animals caused IR (140). In obese humans, TNF-α was shown to be overexpressed in adipose (141,142) as well as muscle tissue (143). In humans, the risk for diabetes is increased with chronic inflammatory diseases. For example, one-third of patients with chronic hepatitis C have type 2 diabetes with TNF-α implicated in this link (144). Thus, obesity-derived inflammation is associated with tissue insulin resistance and presents to be an important mediator of type 2 diabetes.

In obesity-induced inflammation, adipocytes and surrounding macrophages exhibit abnormal production of pro-inflammatory cytokines including TNF-α, and interleukin-6 (IL-6) implicated in tissue insulin resistance (145). Additionally, obesity-related decrease in adipocyte-derived protein, adiponectin and increase in resistin has also been associated with tissue insulin resistance. Inflammatory signals cause insulin resistance primarily through the inhibition of intracellular signaling downstream of the insulin

receptor (133). Several serine/threonine kinases including PKC, JNK, and IKK are activated by inflammatory stimuli and cause inhibition of insulin signaling (146).

1.7.4.1 Role of Inflammatory Cytokines in Insulin Resistance

Tumor Necrosis Factor-α (TNF-α) is an adipocyte-derived cytokine that has been demonstrated to impair the insulin signaling cascade through IRS serine phosphorylation. When infused in rodents, it causes severe IR. In Zucker rat model of obesity and insulin resistance, neutralization of TNF-α with a soluble TNF receptor (TNFR)-immunoglobulin G fusion protein, caused a significant increase in insulin-stimulated autophosphorylation of the insulin receptor and phosphorylation of IRS-1 in muscle tissue isolated from rats which was associated with improved plasma glucose, insulin and FFA levels compared to control animals(147). Gene knockout of TNF-α in high-fat fed mice and genetically obese mice resulted in lower levels of plasma FFA which prevented obesity-associated reduction in the insulin receptor signaling in muscle tissue (148). There was a 46% increase in insulin-stimulated autophosphorylation of the insulin receptor in TNF-α knockout, obese mice compared to obese, control mice. The TNF-α knockout mice also had improved insulin sensitivity compared to obese control mice (148). In accordance, intravenous administration of TNF-α prevented insulin-mediated increase in rat skeletal muscle glucose uptake by 61% (149).

There was a 2.5 fold increase in TNF-α mRNA and a similar increase in TNF-α protein in fat tissue isolated from obese premenopausal women compared to lean controls (141). Moreover, there was a strong positive correlation between TNF-α mRNA expression level in fat tissue and the level of hyperinsulinemia (an indirect measure of

IR). Body weight reduction in these women was characterized by a 45% decrease in adipose TNF-α mRNA expression which was accompanied by improved insulin sensitivity (141). In Native Canadian population, circulating TNF-α concentrations was found to be positively correlated with IR (150). In obese nondiabetic subjects, adipose tissue secretion of TNF-α increased 7.5 fold compared to lean controls, and TNF-α secretion was inversely correlated with insulin sensitivity (151). TNF-α activates downstream enzymes such as the inhibitor of nuclear factor ϰ-B kinase (IKK-B) which can impair the insulin signaling pathway in two ways. It can directly phosphorylate IRS-1 on serine residues and thereby attenuate tyrosine phosphorylation (152). Additionally, it can phosphorylate the inhibitor of NF-kB (IkB), targeting this enzyme for ubiquitination pathway, thus activating NF-kB, a transcription factor involved in the induction of diabetogenic genes. In rats, a 5-hour lipid infusion decreased insulin-stimulated glucose uptake and activation of IRS-1 associated PI3K activity in skeletal muscle. Pretreatment with salicylate, a known inhibitor of IKK-β prevented these lipid-induced effects (99). Moreover, in mice lacking IKK-β, lipid infusion did not lead to decreased insulin-stimulated glucose uptake and activation of IRS-1 associated PI3K activity as seen in wild type mice (99). HFF mice with liver-specific IKK-β gene deletion showed a less pronounced elevation in fasting blood glucose and insulin levels relative to control HFF mice (153). Cultured hepatocytes isolated from control mice, were transiently transduced with an adenovirus expressing a specific inhibitor of NF-ϰB which prevented interleukin-1β (IL-1β)-induced reduction in insulin sensitivity, diminished insulin receptor tyrosine phosphorylation and IRS-1 associated PI3K activity (153). Inhibition of

IKKB by high dose aspirin treatment (salicylates) in diabetic patients improved insulin signaling and action (154). Collectively, the abovementioned studies suggest that IKK-β activation causes insulin resistance through primarily NF-ʁB gene expression. Moreover, these studies strongly implicate the NF-ʁβ pathway in FFA- and inflammation-induced tissue IR.

Apart from TNF-α, interleukin-6 (IL-6), another inflammatory cytokine stimulate both JNK and IKKB pathways leading to induction of IR (133,155). IL-6 is expressed in macrophages and adipocytes. This cytokine is implicated in rodent models of muscle IR (156). In obese, non-diabetic subjects, plasma IL-6 was significantly elevated compared to lean controls and there was a strong inverse relationship with insulin sensitivity (151).

Adiponectin, also referred to as ACRP30, AdipoQ, and gelatin-binding protein-28, is exclusively expressed in adipose tissue (157). The average levels of plasma adiponectin in human range from 3 to 30 μg/ml. In adipose tissue, adiponectin mRNA levels were lower in genetically obese mice than in wild-type mice (158). HFF adiponectin-knockout mice developed severe insulin resistance compared to HFF control mice (159). Furthermore, diabetic mice treated with adiponectin exhibited attenuated hyperglycemia compared to control animals (160).

Using an enzyme-linked immunosorbent assay (ELISA), adiponectin levels were found to be lower in obese humans compared to lean controls (161). Similarly, plasma adiponectin levels were markedly decreased in T2DM and obese patients and the magnitude of reduction was correlated with severity of IR in peripheral tissues including

muscle and liver (162). Therefore, adiponectin levels appear to be reduced in animal models of obesity and T2DM as well as in obese and type 2 diabetic humans indicating that this adipocyte-derived cytokine plays a role in IR.

It has been suggested that obesity-induced reduction in plasma adiponectin levels (hypoadiponectinemia) occurs through obesity-associated pro-inflammatory cytokine downregulation of adiponectin (157). Indeed, TNF-α (163) and IL-6 (164) treatment suppressed adiponectin mRNA and protein expression in 3T3-L1 adipocytes and primary human adipocytes implicating these pro-inflammatory cytokines in the negative regulation of adiponectin expression *in vitro* (165).

Resistin is an adipose-derived peptide hormone that is implicated in obesity and T2DM. Increased resistin levels and expression in adipocytes have been demonstrated in human obesity and T2DM (166,167). Consistent with this, infusion of resistin into healthy animals causes severe hepatic IR but has no effect on muscle IR. Elevated resistin is associated with hepatic but not muscle IR in T2DM humans (168).

Tissue IR is a precedent to IGT (prediabetes), which if left untreated, leads to the development of overt diabetes mellitus. Therefore, diabetes mellitus is the clinical manifestation of prolonged mishandling of glucose by target tissues. In the next section, an overview of diabetes mellitus will be presented to put into context the importance of tissue glucose transport and metabolism in the overall maintenance of whole body glucose homeostasis.

1.8 Diabetes Mellitus

Diabetes mellitus is a group of metabolic diseases characterized by hyperglycemia resulting from defects in insulin secretion, insulin action or both (13). Diminished insulin secretion and insulin action lead to deregulation of glucose and fat metabolism in various tissues and failure to maintain euglycemia (28,31). This prolonged pathological state characterized by hyperglycemia and hyperlipidemia may lead to complications such as retinopathy, neuropathy, nephropathy, microvascular and macrovascular problems (42).

Type 2 diabetes mellitus (T2DM) also known as non-insulin dependent diabetes or adult-onset diabetes accounts for 90-95% of total cases of diabetes mellitus (13). It is characterized by IR and usually relative versus absolute deficiency of insulin. IR, a condition in which major insulin target tissues such as skeletal muscle, fat and liver display diminished responsiveness to normal circulating levels of insulin, result in abnormal fat and glucose metabolism in these tissues and lead to an increase in blood glucose levels due to increased glucose production and decreased glucose utilization, (15). Although, IR in classic target tissues (muscle, liver, fat) may be the predominant contributors underlying T2DM, the pancreas, brain, gastrointestinal tract, and kidneys are additional tissues that become insulin resistant and contribute to the pathophysiology of T2DM (28).

Evidence from genetic studies indicate that the majority of tissue IR present in T2DM is not associated with insulin receptor mutations but rather occurs as a result of post-receptor disturbances primarly involving aberrations in the insulin signaling

pathway (13,15,169). This is also reflected in type A insulin resistance or acanthosis nigricans and pediatric syndromes Leprechaunism and Rabson-Mendenhall syndrome which are characterized by impairments in insulin action caused by insulin receptor gene mutations resulting in metabolic disturbances ranging from hyperinsulinemia and modest hyperglycemia to severe diabetes. However, these account for only a small percentage of total diabetes cases (13,15).

Furthermore, the diminished insulin secretion seen in T2DM is due to pancreatic β-cell dysfunction. The cellular mechanism underlying insulin secretion involves rising blood glucose levels which enters pancreatic β-cells through the facilitated glucose transporter, GLUT2 (14). Once inside the cell, glucose undergoes oxidation resulting in an increase in the ATP/ADP ratio which leads to closing of the ATP-sensitive K^+-channels resulting in cell membrane depolarization and subsequent influx of Ca^{2+} leading to exocytosis of intracellular vesicles where insulin and C-peptide are concomitantly released into the circulation (15,170). This insulin secretory mechanism is compromised when the β cells are chronically exposed to elevated glucose levels (170). Therefore, although acute hyperglycemia is a trigger for insulin release, chronic hyperglycemia leads to β-cell desensitization to glucose and β-cell exhaustion with resultant deficiency in serum insulin levels (171).

As long as β-cell insulin secretion matches the varying degrees of hyperglycemia, normal glucose tolerance will be maintained with fasting plasma glucose levels maintained at 80-115 mg/dL (4.0-7.0 mM) (17,54,170). However, once the compensatory hypersecretion of insulin declines in response to chronic hyperglycemia,

glucose intolerance and subsequent overt diabetes ensues (17). Furthermore, the resultant high plasma glucose levels and poor metabolic control, resulting from declining pancreatic β-cell function, will negatively affect tissue insulin sensitivity, which is determined by the level of tissue responsiveness to insulin and further contribute to the functional decline of the insulin secreting cells. Given that tissue IR and insulin deficiency are closely interconnected, treatments aimed at alleviating IR in major target tissues are highly beneficial in preventing pancreatic β-cell deficiency and at the very least delaying the occurrence of T2DM.

1.8.1 Treatments for Type 2 Diabetes Mellitus

At present, there is no cure for diabetes mellitus as is true for many of the major chronic diseases inflicting the world's population at large (42). For this reason, the majority of current therapeutic strategies for diabetes mellitus is aimed at management and alleviation of the pathological processes underlying this disease. For a T2DM individual, treatment would include drug interventions coupled with lifestyle modifications such as healthy diets, weight management, and regular physical activity (170). There are various classes of oral medications for treatment of T2DM that have different target tissues and mode of action. These include drugs that stimulate insulin release from β-cells (sulfonylureas, meglitinides); inhibit glucose absorption by the gut (α-glucosidase inhibitors); reduce hepatic glucose output through inhibition of gluconeogenesis and increase peripheral glucose transport (biguanides/metformin); and reduce insulin resistance at target tissues (thiazolidinediones or glitazones) (42,171). Given that the current strategy for treatment of T2DM is management, and treatments aimed at

improving tissue IR has proven to be promising, it is warranted to study novel compounds that can bypass tissue IR by exerting an insulin-like effect through either stimulation of the insulin signaling pathway or complementary and convergent pathways with similar effects, and/or by increasing insulin sensitivity, thus potentially widening the spectrum of treatment options for T2DM. Additionally, the study of such novel compounds and their mechanism(s) of action also provide indirect benefits in terms of further elucidation of signaling pathways involved in metabolism, their crosstalk and unifying factors.

1.9 Phytotherapy

The use of plants for healing purposes predates recorded history and forms the origin of much of modern medicine (172). Many conventional drugs originate from plant sources including aspirin (from willow tree bark), digoxin (from foxglove), quinine (from cinchona bark), and morphine (from the opium poppy). The development of drugs from plants continues, with drug companies engaged in large-scale pharmacologic screening of herbs (172,173).

Herbal medicine is still the mainstay of about 75-80% of the world's population, mainly in the developing countries, for primary health care. In the last few years there has been a major rise in the use of herbs in the developed world. In Germay and France, many herbs and herbal extracts are used as prescription drugs and their sales in the countries of European Union were around 6 billion in 1991 and maybe over 20 billion dollars now (173). An herb can be any form of a plant or plant product, including leaves, stems, flowers, roots, and seeds which can be formulated as raw material or extracts.

Maceration of plants with water, alcohol or other solvents results in extraction of their active chemicals including fatty acids, sterols, alkaloids, flavonoids, glycosides, saponins, and others (172).

1.10 Rosemary

Rosemary (*Rosmarinus officinalis*) is a plant belonging to the labiate family (Lamiaceae). It is an aromatic evergreen shrub indigenous to the Mediterranean region and South America (174). The fresh and dried leaves are frequently used as a food preservative and in traditional Mediterranean cuisine as a flavoring agent. Historically, rosemary has been used medicinally to treat renal colic, dysmenorrhea, to stimulate hair growth and relieve symptoms caused by respiratory disorders (174,175). Today, rosemary extracts are often used in aromatherapy to treat anxiety-related conditions and increase alertness (175). Evidence indicates that rosemary possesses anti-inflammatory, anti-microbial, anti-tumorigenic, antioxidant and anti-hyperglycemic effects.

Rosemary contains subclasses of polyphenols including phenolic abietane terpenes, caffeoyl derivatives and flavones (176-179). Thus far, twelve phenolic terpenes have been isolated from rosemary including carnosol, carnosic acid, rosmanol, epirosmanol, isorosmanol, rosmaridiphenol, rosmadial and miltirone (179). Caffeoyl derivatives include caffeic acid, p-coumaric acid, rosmarinic acid, and ferulic acid (180,181) while flavonoids found in rosemary include apigenin, apigenin-7-O-glucoside, and luteolin (180,181).

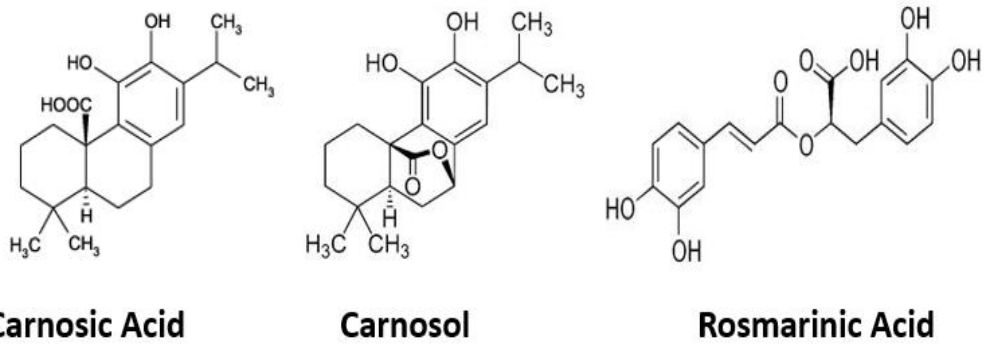

Figure 5: Chemical Structures of Rosemary's Major Polyphenols

The polyphenols found in highest quantity in rosemary are carnosic acid (CA), carnosol and rosmarinic acid (RA) (176,178,182,183) (Figure 5). The reported concentrations of CA, and RA found in rosemary range between 0.1-5.0% (184) and 0.02-30.0% (185,186). The production of these polyphenols in the plant is influenced by intrinsic factors such as genetics, subspecies, and age as well as extrinsic factors such as climate (sunlight exposure) and cultivation conditions (soil quality, and water availalbility) or the isolation/extraction method (172,184). It has been reported that anatomical regions of this herbal plant have varying levels of total phenolic content whereby the leaves contain the highest concentration of polyphenols in comparison to stem, branch and flower regions (183). Furthermore, the choice of solvent and extraction method affects the chemical composition of the extract with the possibility of losing lipid-soluble chemicals by an aqueous-based extraction method and water-soluble chemicals by nonpolar solvent- (ethanol, methanol) based extraction (174). Regardless of the extraction method used, both polar and non-polar based rosemary extracts, with differential concentrations of polyphenols, have been shown to have

antioxidant, anti-inflammatory, and anti-hyperglycemic effects. These biological effects are highly correlated with the polyphenolic content with carnosic acid, carnosol and rosmarinic acid shown to be responsible (187-192).

1.10.1 Antioxidant Properties of Rosemary Extract: *In Vitro* Studies

Numerous physiological and biochemical processes in the human body produce reactive oxygen species such as superoxide, and hydrogen peroxide as byproducts. Overproduction of such free radicals causes oxidative damage to biomolecules (membrane lipids, nucleic acids, and proteins) resulting in cellular damage and leading to many chronic diseases such as atherosclerosis, cancer, and diabetes (193). On the other hand, the intake of natural antioxidants has been associated with reduced risks of cancer, cardiovascular disease, and diabetes (173). Plants (fruits, vegetables, medicinal herbs etc.) contain a wide variety of free radical scavenging molecules, such as phenolic compounds, nitrogen compounds, vitamins, terpenoids, and some other endogenous metabolites, that have been found to be rich in antioxidant activity (172,193). A number of studies have shown rosemary's antioxidant properties. A study examining aqueous, and methanol extracts of rosemary leaves using a cell-free assay [2,2-diphenyl-1-picrylhdrazyl (DPPH) assay] found that the latter extract had a higher antioxidant activity attributable to its relatively high total phenolic content compared to the former extract (183) (Table 2). The DPPH assay is used for the assessment of radical scavenging properties. DPPH colour change from purple to yellow is the result of the reducing ability of antioxidants toward DPPH stable radical (194). The decrease in DPPH stable radical in response to antioxidants is assessed by absorbance at 515 nm (194). Similarly,

methanol extract of rosemary exhibited high antioxidant activity which was attributed to its high phenolic content (194-196). Additionally, methanol extract of rosemary was demonstrated to have anti-lipid peroxidation activity in a linoleic acid emulsion system further supporting its antioxidant properties (194). In contrast, aqueous extract of rosemary was found to have greater antioxidant activity compared to the methanol extract of rosemary which was attributed to greater phenolic content in the former extract (197) (Table 2). Aqueous extract of rosemary showed the highest inhibitory activity against the peroxidation of arachidonic acid in liposomes while the methanol extract displayed less pronounced protective effects (197). Another study reported antioxidant activity of aqueous rosemary extract that was dose-dependent using the cell free DPPH assay (198). Moreover, the aqueous extract of rosemary was examined in liposomes composed of egg lecithin with Fe^{3+}/ascorbic acid/H_2O_2 and demonstrated to have strong inhibitory effects against the oxidation of liposome indicative of potent antioxidant activity (198).

Several studies have indicated that rosemary extract's antioxidant activity is mainly attributed to carnosic acid and carnosol (199). Carnosic acid is reported to be the most powerful antioxidant among phenolic diterpenes (200). One study reported that approximately 90% of the total antioxidant activity of rosemary extract is mainly derived from carnosic acid and carnosol (201). Romano et al. (192) found that the antioxidant power of methanol extract of rosemary leaves was more similar to the antioxidant power of carnosic acid than to that of rosmarinic acid suggesting that the extract derives its antioxidant activity predominantly from carnosic acid. Similarly, the relative

antioxidant activity of rosemary extract was contingent on the content of carnosic acid (202). In agreement, three commercial oil-soluble rosemary extracts standardized on increasing concentration of carnosic acid (25.9%, 36.2%, 42.2% of extract formulation) were demonstrated to have strong antioxidant activity with the extract containing the highest concentration of carnosic acid exhibiting greatest antioxidant activity (203) (Table 2, refer to page 51).

In contrast, rosmarinic acid isolated from aqueous extract of rosemary leaves exhibited the strongest antioxidant activity assessed by a cell free DPPH assay across all micro-molar concentrations used compared to carnosic acid and carnosol (204). Similarly, it was demonstrated using the DPPH assay that the main active compound contributing to the antioxidant activity of methanol extract of rosemary is rosmarinic acid (205).

The relative antioxidant activity of whole extract of rosemary and pure polyphenolic constituents was evaluated using the DPPH assay and the former was found to have greater antioxidant capacity (206). Additionally, the pure polyphenolic constituents CA and RA were demonstrated to be readily oxidized in solution compared to their levels in the whole rosemary extract (206,207). These findings indicate that the presence of the other polyphenols provides a protective effect on the stability of each compound in the extract. A commercial oil-soluble rosemary extract containing 40% carnosic acid exhibited greater antioxidant activity in comparison to pure carnosic acid (207) (Table 2). These findings indicate additivity/synergy of various polyphenols present

in rosemary extract whose overall antioxidant activity is greater than pure polyphenolic constituents.

All of the above studies indicate that different rosemary extract formulations consistently exhibit *in vitro* antioxidant activity with carnosic acid, carnosol and rosmarinic acid being the principle phytochemicals contributing to rosemary's antioxidant properties.

Table 2: Phenolic Content and Antioxidant Activity of Rosemary Extract

Study ID	Rosemary Constituents	Assessment	Total Phenolic Content	Isolated Compounds	Activity
(194)	Methanol extract of rosemary; CA; RA	DPPH radical assay	162 mg GAE/g	Extract contained 6% CA & 8% RA	Extract had potent DPPH scavenging activity. CA had stronger radical scavenging activity compared to RA.
(195)	Methanol (M), ethanol (E), water (W) extract of rosemary.	DPPH radical assay	M: 90 mg CAE/ g > E:78 mg CAE/g > W 50 mg CAE/g	n/a	M>E>W in terms of antioxidant activity and phenolic content.
(196)	Methanol extract of rosemary leaves	DPPH radical assay	98.31 mg GAE/g Flavonoid content: 113.5 mg QE/g	CA>RA> caffeic acid.	Extract exhibited strong DPPH activity. Superoxide anion scavenging reduced by 69% at 300 µg/ml of extract. Extract exhibited antibacterial and antifungal activities.
(197)	Methanol (M) and water (W) extract of rosemary	DPPH, superoxide, and hydroxyl radical tests	W: 47.9 µg QE/mg M: 24.0 µg QE/mg	n/a	Both extracts had significant activity against both radicals. W>M in terms of antioxidant activity and phenolic content.
(198)	Aqueous extract of rosemary leaves (RL)	DPPH	185.04 mg GAE/g	n/a	100 ug/ml of RE displayed good radical scavenging.
(199)	24 different pilot plant and commercial rosemary extracts	Methyl linoleate in lipophilic solvent system.	n/a	CA, COH, RA amongst various other derivatives	All formulations of rosemary tested had significant antioxidant activity. Extracts containing a higher percentage of RA displayed greater ATOX activity

(192)	Methanol extract of rosemary.	DPPH assay	n/a	CA: 30%; COH: 16%; RA: 5% found in extract.	RE>constituents in terms of ATOX activity. RA >CA in terms of ATOX activity. Concluded that extract's ATOX is explained by combinatory ATOX activities of its main polyphenols CA & RA.
(202)	Super critical fluid extract of rosemary	DPPH assay	n/a	CA: 3.12-30.0% in different extracts.	Extract with higher percentage of CA displayed stronger ATOX activity.
(203)	Commercial oil soluble rosemary extract standardized on CA.	Superoxide anion, hydroxyl and DPPH radical activity	n/a	VivOX20 <VivOX40 < Inolens 50 in terms of CA content.	All extracts had significant ATOX with all 3 tests. Inolens 50 showed strongest activity.
(204)	Rosemary derived CA, COH & RA (0.01, 0.1, 1.0 µM)	DPPH radical assay	n/a	CA, COH, & RA	All 3 compounds showed dose dependent DPPH activity. RA: most potent across [µM].
(205)	Methanol extract of rosemary.	DPPH assay	n/a	RA: 2.2-9.7 mg/g wet weight of rosemary	RA exhibited strongest antioxidant activity amongst various phenolic compounds tested.
(206)	Methanol (M), & water (W) extract of rosemary leaves (L), flower (F), and branch (B) parts	DPPH radical assay; Folin-Ciocalteau method; HPLC analysis	M: 20 g GAE/ 100 g (200 mg GAE/g)* W: 3 g GAE/100 g (30 mg GAE/g)	L & F contained higher phenolic content. M contained CA, COH, & RA. W contained RA.	M had greater antioxidant activity compared to W.
(207)	Commercial V40 rosemary extract	DPPH radical assay	n/a	CA in larger quantity. COH in trace amounts. No RA.	V40 greatest antioxidant activity and CA among pure compounds tested. RE displayed antilisterial activity greater than CA.

CA, carnosic acid; CAE, chlorogenic acid equivalents; COH, carnosol; DPPH; 2,2-diphenyl-1-picrylhydrazyl; GAE, gallic acid equivalents; QE, quercetin equivalents; n/a, not applicable

1.10.2 Antioxidant Properties of Rosemary Extract: *In Vivo* Studies

Membrane phospholipids of red blood cell (RBC) are more susceptible to peroxidation and formation of phospholipid hydroperoxidses (PLOOH), key products of oxidative damage. Supplementation with 1% (w/w of diet) rosemary extract for one week in mice lowered the level of RBC PLOOH by 65-74% compared to the control group indicating high antioxidant activity of rosemary (208) (Table 3). Another study examined whether two concentrations (0.2% and 0.02%) of a rosemary extract containing 20% carnosic acid could enhance antioxidant status in aged rats by assessing its effects on the activities of catalase (CAT), glutathione peroxidase (GPx), superoxide dismutase (SOD) and nitric oxide synthase activity (NOS) as well as lipid peroxidation (191). Ageing causes changes in rodent antioxidant enzymes such as increased activity of CAT especially in heart and brain tissue. While there were no significant changes in SOD and GPx activity in response to rosemary extract supplementation, CAT activity in brain and heart tissues of rats was found to be diminished clearly indicating the antioxidant potential of the extract because the extract reversed the effects of ageing and the associated higher levels of reactive oxygen species (ROS) production on inducing increased CAT activity (191) (Table 3). Supplementation with 0.02% rosemary extract decreased NOS activity in heart, indicative of its protective role in this tissue. Furthermore, there was a significant dose-dependent inhibition of lipid peroxidation in the cerebral cortex of rats (191). The administration of 200 mg/kg of aqueous extract of rosemary to STZ-induced diabetic rats caused a significant restoration of total antioxidant capacity (enzymatic and non-enzymatic antioxidants) compared to control animals (209). Similarly, rosemary extract

significantly protected against increases in lipid peroxidation markers such as malondialdehyde (MDA) and decreases in plasma antioxidant enzymes including SOD, CAT and GPx and non-enzymatic antioxidants including ascorbate and glutathione in STZ- diabetic rats (210) and alloxan-induced diabetic rabbits (211). Currently, there are no studies directly examining the antioxidant effects of rosemary extract or its major constituents in humans. However, there have been a few studies indirectly examining the effects of rosemary supplements with non-conclusive results. An observational, prospective, monocenter study examined the effect of 21 days of oral supplementation of aqueous rosemary extract containing 77.7 mg rosemary extract with 0.97 mg carnosol, 8.60 mg carnosic acid, and 10.30 mg rosmarinic acid in twelve healthy young volunteers (212) (Table 3). There were no significant differences in serum SOD, intercellular adhesion molecule 1 (ICAM-1), vascular cell adhesion molecule 1 (VCAM-1), GPx, high-sensitivity capsular reactive protein (hs-CRP), TNF-α, and fibrinogen levels between extract supplemented group and control group. However, there was a significant decrease observed in plasminogen activator-inhibitor-1 (PAI-1) levels suggesting that rosemary extract may have anti-inflammatory and anti-blood clotting activity *in vivo*. Another observational study demonstrated rosemary extract and oleanolic acid, twice to thrice a day for four to eight weeks in patients with osteoarthritis, fibromyalgia, and rheumatoid arthritis, was protective against inflammatory rheumatic diseases (213) (Table 3). Thus, these studies provide strong evidence of antioxidant activites of rosemary extract *in vivo* (Table 3) and are in agreement with the *in vitro* (Table 2) studies.

Table 3: Antioxidant Properties of Rosemary Extract: In Vivo Studies

Reference	Animals	Treatment	Assessment	Results	Conclusion
(208)	ddY mice	1% (w/w) of diet supplemented with hexane extract of rosemary.	Lipid peroxidation (PLOOH)	Extract significantly reduced RBC plasma PLOOH levels to 65-74% of control cells.	Extract displays strong antioxidant effects.
(191)	Aged male wister rats (550-700 g)	Supercritical fluid extract of rosemary (SFE) with 20% CA supplemented in diet at 0.2% & 0.02%	Heart, and brain tissue CAT, GPx, SOD; NOS; LP	Cortex: Dose-dependent inhibition of LP by extract Hippocampus: Decrease in LP at 0.2% ($p<0.05$). CAT Heart and cortex: CAT activity significantly decreased. NOS activity decreased in heart at 0.02% extract.	Extract decreased cerebral catalase activity, and LP; and decreased catalase and NOS activity in the heart.
(209)	STZ-induced adult male albino rats (150-200 g)	Aqueous extract of rosemary supplemented at 200 mg/kg b.w for 21 days.	Total antioxidant activity (TAC)	TAC significantly decreased in diabetic animals compared to control animals. Extract significantly increased TAC levels compared to treated normal animals.	Extract displayed antioxidant properties *in vivo*.
(210)	STZ-induced diabetic adult male albino rats (150-200 g)	Aqueous extract of rosemary supplemented at 200 mg/kg b.w daily for 3 weeks.	MDA, NO, CAT, SOD, GPx, vitamin C, glutathione levels (G)	Diabetic rats displayed decreased levels of CAT, SOD, GPx, vitamin C, G & increased levels of MDA and NO compared to control. Extract increased all antioxidant enzyme activity and non-enzyme levels; and decreased MDA and NO levels ($p<0.05$).	Extract displayed antioxidant properties *in vivo*.
(211)	Alloxan-induced, adult New Zealand rabbits (2.2-3.1 kg)	200 mg/kg b.w of ethanolic extract of rosemary (RE) for a week	MDA, SOD, CAT	SOD, CAT significantly increased and MDA increased in diabetic rabbits compared to control. RE significantly inhibited serum MDA elevations by 33.3% and increased serum SOD and CAT activity by 24% and 35% compared to diabetic control animals.	Antioxidant effects demonstrated *in vivo*.

(212)	12 healthy, young volunteers	21 days of rosemary extract supplementation. 77.7 mg of crude extract: 0.97 mg COH, 8.60 mg CA, 10.30 mg RA.	Serum lipid profile, SOD, ICAM-1, VCAM-1, GPX, hs-CRP, TNF-α, PAI-1 and fibrinogen levels	Amongst the various markers examined, the supplementation significantly decreased PAI-1 levels in treatment group compared to control.	Rosemary may possess anti-clotting and anti-inflammatory properties.
(213)	72 patients with rheumatic disease including osteoarthritis (OA), rheumatoid arthritis (RAT) and fibromyalgia (FM).	Supplemented with 440 to 880 mg of Met050, a proprietary standardized combination of rosemary extract & oleanolic acid, 2-3 times a day for 8 weeks.	C-reactive protein (CRP)	Significant decrease in CRP in treatment group particularly in those with initial serum CRP levels >7.0 mg/L.	Meta050 may provide beneficial relief encountered in rheumatic diseases especially in patients with OA.

BHT, butylated hydroxytoluene; CA, carnosic acid; CAT, catalase; COH, carnosol; FM, fibromyalgia; GPx, glutathione peroxidase; CRP, C-reactive protein; ICAM-1, intercellular adhesion molecule-1; LP, lipid peroxidation; MDA, malondialdehyde; NOS, nitric oxide synthase; OA, osteoarthritis; PAI-1, plasminogen activator inhibitor-1; PLOOH, phospholipid hydroperoxides RA, rosmarinic acid; RAT, rheumatoid arthritis; RBC, red blood cell; SOD, superoxide dismutase; TAC, total antioxidant capacity; TBARS, thiobarbituric acid reactive substances; VCAM-1, vascular cell adhesion molecule-1.

1.10.3 Evidence of Anti-hyperglycemic Effects of Rosemary Extract: *In Vitro* Studies

Rosemary extract and its phenolic compounds CA, and RA were shown to significantly suppress gluconeogenesis in HepG2 hepatocytes via inhibition of the cAMP/PKA/CREB pathway (214). Specifically, the cAMP responsiveness of the phosphophenolpyruvate carboxykinase (PEPCK) and glucose-6-phosphatase (G6Pase), the key gluconeogenic enzymes, were significantly inhibited by RE and its phenolic components (214). Moreover, rosemary extract was shown to significantly increase glucose consumption in hepatocytes in a dose-dependent manner (215). Additionally, exposure of hepatocytes to RE significantly increased phosphorylation of 5' AMP-activated kinase (AMPK), an enzyme with regulatory effects on cellular lipid and glucose metabolism (Table 4)(215). Carnosic acid, a major polyphenolic constituent of RE, prevented palmitate-induced lipid accumulation in hepatocytes with concomitant activation of both AMPK and its downstream enzyme, acetyl coA carboxylase (ACC) (215). Furthermore, co-treatment with compound C, a specific inhibitor of AMPK, abolished these effects of carnosic acid suggesting that AMPK may be involved in the protective effects of carnosic acid against lipid accumulation in liver cells (216) (Table 4). Administration of ethanol extract of rosemary enriched with 40% CA in lean rats did not affect AMPK phosphorylation in adipose tissue and liver while muscle tissue was not examined (188) (Table 5). In contrast, in adipose tissue of leptin receptor deficient obese rats treated with rosemary extract, there was a decrease in phosphorylated AMPK levels compared to control obese

animals while this enzyme was undetectable in liver tissue (188). The authors indicated that the finding of increased phosphorylated AMPK levels in adipose tissue of control obese rats may have been a consequence rather than a cause of the higher levels of circulating adipokines in an attempt to attenuate the dysfunction and inflammation in this tissue of these animals.

Apart from the abovementioned studies, rosemary extract's polyphenolic constituents have been previously reported to modulate PPARγ, a transcription factor regulating genes involved in adipocyte differentiation, lipid metabolism and regulation of insulin sensitivity. PPARγ represent the major target for thiazolidinediones, the anti-diabetic class of drugs. Extracts of rosemary were found to increase human PPARγ activity in an *in vitro* cell-free assay and decrease adipocyte differentiation (217). Similarly, 80% aqueous ethanol extract of rosemary activated human PPARγ in a concentration-dependent manner with half maximal effective concentration (EC_{50}) value of 22.8 ± 8.4 mg/L (218). Furthermore, carnosic acid and carnosol were determined to be the principle constituents contributing to PPARγ activation (218). In hepatocytes, CA at 10 and 20 µM concentrations was demonstrated to abolish the palmitate-induced reduction in mRNA and protein levels of PPARγ through increased activation of the EGFR/MAPK pathway leading to reduced lipid accumulation (189). Similarly, rosemary extract and carnosic acid were demonstrated to inhibit 3T3-L1 adipocyte differentiation, in part through inhibition of PPARγ expression (187). Thus, rosemary and its polyphenolic constituents have been shown to modulate PPARγ expression and activity, which may have secondary implications for increased insulin sensitivity.

Rosemary extract's polyphenolic constituents may also provide protection against chemically-induced reactive oxygen species production and cell death. RA exhibited significant cytoprotective effects against mycotoxin-induced reactive oxygen species (ROS) production, protein and DNA synthesis inhibition, and induction of apoptosis through inhibitory effects on caspase-3 activation in human hepatocytes (219). Similarly, RA inhibited lipopolysaccharide (LPS)- and phorbol 12-myristate 13-acetate (PMA)-induced reactive oxygen and nitrogen species production and cell death in RAW264.7 macrophages (220). The proposed underlying mechanism was reported to be inhibition of LPS-induced Iκ-Bα phosphorylation of Ser32 and Ser36 residues (220). On the other hand, 50-100 μM CA caused a decrease in intracellular ATP levels without affecting caspase3/7 activity and lactate dehydrogenase (LDH) release in human hepatocytes indicating that CA may be acting as a mitochondrial toxin, indicating that it may inhibit a component of the mitochondrial respiratory complex (221).

Digestive enzymes convert starch to maltose and iso-maltose which then travel to the small intestine where they are converted along with sucrose to monosaccharides (glucose and fructose) and absorbed by intestinal α-glucosidase (sucrase and maltase) thereby increasing blood glucose levels. Inhibitors of α-glucosidase are used in the management of hyperglycemia present in T2DM. Rosemary extract was found to have significant α-glucosidase inhibitory activity (222) which was the most potent among 31 other extracts of herbs and spices tested (223) (Table 4). Moreover, rosmarinic acid, a major polyphenolic constituent of rosemary extract, was demonstrated to significantly inhibit porcine pancreatic amylase activity *in vitro* (224), although the same has not been reported for CA, another major polyphenolic constituent of rosemary extract.

These studies indicate that rosemary extract and its polyphenols may play a role in carbohydrate digestion and absorption in the bloodstream and exert beneficial effects in pathological states such as insulin resistance and T2DM. From the above studies, it is evident that only a limited number of studies have examined the potential anti-hyperglycemic effects of rosemary extract in *in vitro* systems. There are no studies examining the direct effect of rosemary extract or any of its constituent polyphenols on glucose uptake and metabolism in skeletal muscle cells or adipocytes, key insulin target tissues. On the other hand, extracts of sage, an herb classified in within the rosemary family of *Lamiaceae*, were shown to significantly enhance insulin-stimulated glucose uptake in a dose-dependent manner in adipocytes (217) (Table 4).

Other effects of rosemary extract that may contribute to regulation of glucose homeostasis may be due to its effects on lipid/fat metabolism. Lipids are stored in cells particularly adipocytes in the form of triglycerides (TG). The breakdown of TG is controlled by enzymes called lipases. Excessive activation of hormone sensitive lipase leads to increases in plasma lipid levels such as free fatty acids (FFA) contributing to insulin resistance and T2DM. The effects of rosemary extract were assessed on hormone sensitive lipase (HSL), and pancreatic lipase (PL) and was shown to significantly inhibit both enzymes in a dose-dependent manner (225). Pure rosmarinic acid was shown to inhibit PL and HSL in a dose-dependent manner (225). Moreover, the extract had greater inhibitory activity compared to purified compounds suggesting that the extract contains a variety of constituents that may contribute synergistically in the inhibition of these enzymes (225). Additionally, *in vitro* analysis indicated that carnosic acid rich rosemary

extract inhibited PL activity by 70% (190). These studies clearly indicate that RE and its constituents CA and RA have antilipolytic activity *in vitro*.

Table 4: Anti-hyperglycemic Effects of Rosemary Extract and/or its Polyphenolic Constituents: *In Vitro* Studies

Study ID	Cell/Model	Treatment	Effects	Effects on Signaling Molecules
(214)	HepG2 hepatocytes	Methanol rosemary extract	Rosemary extract and its polyphenolic constituents suppressed gluconeogenesis through inhibition of the cAMP/PKA/CREB pathway.	Supressed cAMP responsiveness of PEPCK and G6Pase promoters in hepatocytes by > 60% quantified by the luciferase reporter gene
(226)	HepG2 hepatocytes	0.4, 2, 10, 50 µg/ml methanol rosemary extract	2-50 µg/ml increased glucose consumption by 6 %, 13 %, 21%	10-50 µg/ml ↑AMPK & ACC phosphorylation
(216)	HepG2 hepatocytes	10-20 µM CA	Inhibited palmitate-induced cellular fat accumulation.	CA ↑AMPK phosphorylation in a time-dependent manner. ↓PPARγ (↑EGFR/MAPK signaling)
(218)	Cos7 cells transfected with hPPARγ	80% aqueous ethanol rosemary extract	Rosemary extract activated PPARγ in a concentration-dependent manner, with EC (50) values of 22.8 +/- 8.4 mg/L. CA & COH, active principles of extract had EC (50) values of 19.6 +/- 2.0 µM, and 41.2 +/- 5.9 µM respectively.	↑PPARγ activation.
(187)	3T3-L1 adipocytes	Acetone rosemary extract; CA	Rosemary extract (10-30 µg/ml) & CA (0.3-20 µM) significantly inhibited adipocyte differentiation.	↓PPARγ expression.
(219)	HepG2 hepatocytes	RA (25-50 µM)	RA significantly reduced AFB1- & OTA-induced ROS production, DNA & protein sythnesis inhibition, & apoptosis.	↓activation of caspase 3
(220)	RAW264.7 macrophages	RA (10-50 µM)	RA significantly reduced LPS-induced NO production, and decreased iNOS protein expression; PMA-induced ROS production.	↓Iκ-Bα phosphorylation at Ser32 & Ser36 residues

(221)	HepG2 hepatocytes	50-100 µM CA	CA caused hepatoxicity, with associated decrease in ATP levels and lack of caspase 3/7 activity or LDH release after 4 hours of treatment indicating that CA may be acting as a mitochondrial toxin.	↓ATP levels ↔ caspase 3/7 ↔ LDH levels
(223)	Rat intestinal α-glucosidase (AGc)	50 % ethanol rosemary extract	Inhibited AGc with IC50 value of 683-711 µg/ml	
(227)	PPAM	100 mg of different RA extract in 3 mL of 50% ethanol. Oregano (7% RA) (O); Lemon balm (50% RA) (LB); Pure RA (97%) (PRA)	PRA, LB, O inhibited amylase activity by 85%, 50%, & 42%. Inhibitory amylase activity was correlated with RA content of extracts	
(225)	Porcine pancreatic lipase (PL); Rodent hormone sensitive lipase (HSL)	6.3-200 ug/ml of methanol rosemary extract & its constituent RA	Both inhibited PL & HSL activity. *Extract > inhibitory activity versus pure RA	
(190)	Human PL	100 µg/ml rosemary extract rich in CA	Inhibited human PL (70%)	
(217)	3T3-L1 adipocytes	Extract of sage	Increased insulin-stimulated glucose uptake in a dose-dependent manner	↑PPARγ transactivation ↓adipocyte differentiation

CA, carnosic acid; COH, carnosol, RA, rosmarinic acid; PPAM, porcine pancreatic α-amylase; PL, AGc, α glucosidase, porcine pancreatic lipase; HSL, hormone sensitive lipase; PPARγ, peroxisome proliferator activated receptor-γ; EGFR, epidermal growth factor receptor; MAPK, mitogen activated protein kinase; AMPK, AMP-activated protein kinase; ACC, acetyl coA carboxylase.

1.10.4 Evidence of Anti-Hyperglycemic Effects of Rosemary Extract: *In Vivo* Studies

In streptozotocin-(STZ) induced diabetic rats, aqueous rosemary extract resulted in significant improvements in fasting plasma glucose levels (228) (Table 5). Administration of 50% ethanol extract of rosemary in streptozotocin (STZ)-induced diabetic rats significantly decreased plasma glucose levels (223). This effect was due to inhibition of glucosidase enzymes involved in glucose absorption (Table 5). In a more recent study, daily administration of 200 mg/kg b.w of aqueous extract of rosemary for three weeks caused significant reductions in blood glucose levels of both normal and STZ-induced diabetic rats (210) (Table 5). Similar effects were seen on blood glucose levels in STZ-induced diabetic rats given aqueous rosemary extract (1.16 g/ml) for 4 weeks *(229).* In addition, the extract significantly reduced plasma triglycerides, cholesterol and LDL while increasing plasma HDL levels (229). In agreement with the above studies, blood glucose levels as well as total cholesterol and triglyceride levels were significantly reduced in STZ-induced diabetic rats given aqueous rosemary extract 2 weeks before and 2 weeks after STZ injection (209,230). Insulin resistance and Type 2 diabetes is associated with increased plasma lipid levels in humans and studies both *in vitro* and *in vivo* provide clear evidence that enhanced lipid levels can cause insulin resistance as discussed in section 1.7. Therefore, the significant reduction in plasma lipid levels seen in the abovemetioned studies using the STZ-induced diabetic animals provide strong evidence for RE's indirect anti-diabetic effects. Furthermore, administration of aqueous extract of rosemary prior to streptozotocin injection in rats significantly protected

against STZ-induced elevations in blood glucose levels which was correlated with a significant protection against pancreatic β-cells (231). In addition, rosmarinic acid, a major polyphenolic constituent of rosemary, was demonstrated to significantly increase total antioxidant capacity and estrogen levels in STZ-induced diabetic female rats suggesting that it may have indirect effects on hyperglycemia-induced reactive oxygen species production and associated T2DM complications (232). Although, the abovementioned studies used STZ-induced diabetic animals to investigate the effects of RE, its effects on different insulin target tissues and the mechanism involved are not clear largely due to the fact that the different studies examined different parameters and there was a lack of systematic examination of factors involved in glucose homeostasis. All of the studies are summarized in Table 5 (refer to pages 71-74) to provide an overview of the existing literature on the topic and simultaneously reveal potential areas of interest for future research to better clarify rosemary extract's effects on glucose homeostasis and its mechanism of action.

In addition to the STZ-induced diabetic model, the alloxan-induced diabetes animal model is also used extensively. Alloxan causes diabetes by rapid depletion of pancreatic β-cells leading to inflammation and sustained hyperglycemia secondary to a reduction in insulin release into circulation. In alloxan-induced diabetic rabbits, 200 mg/kg b.w of ethanol extract of rosemary lead to a significant reduction in fasting plasma glucose levels (211) (Table 5). Another recent study evaluated the effects of rosemary extract on blood glucose levels and liver function and structure in alloxan-induced diabetic rats (233). Diabetic rats were supplemented with powdered rosemary extract added as 20%

of diet or 20% aqueous rosemary extract was orally administration through a tube (233) (Table 5). There was a significant decrease in fasting plasma glucose levels in both treatment groups compared to control. Additionally, aqueous extract of rosemary was demonstrated to have regenerative properties against alloxan-induced hepatocyte vacuolar degeneration, necrosis, small hemorrhages and dilatation of hepatic sinusoids indicating hepatoprotective effect of this herbal extract (233). Moreover, administration of 100-200 mg/kg b.w of rosmarinic acid to alloxan-induced rats for eight weeks significantly inhibited glomerular hypertrophy, glomerular number loss and glomerulosclerosis compared with diabetic control indicating rosmarinic acid's renoprotective properties (234).

Oral administration of carnosic acid (0.05% (w/w)) to obese leptin receptor deficient (db/db) mice for five weeks resulted in significant protection against fat-induced fasting and non-fasting hyperglycemia. Carnosic acid also significantly inhibited weight gain, decreased regional areas of visceral fat, and prevented against fat accumulation in white adipose tissue as well as liver. Moreover, animals supplemented with carnosic acid exhibited decreased serum levels of triglycerides, cholesterol, and alanine aminotransferase; as well as significantly decreasing hepatic lipids (189) (Table 5).

Apart from animal models of genetic and chemically-induced obesity and T2DM, the effects of rosemary extract have been examined in dietary animal models of obesity and T2DM. The preventive effects of aqueous rosemary extract standardized to contain 20% carnosic acid on glycemic levels, and lipid homeostasis was examined in mice that

were started on a high-fat diet (HFD) as juveniles (190). Daily, dietary supplementation of 500 mg/kg b.w of rosemary extract standardized to contain 20% carnosic acid for 16 weeks significantly protected against HFD-induced elevations in plasma glucose levels and total cholesterol levels compared with HFD control mice (190). Notably, fasting insulinemia remained low during the length of the study and no significant differences were observed between the groups. Correlating with the observed reductions in total cholesterol levels, HFD mice supplemented with rosemary extract displayed significant decreases in fat mass and one to twofold increase in total fecal content compared to HFD-fed control mice (190). Similarly, daily administration of 100 mg/kg b.w of aqueous rosemary extract to high-cholesterol fed mice for 36 days resulted in significant declines in tryiglycerides, plasma total cholesterol, LDL-C, and increase in HDL levels compared to control mice (235). Furthermore, administration of aqueous extract of rosemary and non-esterified phenolic extract of rosemary at concentrations of 70 mg/kg b.w and 140 mg/kg b.w to diet-induced hypercholesterolemic rats for four weeks resulting in significant reduction in total cholesterol and non-HDL-c levels compared with control rats only in response to the former herbal supplementation (Afonso et al., 2013). However, there were no effects on triglyceride and HDL-C levels. In addition, high-fructose fed (HFR) mice given daily dose of 100 mg/kg b.w of rosmarinic acid for 60 days significantly prevented against HFR-induced glucose intolerance compared to HFR control mice (236). Glucose disposal in the diaphragm of mice *in vitro* also increased significantly in response to rosmarinic acid and rosmarinic acid in combination with insulin compared to control.

In contrast, obese mice and their lean counterparts fed 0.5% ethanol extract of rosemary enriched with carnosic acid (40%) incorporated in their standard chow for 64 days did not show significant differences in their glucose levels compared to control rats, although circulating insulin levels were found to be significantly decreased only in the lean rats (188) (Table 2). Noteworthy, the plasma glucose levels in all animals were within normal physiological range with a non-significant, slight increase in obese counterparts. The study also demonstrated a significant inhibition of gastric lipase (GL) in the stomach and pancreatic lipase (PL) in small intestine of rats consuming the rosemary extract (237). Furthermore, there was a significant attenuation of circulating plasma TNF-α, IL-1β, leptin and elevation of adiponectin levels, adipocytokines implicated in peripheral tissue insulin resistance and T2DM (188).

Thus the anti-hyperglycemic effects of rosemary extract are observed in animal models of obesity and T2DM. The mechanisms underlying the anti-hyperglycemic effects of *rosemary* extract *in vivo*, however, remain to be determined.

Table 5: Anti-hyperglycemic Effects of Rosemary Extract and/or its Polyphenolic Constituents: In Vivo Studies

Study	Animal Model	Dose	Glucose	Insulin	Other Measures
(228)	STZ-induced diabetic Swiss albino mice (25-30 g)	Ad libitum (10 g leaves in 1 L boiling water) for 3 months	↓FPG in healthy and diabetic animals		↔ alkaline phosphatase, bilirubin, ALT, AST, creatinine, urea-N, total protein, albumin
(223)	STZ-induced diabetic male ddY mice (19-21 g)	20 mg/mice of 50% ethanol & aqueous rosemary extract	↓ Plasma glucose levels.		Both exerted strong α-glucosidase (AGc) inhibitory activity
(210)	STZ-induced diabetic male albino rats (150-200 g)	Oral 200 mg/kg/day of aqueous rosemary extract for 3 weeks	↓ FPG		↑CAT, SOD, GPx, vitamin C, vitamin G ↓MDA ↓NO
(229)	STZ-induced diabetic male albino rats (140-155 g)	Oral 1.11 g/ml of aqueous rosemary extract for 4 weeks	↓ FPG (20%)		↓ total cholesterol, TAG, LDL-c (22%, 24%, 27%) ↑ HDL-c (18%)
(230)	STZ-induced diabetic male albino rats (150-200 g)	Oral 200 mg/kg/day of aqueous rosemary extract for 2 weeks prior to STZ injection; for 3 weeks after STZ injection.	↓FPG (36.9%)		↑Hb levels ↓total cholesterol, TG, LDL-c (72.9%, 33%, 79%). ↑HDL-c (40%) ↓ serum AST, CDK, LDH

(209)	STZ-induced diabetic male albino rats (150-200 g)	Oral 200 mg/kg/day of aqueous rosemary extract for 21 days	↓FPG		↓total cholesterol, TAG ↑TAC
(231)	STZ-induced diabetic male albino rats (150-200 g)	Oral 200 mg/kg/day of aqueous rosemary extract for 2 weeks prior to STZ injection; & for 3 weeks after STZ injection	↓FPG in both groups	↑serum insulin & C-peptide	↓ serum AST, ALT, ALP, ↑total protein, albumin
(232)	STZ-induced diabetic, female albino Wistar rats (250 g)	Oral 5 mg/rat RA for 8 weeks			↓MDA ↑Total antioxidant capacity.
(211)	Alloxan-induced diabetic New Zealand rabbits (2.2-3.1 kg)	Oral 50, 100, 200 mg/kg of ethanol rosemary extract for 6 hours (acute); for 1 week (subacute)	<u>Healthy animals</u> Acute: ↓FPG (14.5%) ↓ OGTT glucose levels <u>Diabetic animals</u> Acute: ↓FPG (22.3) Subacute: ↓ FPG (29.5%)	↑insulin levels in healthy & diabetic animals *200 mg/kg extract for 1 week increased plasma insulin levels by 77.8%	↓MDA (33.3%) ↑SOD, & CAT activity (24%, 35%)
(233)	Alloxan-induced Sprague-Dawley male albino rats (130-200 g)	20% of diet powdered rosemary; 20% of rosemary extract administered through the tube	↓FPG		Significant regenerative properties against alloxan-induced hepatocyte vacuolar degeneration, necrosis, small hemorrhages, and dilatation of hepatic sinusoids

(234)	Alloxan-induced Sprague-Dawley uninephrectomized rats	100-200 mg/kg/day of RA for 8 weeks			Inhibited glomerular hypertrophy, glomerular number loss, & glomerulosclerosis. ↓serum MDA, creatinine, urea
(237)	Female Zucker lean (fa/+) and obese (fa/fa) rats (105.5-148.5 g)	0.5% w/w of aqueous rosemary extract enriched with CA for 64 days	↔ plasma glucose levels *(levels were normal range throughout entire study period)	↓insulin levels in lean animals.	Inhibited gastric lipase activity in both lean (70%) and obese animals (80%) ↓total cholesterol, TAG, LDL-c ↑HDL-c
(189)	Male ob/ob mice	0.05% w/w CA for 5 weeks	↓BPG ↓OGTT glucose levels		↓ total cholesterol, TAG ↓ALT ↓hepatic lipids and total TAG content (28%, 47%)
(190)	HFD-treated male C57BL/6J mice	Oral 500 mg/kg/day of aqueous rosemary extract standardized to contain 20% CA for 16 weeks	↓FPG (72%)		↓ total cholesterol (68%) ↑total fecal content (1-2 fold)
(235)	Diet-induced HC female BALB/c mice	Oral 100 mg/kg/day of aqueous rosemary extract for 36 days; 10, 50, 100 mg/kg/day of rosemary extract for 8 weeks			↓total cholesterol, TAG, LDL-c ↑HDL-c

(238)	Diet-induced HC Wistar rats (101 g)	Oral 70 & 140 mg/kg/day of aqueous rosemary extract (AQ); 7 & 14 mg/kg/day of non-esterified phenolic extract of rosemary (NEPF)			↓total cholesterol, non-HDL-c (39.8%, 44.4%)
(236)	Fructose-fed (FF) swiss albino mice (25-30 g)	Oral 100 mg/kg/day of RA for 60 days	↓FPG levels ↓OGTT glucose levels	↓ plasma insulin levels	↑diaphragm glucose utilization* (RA plus insulin resulted in greater effects) ↓Glycated plasma Hb levels
(237)	Female Zucker lean (fa/+) and obese (fa/fa) rats (105.5-148.5 g)	0.5% w/w of ethanolic rosemary extract enriched with CA for 64 days	↔ plasma glucose levels *(levels were normal range throughout entire study period)	↓insulin levels in lean animals.	Inhibited gastric lipase activity in both lean (70%) and obese animals (80%) ↓total cholesterol, TAG, LDL-c ↑HDL-c
(188)	Female Zucker lean (fa/+) and obese (fa/fa) rats (105.5-148.5 g)	0.5% w/w of ethanolic rosemary extract enriched with CA for 64 days			↓leptin, TNF-α, IL-1β (lean rats) ↓AMPK phosphorylation in adipose tissue of obese rats. Undetectable Phospho-AMPK in liver or hypothalamus of both obese and lean rats.

AGc, α-glucosidase activity; ALT, alanine aminotransferase; CA, carnosic acid; COH, carnosol; FF, fructose-fed; FPG, fasting plasma glucose; HFD, high-fat diet; HC, hypercholesterolemia; HDL-c, high-density lipoprotein; LDL-c, low-density-lipoprotein; MDA, malondialdehyde; RA, rosmarinic acid; SGLT, sodium glucose cotransporters; STZ, streptozotocin; TAC, total antioxidant capacity; TC, total cholesterol; TG, triglyceride;

Chapter 2

2.1 Research Proposal

The vast majority of pharmacological treatments for insulin resistance and T2DM including biguanides, thiazolidinediones, sulfonylureas and α-glucosidase inhibitors are lacking in drug efficacy, and/or have unwanted side-effects. Biguanides (metformin) are insulin-sensitizing or insulin-mimetic drugs without affecting insulin secretion (42). The major adverse effects of metformin are lactic acidosis. Thiazolidinediones (TZDs) are a new class of oral antidiabetic drugs that improve metabolic control in patients with type 2 diabetes through the improvement of insulin sensitivity (239). TZDs exert their antidiabetic effects through a mechanism that involves activation of the gamma isoform of the peroxisome proliferator-activated receptor (PPAR-γ), a nuclear receptor. TZDs improve insulin resistance in muscle, adipose tissue and liver through PPAR-γ induction of genes involved in glucose and lipid metabolism including glucokinase and the GLUT4 glucose transporter. The major adverse effects associated with TZDs are edema and fluid retention (239). Sulfonylureas are antidiabetic drugs that stimulate β-cells of the pancreas to release insulin. Several studies have also shown that sulfonylureas can midly reduce endogenous glucose output and improve peripheral insulin resistance (42). The adverse effects associated with sulfonylureas are severe hypoglycemia, gastrointestinal intolerance, hemolytic anemia and cholestatic jaundice due to hepatotoxicity. Alpha-glucosidase inhibitors delay the digestion of complex carbohydrates and disaccharides (starch, sucrose) to monosaccharides by reversibly inhibiting α-glucosidases within the intestinal brush border which results in reduced glucose absorption and attenuated rise

of postprandial hyperglycemic. The currently available α-glucosidase inhibitors are acarbose, miglitol and voglibose. The major adverse effects associated with acarbose therapy are gastrointestinal complaints including flatulence and abdominal discomfort.

There is growing interest in search of new compounds found in plant extracts and herbal supplements in the treatment of insulin resistance and T2DM (173,225). The plant polyphenol resveratrol found in high concentrations in red wine has been demonstrated to increase glucose uptake *in vitro* (88) and reduce blood glucose levels in different animal models of type 2 diabetes (90,91,240). Resveratrol has been shown to activate AMPK in myotubes (88) and as previously mentioned the beneficial effects of resveratrol against fat-induced insulin resistance are abolished in animals lacking AMPK (91) providng strong evidence that AMPK activation is very important.

Rosemary extract has been demonstrated to decrease plasma glucose levels in animal models of obesity and diabetes, an effect similar to resveratrol. Studies have indicated that rosemary extract has *in vitro* and *in vivo* antioxidant activity. Given that oxidative stress and increased production of reactive oxygen species (ROS) is linked to insulin resistance (IR) and T2DM (36), rosemary extract's reported antioxidant activity may indirectly affect glucose homeostasis and exert beneficial effects in pathological states of IR and T2DM. Moreover, previous *in vivo* studies have demonstrated that RE protects against hyperlipidemia and hyperglycemia in genetic, chemically-induced and dietary animal models of obesity and T2DM. Daily administration of RE significantly improved plasma glucose levels in streptozotocin (STZ)-induced diabetic rats

(210,223,229); and in alloxan-induced diabetic rats (231) and rabbits (211). In genetically obese mice, carnosic acid, a polyphenolic component of RE protected against fat-induced fasting and non-fasting hyperglycemia and hyperlipidemia (189). Similarly, in a dietary rodent model of obesity, RE significantly protected against high-fat diet (HFD) induced elevations in plasma glucose and total cholesterol levels (190). Collectively, these studies (refer to Table 5) demonstrate RE's *in vivo* anti-hyperglycemic properties. However, there are currently no studies that delineate the mechanism underlying the reported *in vivo* effects of RE. It is possible that the antihyperglycemic effects of the extract of rosemary *in vivo* may be due to effects on skeletal muscle; however, the exact action of rosemary extract and its polyphenolic constituents on glucose uptake in muscle tissue, quantitatively the most important insulin target tissue, have not been examined.

2.2 Hypotheses

Rosemary extract (RE) and its two major polyphenolic constituents carnosic acid (CA) and rosmarinic acid (RA) increase skeletal muscle glucose uptake via activation of AMPK.

2.3 Objectives/Aims

1. Examine the effects of rosemary extract (RE) on glucose uptake in skeletal muscle cells.
2. Examine the effects of pure rosemary extract constituents including carnosic acid (CA), and rosmarinic acid (RA) on glucose uptake in skeletal muscle cells.

3. Investigate the intracellular signaling molecules and signaling cascade activated by rosemary extract (RE).
   3.1 Examine the effects of rosemary extract and its main polyphenols on activation of Akt and determine the role of Akt.
   3.2 Examine the effects of rosemary extract and its main polyphenols on activation of AMPK and determine the role of AMPK.
   3.3 Examine the effects of rosemary extract (RE) and its main polyphenols on glucose transporter GLUT1 and GLUT4 translocation

2.4 Methodology

2.4.1 Materials

Minimum essential media (α-MEM), fetal bovine serum (FBS), trypsin, and antibiotic were purchased from GIBCO Life Technologies (Burlington, ON, Canada). Akt, and AMPK (Total and Phospho-specific) antibodies, horse-radish peroxidase (HRP)-conjugated anti-rabbit secondary antibody, and LumiGLOW reagents were purchased from New England Biolabs (Mississauga, ON, Canada). Insulin (Humulin R) was purchased from Eli Lilly and Company (Indianapolis, IN, USA). Bovine serum albumin and compound C were purchased from Calbiochem (Gibbstown, NJ, USA). Bradford protein assay dye reagent concentrate, polyvinylidene difluoride (PVDF) membranes, molecular weight protein standards, and electrophoresis reagents were purchased from BioRad. [3H]-2-deoxy-D-glucose were purchased from PerkinElmer (Boston, MA). Cytochalasin B, and cold 2-deoxy-D-glucose were purchased from Sigma Chemicals (St. Louis, MO). Dimethyl sulfoxide (DMSO) hybri-max was purchased from Sigma Life Sciences. Rosmarinic acid

(≥98%, powder, from *Rosmarinus officinalis*) and carnosic acid (≥91%, powder, from *Rosmarinus officinalis*) were purchased from Sigma Aldrich. Whole dried rosemary (*Rosmarinus officinalis* L.) leaves were purchased from Compliments/Sobeys (Mississauga, ON, Canada). Parental, GLUT1 and GLUT4 overexpressing L6 cells were a kind gift from Dr. A Klip (Hospital for Sick Children, Toronto, ON, Canada).

2.4.2 Cells

L6 cells which are an immortalized myogenic cell line derived from rat hindlimb skeletal muscle, undergo proliferation as mononucleated myoblasts when grown in 10% FBS containing α-minimum essential media (α-MEM) and spontaneously differentiate into multinucleated myotubes when placed in 2% FBS containing media. L6 cells express insulin receptor, insulin-like growth factor-1 receptor (IGF-1), and facilitated glucose transporters (GLUTs) namely GLUT1, GLUT3, and GLUT4 (241). During differentiation from myoblasts into myotubes, insulin receptor and insulin-sensitive glucose transporter (GLUT4) expression increases resulting in established insulin responsiveness. Following cell treatment with insulin, all three GLUT isoforms translocate to the plasma membrane but the largest relative change occurs with the GLUT4 (242). In accordance with relative change in GLUT expression between myoblasts and myotubes, glucose transport activity also differs as the cells differentiate. Basal glucose transport is highest in myoblasts and decreases as the cells differentiate into myotubes while insulin-stimulated glucose uptake is observed only upon cell alignment and increases as they differentiate to the myotube stage (243).

Cultured cells are extensively used to study metabolic and hormonal processes. The advantages of studying molecular mechanisms of hormone action and transport function/regulation in a cell culture system are the homogeneity of muscle cell population with limited intercellular space unlike intact tissue preparation, as well as a closely controlled external environment without influences by other factors found in *in vivo* studies (241). Additionally, cell cultures have an extended viability and provide a conducive model to examine acute and chronic effects of a particular substance/chemical under investigation.

Isolation of human skeletal muscle strips is possible only during a surgical procedure and therefore availability is greatly limited. Additionally, there is a risk of compromising membrane integrity upon removal of muscle tissue (242). In primary cell culture, stimulation of glucose transport in response to physiological concentrations of insulin has been demonstrated ineffective (241). Furthermore, there is difficulty associated with establishing primary muscle cell culture and is not generally used.

Other than L6 skeletal muscle cells, mouse C_2C_{12} cells, which express both the glucose transporters GLUT1 and GLUT4 have been used as an *in vitro* model of skeletal muscle (241).

L6 cells display greater ratios of GLUT1 and GLUT3 and lower GLUT4 transporter expression compared to adult rat muscles resulting in an inequitable representation of adult skeletal muscle, however these cells express many morphological and functional characteristics of skeletal muscle. Most importantly, the L6 cell line is amongst few cell

lines that differentiate in culture, and the only cell line that express GLUT1, GLUT3 and GLUT4 (241,242).

L6 cells are extensively used and represent the best available cell culture model of skeletal muscle (242). These cells grow in monolayers, which makes them readily accessible to substrates rendering them a good model for studying the influence of substances/chemicals on glucose transport.

In addition to using the parental L6 cell line, the L6 GLUT4myc and GLUT1myc overexpressing cell lines were used in the present study. The L6 GLUTmyc overexpressing cell line was constructed by inserting a human c-myc epitope tag within the first exofacial loop of the GLUT1 or GLUT4 trasnporter (241,244). These cells differentiate normally from myoblasts to fused myotubes, at which stage they respond to insulin with a two-fold stimulation of glucose uptake. Additionally while the GLUT4myc cell line responds to insulin treatment with a two-fold increase in GLUT4 translocation, there is a modest increase in GLUT1 translocation in GLUT1myc cells. The Michaelis-Menten constant (K_m) of glucose uptake is similar in L6 GLUTmyc cells to that of the parental cells (71,241). Similar to L6 parental cells, L6 GLUTmyc cells respond to insulin by IRS-1 phosphorylation and subsequent PI3k and Akt/PKB activation, which are necessary for stimulation of glucose uptake.

2.4.3 Cell Culture Technique

L6 rat skeletal muscle cells were grown in α-MEM (pH 7.4) containing 5 mM glucose, 10% (v/v) FBS, and 1% (v/v) antibiotic-antimycotic solution (100 U/ml penicillin, 100

μg/ml streptomycin, and 250 ng/ml amphotericin B) in a humidified atmosphere of 5% CO_2, 95% air at 37^oC. Cells were grown in 250 cm^3 flasks and seeded into 12-well tissue culture plates for glucose uptake measurements and 6-well plates for immunoblotting analysis. Upon reaching 100% confluency, the cells were exposed to 2% (v/v) FBS to allow the cells to differentiate from mono-nucleated myoblasts into multi-nucleated myotubes. Myotubes were used for all experiments. Prior to treatments, myotubes were growth-arrested by incubation with serum-free α-MEM media for 2.5-3 hours. Serum deprivation decreases the rate of basal glucose transport so that the cells are not at maximum capacity before stimulation, thereby making an increase in glucose transport in response to treatments more detectable (Mitsumoto et al., 1991).

2.4.4 Preparation of Rosemary Extract (RE)

A methanol extract of rosemary (RE) was prepared. Whole dried rosemary (*Rosmarinus officinalis* L.) leaves (purchased from Compliments/Sobey's, Mississauga, ON, Canada), were ground and passed through a mesh sieve and extracted following protocols established by the National Cancer Institute of the U.S. (223,226). The ground plant (5 g) was steeped overnight (16 hours) in dichloromethane-methanol (1:1) (30 mL). The filtrate was collected under slight vacuum followed by a MeOH (30 mL) extraction for 30 min. The solvent was removed by rotary evaporation. Aliquots were prepared in dimethyl sulfoxide (DMSO) (10 mg/ml) and stored at -20 ˚C (226). Preparation of the rosemary extract was performed in collaboration with Dr.Stamatatos's chemistry lab at Brock University.

2.4.5 Analysis of Rosemary extract (RE) Using High Performance Liquid Chromatography (HPLC) Technique

Methanol extract of rosemary, and standards (carnosic acid and rosmarinic acid) (purchased from Sigma Aldrich) were dissolved in sterile DMSO at a concentration of 2 mg/mL. Before HPLC analysis, all the samples were filtered through a 0.45 µM filter. Aliquots of 2.5 µL were injected into a reverse phase Agilent 110 series HPLC instrument equipped with an autosampler. Separation and quantification were achieved at 25 ^{o}C by using a mobile phase consisting of solvent A and solvent B. Solvent A was 0.1% formic acid in HPLC grade water, and solvent B was acetonitrile. A linear gradient of 95% solvent A and 5% solvent B was achieved over 30 minutes. The flow rate was 0.4 ml min^{-1} and the detection was set at 254 nm. Identification of individual compounds was based on the comparison of the actual retention time to those of reference authentic standards (carnosic acid, rosmarinic acid). Quantification of each compound was performed by the calculation of the peak areas after HPLC separation. Mean total content was expressed in % (g/100 g dry weight extract). It should be noted that the HPLC analysis was performed in collaboration with Dr.Hudlicky's chemistry lab at Brock University.

2.4.6 Cell Treatment

L6 myotubes were treated with different concentrations of methanol extract of rosemary leaves with different exposure times. The concentrations used were 0.1, 1.0, 5.0, 10, 20, 30, 40, 50 ug/ml of methanol extract of rosemary leaves. The exposure times were 0.5, 1, 2, 4, 6, 16 hours. Cells were exposed to 100 nM insulin (30 min. exposure)

or 5 mM metformin (16 hours exposure) (211,228,236). L6 myotubes were also exposed to 0.1, 0.3, 2.0 µM carnosic acid (CA), and 2.0, 5.0 µM rosmarinic acid (RA) for four hours. Selection of these concentrations was derived from the HPLC analysis of the extract and other *in vitro* studies that used these compounds. A vehicle-treated control (% of DMSO) was used in parallel with the treated groups.

2.4.7 Glucose Uptake Assay

The radiometric glucose uptake assay measures specific carrier (GLUT)-mediated glucose transport utilizing a radiolabelled, non-metabolizable glucose analog, [^{3}H]-2-deoxy-D-glucose. At the end of the incubation period, the cells were rinsed three times with HEPES-buffered saline solution (HBS; 14mM NaCl, 5mM KCl, 20 mM HEPES, 2.5mM MgSO4 and 1mM CaCl2, pH 7.4). Subsequently, 2-deoxy-D-glucose uptake measurements were carried out by exposing cells to 250µl of HEPES-buffered saline containing 10µM [^{3}H]-2-deoxy-D-glucose for 10 minutes. Nonspecific uptake of 2-deoxy-D-glucose were determined in the presence of 10µM cytochalasin B (GLUT inhibitor), and subtracted from total uptake (absence of CB) to determine specific carrier-mediated glucose transport. The transport assay was terminated by washing the cells three times with 1 ml ice-cold 0.9% NaCl solution. Cells were solubilized by 1 ml of 0.05N NaOH solution. Cell lysates were collected into scintillation vials followed by addition of 10 ml of scintillation fluid. All experiments were assayed in triplicates and performed 4-8 times. 50µl of cell lysates were pipetted into 2 ml eppendorf tubes and stored at -20^{o}C for analysis of cellular protein content using the Bradford Protein Assay method. Radioactivity was measured using the Beckman Scintillation Counter.

2.4.8 Cell Lysis

L6 cells were grown in 6-well plates until they were fully confluent, followed by treatments as indicated in the cell treatment section. After treatments, cells were be washed two times with PBS and placed on ice. PBS was removed and 100µl of cell lysis buffer was added to each well of the 6-well plates. Cells were lysed and collected into 1.5 mL eppendorf tubes, and an equal amount of SDS (sodium dodecyl sulfate) sample buffer was added to each tube. The cell lysates were then boiled for 5 minutes and stored in the freezer at -20°C.

2.4.9 Protein Assay

Protein assay dye (BioRad) was prepared (1 part dye concentrate: 4 parts DD H_20) and filtered for protein concentration determination. BSA protein standards (0, 0.1, 0.2, 0.4, 0.6, 0.8, 0.9, 1.0mg/ml) were used to create a standard protein curve. 10µL of each protein standard and lysed samples was pipetted into separate wells of a 96-well plate in triplicate. 200µL of protein assay dye was then added into each well. The absorbance was measured using a microplate reader at 595nm, and the final concentration of the protein samples was calculated in Microsoft Excel 2010.

2.4.10 Western Blot Analysis

At the end of the treatment period, the cells were rinsed three times with HBS and then lysis buffer (20mM Tris (pH 7.5), 150mM NaCl, 1mM EDTA, 1mM EGTA, 1% Triton X-100, 2.5mM NA407P2, 1mM β-glycerolphosphate, 1mM Na3V04, 1µg/ml leupeptin, 1mM PMSF) was added and the lysate was scraped off and solubilized in electrophoresis sample buffer, followed by separation by sodium dodecyl sulfate polyacrylamide gel

(10%) electrophoresis. The samples were subsequently transferred electrophoretically to PVDF membranes. The membranes were incubated for 1 h at room temperature with 5% (w/v) nonfat dry milk in Tris- buffered saline and then overnight at 4°C with the primary antibody. The following primary antibodies were used: Phospho- Akt (Ser473) polyclonal antibody (1:1000 dilution), Total- Akt polyclonal antibody (1:1000), Phospho-AMPKα1/2 polyclonal antibody (1:1000), Total-AMPkα1/2. Immunoblotting of total and phosphorylated forms of the specific protein were performed on separate PVDF membranes. The primary antibody was detected with either the HRP-conjugated anti-rabbit secondary antibody (1 :2000) or the HRP- conjugated anti-mouse secondary antibody (1 :2000), and LumiGLOW reagent (New England Biolabs) using Alpha Innotech FluorChem (quantitative imaging system for fluorescent and chemiluminescent blots; Johannesburg, S.A).

2.4.11 Measurement of GLUT1myc and GLUT4myc Translocation

The amount of myc-tagged GLUT1 and GLUT4 at the surface of intact cells was measured by an antibody-coupled colorimetric assay as previously described (245). Following the treatment period, the monolayer of myotubes was fixed with 3% paraformaldehyde for 10 minutes at 4^{o}C, incubated with 1% glycine for 10 minutes to reduce the remaining paraformaldehyde, blocked with 5% goat serum in PBS, and then exposed to anti-myc antibody (1:500) for 60 minutes, and followed by incubation with horseradish peroxidase (HRP)-conjugated goat anti-rabbit IgG (1:1000) for 45 minutes, all at 4^{o}C. Cells were washed extensively, and 1 ml of OPD reagent was added for 30 minutes at room temperate. The reaction was stopped by 0.25 ml of 3 N HCL. The

supernatant was collected, transferred to a 96-well ELISA plate and the absorbance was measured at 492 nm. Nonspecific IgG binding, as measured by a HRP-conjugated goat anti-rabbit IgG was subtracted from experimental values. Values were expressed as percentage of control.

2.4.12 Statistical Analysis

Statistical analysis was performed using the SAS software 9.3. All data from several experiments were pooled and then presented as mean ±SE. The means of the groups (treatments compared to control group) were compared with one-way analysis of variance (ANOVA) followed by Tukey's post hoc test for multiple comparison

Chapter 3: Results

3.1 Effects of rosemary extract (RE) on glucose uptake in L6 skeletal muscle cells.

We investigated whether rosemary extract (RE) stimulates glucose uptake in L6 skeletal muscle cells. For this purpose L6 myotubes were treated with 0.1, 1.0, 5.0, 10, 20, 30, 40, and 50 µg/ml of RE for 4 hours followed by glucose uptake measurements. An incubation time of 4 hours was initially chosen based on another study that has investigated the effects of methanol extract of rosemary in HepG2 cells (226). RE at 0.1 and 1.0 µM did not have a significant effect on glucose uptake (119± 4.73% and 129%±6.54% of control, $p>0.05$ respectively). However, RE at 5 µg/ml and 10 µg/ml significantly increased glucose uptake (184±5.05% and 178±7.84% of control, $p<0.001$ respectively) (Figure 6). Concentrations at 20 µg/ml resulted in significant increase in glucose uptake (145±5.05% of control, $p<0.01$) while concentrations higher than 20 µg/ml did not have significant effects (data not shown; 30 µg/ml: 134±6.69%, 40 µg/ml: 124±14.81%, 50 µg/ml: 95±12.89% of control, $p>0.05$). Microscopic examination of cell morphology did not reveal any changes with any concentrations used, indicating no changes in cell viability. Although no microscopic evidence of toxicity were observed at RE concentrations of 30-50 µg/ml, the lack of stimulation of glucose uptake may indicate an excessive pharmacological dose with possible associated cytotoxic effects and therefore such high doses are not recommended to be used in future studies.

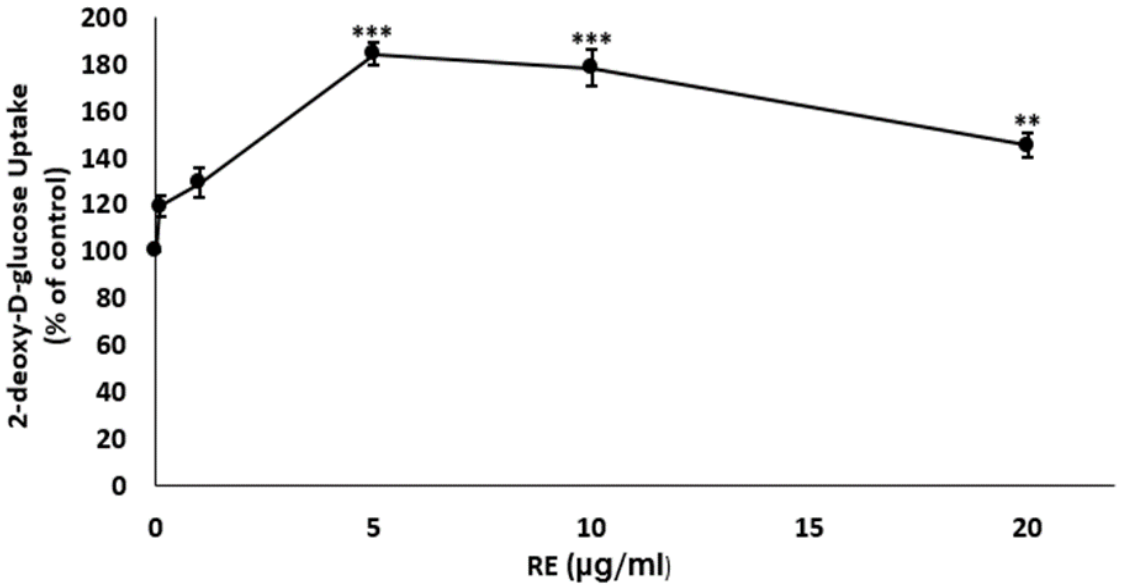

Figure 6: Effects of rosemary extract (RE) on glucose uptake in L6 myotubes: Dose-response. Serum deprived L6 myotubes were incubated with the indicated concentrations of RE for 4 hours. 2-deoxy-D-glucose uptake was measured according to the methods. Data are expressed as percentage of control. Results are the mean ± SE of six to eight independent experiments. ** P<0.01, ***P<0.001, vs. control.

Next, in order to examine whether the effect of RE in increasing glucose uptake in myotubes is time-dependent, the cells were incubated with 5 µg/ml of RE for 0.5, 1, 2, 4, 6 & 16 hours followed by glucose uptake measurements (Figure 7). Incubation of myotubes with RE for 0.5 & 1 hour did not result in a significant increase in glucose uptake (115±4.10%, 123±5.21%, p>0.05). However, RE at 2, 4, 6 and 16 hours increased glucose uptake time-dependently (154±5.93%, 184±5.07%, 197±7.28% and 157±8.66% of control, p<0.001 respectively). Maximum stimulation was seen with 6 hours (197±7.28% of control, p<0.001 respectively). Importantly, longer incubation time with RE (16 hours) resulted in a significant increase in glucose uptake.

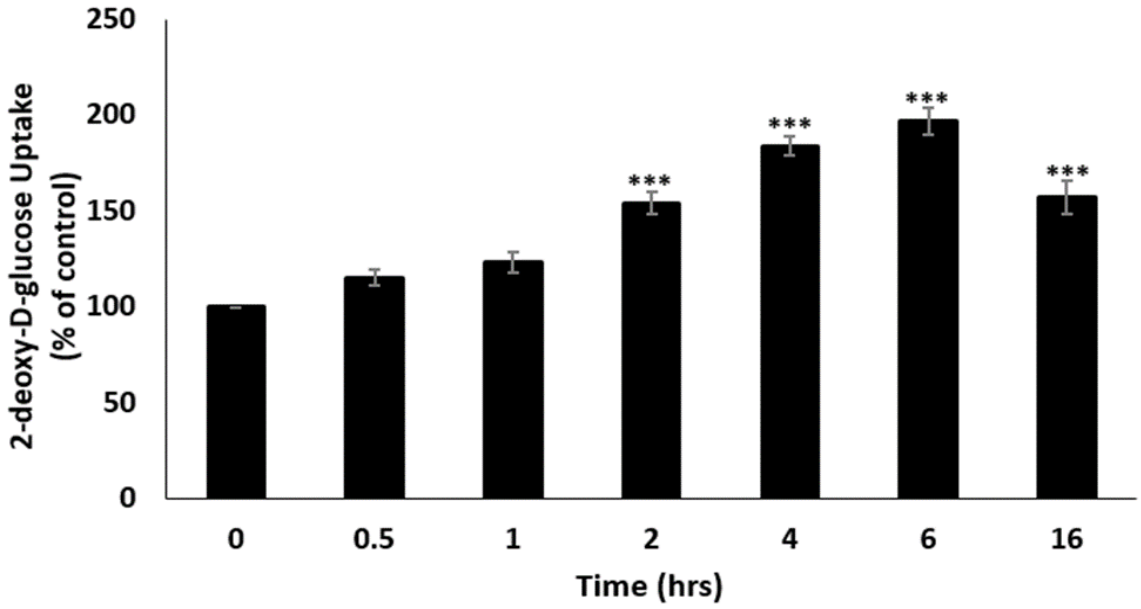

Figure 7: Effects of rosemary extract (RE) on glucose uptake in L6 myotubes: Time-course. Serum deprived L6 myotubes were incubated with 5 µg/ml of RE for the indicated times. 2-deoxy-D-glucose uptake was measured according to the methods. Data are expressed as percentage of control (0 hrs). Results are the mean ± SE of eight to ten independent experiments. *** P<0.001 vs. control.

We next examined whether this effect of RE is similar to insulin. Insulin (100 nM, 30 minutes) significantly stimulated glucose uptake in myotubes (207±5.26% of control, p<0.001) (Figure 8). Similarly, RE at 5 µg/ml for four hours caused a significant increase in glucose uptake (184±5.07% of control, p<0.001) which was comparable to insulin (Figure 8). Furthermore, this effect of RE is comparable to metformin (2 mM for 16 hours), an oral anti-diabetic drug (216±8.77%, P<0.001). These results indicate that RE significantly stimulates glucose uptake in a dose- and time-dependent manner that is independent of insulin. Importantly the increase in glucose uptake by RE is to the same level as the increase seen with maximum insulin and metformin stimulation.

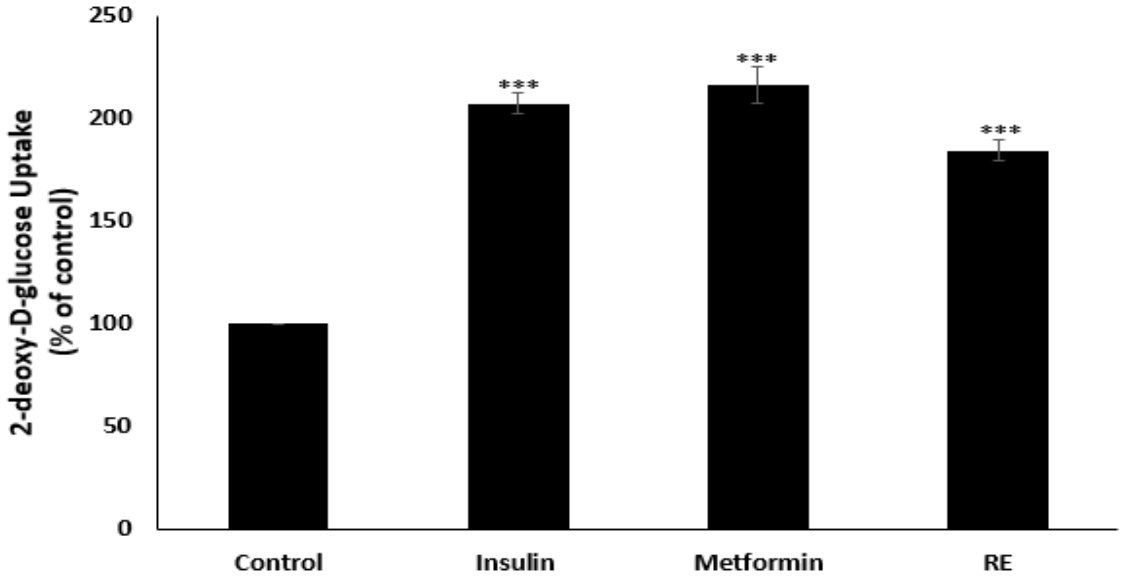

Figure 8: Stimulation of skeletal muscle glucose uptake by insulin, metformin, and rosemary extract (RE). L6 myotubes were incubated with 100 nM insulin (30 minutes), 2 mM metformin (16 hours) or 5 µg/ml of RE (4 hours). 2-deoxy-D-glucose uptake was measured according to the methods. Data are expressed as percentage of control. Results are the mean ± SE of four to eight independent experiments. ***P<0.001 vs. control.

3.2 Effects of rosemary extract (RE) on insulin-stimulated glucose uptake in L6 skeletal muscle cells.

Next, we examined the effect of rosemary extract (RE) on insulin-stimulated glucose uptake. Myotubes were treated with or without 5 µg/ml RE (4 hours) and different concentrations of insulin (1 nM, 3 nM, 10 nM, 100 nM) were added in for the last 30 minutes followed by glucose uptake measurements.

Insulin increased glucose uptake in a dose-dependent manner (157±9.30%, 161±7.92%, 188±11.45%, 203± 9.5% of control, p<0.001) (Figure 9). Pre-treatment with RE did not affect the insulin response in any of the concentrations used (181±5.84%,

185±5.01%, 194±6.35% and 199±7.55% of control, p>0.05) (Figure 9). There was a tendency of RE to increase glucose uptake at insulin concentrations of 1 nM and 3 nM but it did not reach significance. The results indicate that RE does not have additive or synergistic effects on insulin-stimulated glucose uptake.

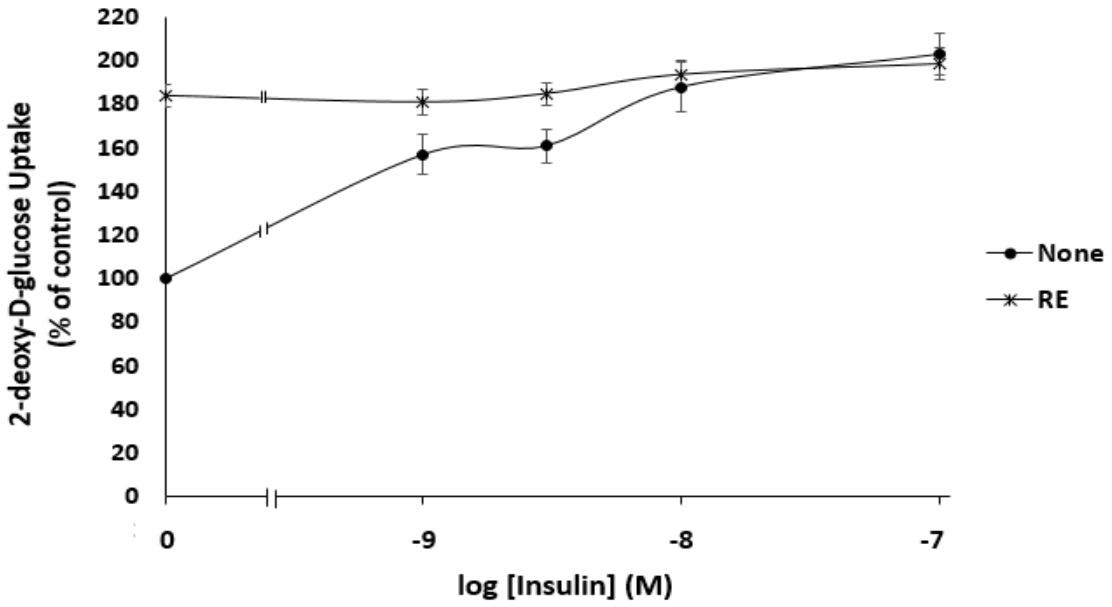

Figure 9: Effect of rosemary extract (RE) on insulin-stimulated glucose uptake. Serum deprived L6 myotubes were incubated with 5 µg/ml RE for 4 hours and then exposed to different insulin concentrations for the last 30 minutes followed by glucose uptake measurements. Data are expressed as percentage of control. Results are the mean ± SE of three to five independent experiments.

3.3 Effects of the PI3K inhibitor wortmannin on rosemary extract (RE)-induced glucose uptake.

PI3K has been established as a key molecule involved in the insulin signalling cascade that leads to glucose uptake in skeletal muscle and its activity is required in this action. Therefore we investigated whether PI3K may be a mediator of RE-stimulated glucose uptake by using the PI3K inhibitor, wortmannin. Myotubes were pre-treated with 100 nM of wortmannin for 15 minutes followed by treatment with or without 5 µg/ml RE for

4 hours or 100 nM insulin for 30 minutes. After treatments, glucose uptake measurements were performed.

Insulin significantly increased glucose uptake (210±9.47% of control, p<0.001), and this effect was significantly reduced by wortmannin pre-treatment (140±6.08% of control, p<0.001) (Figure 10). RE significantly increased glucose uptake (208±13.62% of control, p<0.001) but this was not affected by wortmannin pretreatment (201±9.32% of control, p>0.05) (Figure 10). These results suggest that PI3K is not involved in the regulation of glucose uptake by RE.

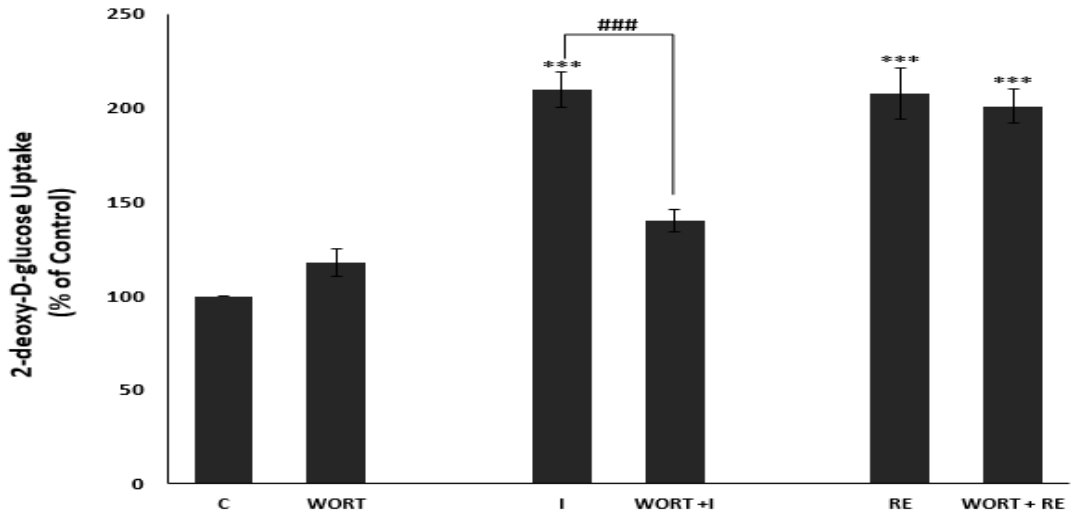

Figure 10: Effect of wortmannin on insulin- and rosemary extract (RE)-induced glucose uptake. Cells were pre-incubated in the absence or presence of 100 nM wortmannin for 15 minutes followed by treatment with or without 5 µg/ml of RE for 4 hours or 100nM of insulin for 30 minutes. 2-deoxy-D-glucose uptake was measured according to the methods. Data are expressed as percentage of control. Results are the mean ± SE of six to seven independent experiments. ***P<0.001 vs. control. ###P<0.001 vs. treatments alone (without inhibitors).

3.4 Effect of rosemary extract (RE) on Akt phosphorylation

Although the use of wortmannin, the PI3K inhibitor, indicated that the PI3K-Akt cascade may not be activated by RE, we wished to confirm these findings and therefore we next examined the effects of RE on Akt, the molecule downstream of PI3K. Phosphorylation of Akt on Ser473 residue leads to its activation and ser473 phosphorylation has been established as an indicator of Akt activity (246). Therefore, the effect of RE was examined using phospho-specific antibodies against Akt (Ser473) in western blot analysis. As shown previously in our lab (88,247) and others, insulin treatment (100 nM for 15 minutes) strongly stimulates phosphorylation of Ser473 residue of Akt (260±11.5%, $p<0.05$) (Figure 11). RE at 5 μg/ml and 10 μg/ml (4 hours) did not affect Akt phosphorylation (Figure 11). The action of insulin on Akt phosphorylation is an acute event. It is possible that RE may activate Akt and we missed such activation by looking at 4 hour time point (Figure 11). To ensure that we did not miss potential earlier phosphorylation of Akt by RE, cells were exposed to 5 μg/ml of RE for 0.25, 0.5, 1, 2, and 4 hours and Akt phosphorylation was examined. RE did not lead to phosphorylation of Akt at any of the time points (Figure 12). Insulin consistently phosphorylated Akt. Metformin, resveratrol and AICAR were also used and none of them, as it is previously established, induced Akt phosphorylation (Figure 12). Total Akt levels were not changed by any treatment (Figure 11 & 12). These results indicate that the effect of RE on glucose uptake is Akt-independent.

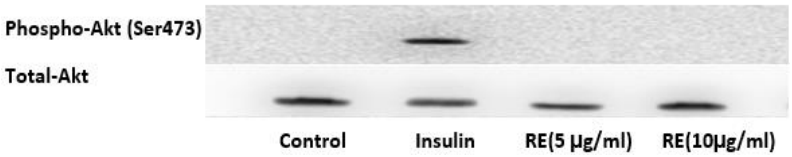

Figure 11: Effect of rosemary extract (RE) on Akt phosphorylation. L6 myotubes were serum-deprived for 2 hours followed by treatment with 100 nM insulin for 15 minutes, 5 µg/ml or 10 µg/ml of RE for 4 hours. Whole cell lysates were prepared and immunoblotted for Akt and Phospho-Akt (Ser473).

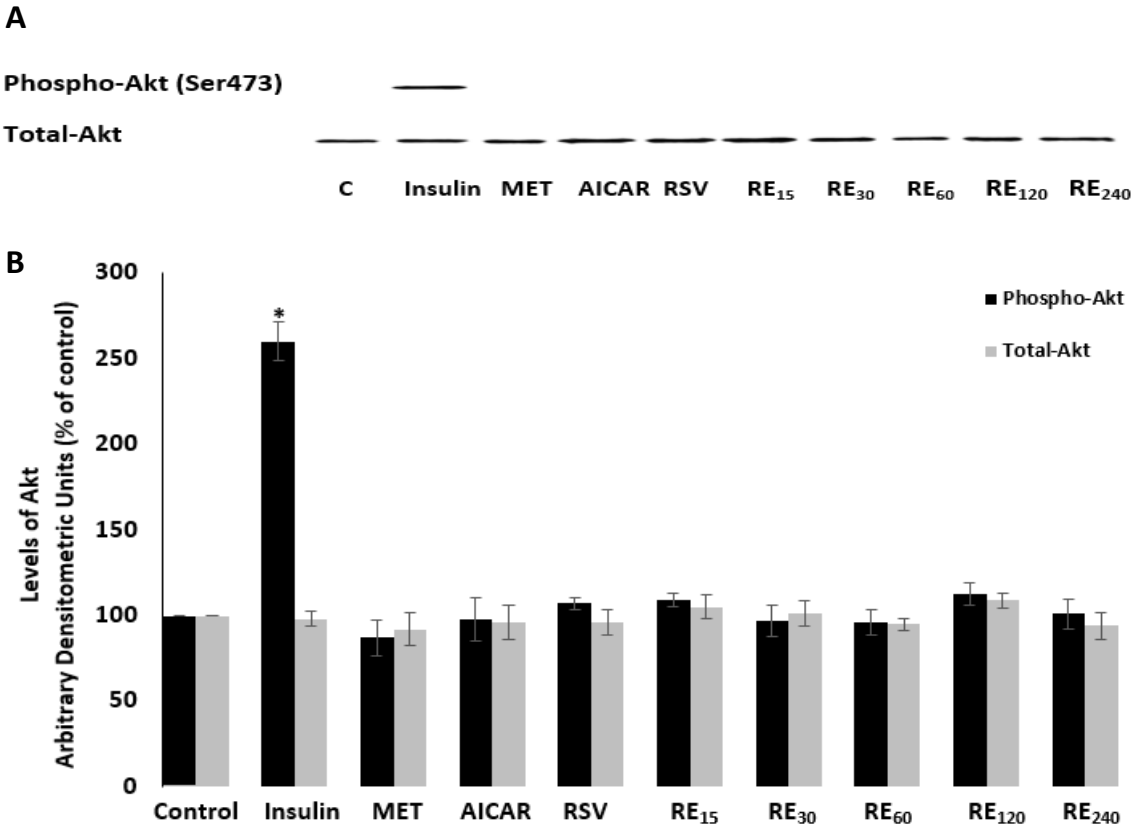

Figure 12: Effect of rosemary extract (RE) on Akt phosphorylation: Time-Course. L6 myotubes were serum-deprived for 2 hours followed by treatment with 100 nM insulin (15 minutes), 2 mM metformin (MET) (120 minutes), 2mM AICAR (120 minutes), 100 µM resveratrol (RSV) (120 minutes), or 5 µg/ml of RE for the indicated times Whole cell lysates were prepared, resolved by SDS-PAGE and immunoblotted for specific antibodies that recognize Akt or Phospho-Akt (Ser473). (A) Representative immunoblots. (B) Immunoblots were scanned to quantitate the density of the bands. Values are arbitrary densitometric units compared to control. Results are the mean± SE of 3-4 experiments. *$p<0.05$ compared to control (B).

3.5 Effects of the AMPK inhibitor compound C (CC) on rosemary extract (RE)-induced glucose uptake.

As previously discussed (section 1.6), activation of AMPK in skeletal muscle has been shown to be another mechanism stimulating glucose uptake. This mechanism is employed by exercise/contraction, and various compounds including metformin, AICAR, and the polyphenol resveratrol. Therefore AMPK may be a mediator of RE-stimulated glucose uptake. We investigated the possible involvement of AMPK by using the AMPK inhibitor compound C. Myotubes were pre-treated with 25 µM compound C for 30 minutes followed by treatment with or without 5 µg/ml RE, or 2 mM metformin (2 hours). After treatments glucose uptake measurements were performed.

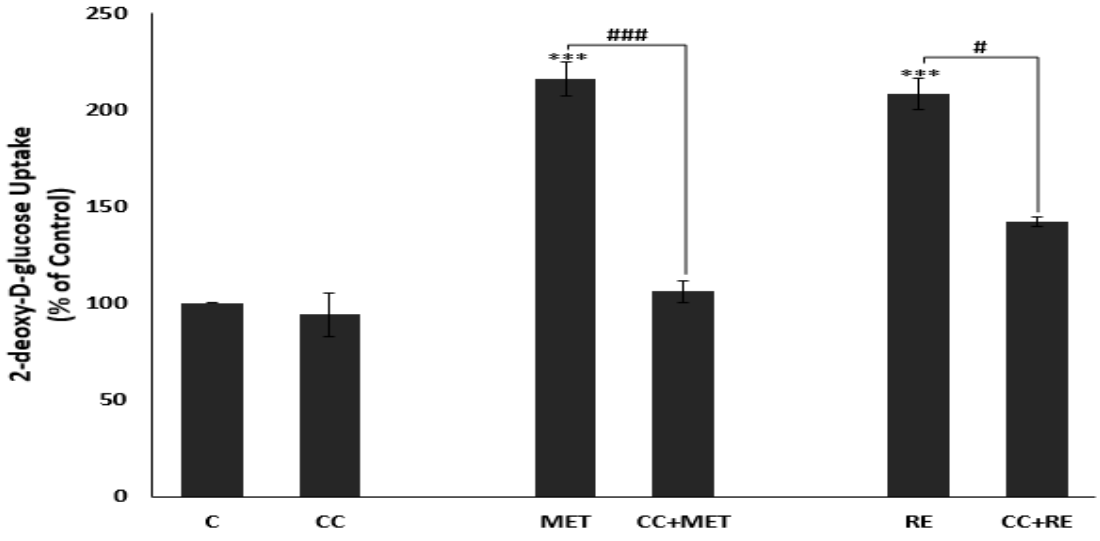

Figure 13: Effect of compound C (CC) on metformin and RE-induced glucose uptake. Cells were incubated in the absence or presence of 25 µM compound C (CC) for 30 minutes followed by the addition of 2 mM metformin (MET) for 2 hours or 5 µg/ml of RE for 4 hours. 2-deoxy-D-glucose uptake was measured according to the methods. Data are expressed as percentage of control. Results are the mean ± SE of six to seven independent experiments. ***P<0.001 vs. control. #P<0.05, ###P<0.001 vs. treatments alone (without inhibitors).

Metformin treatment increased glucose uptake (216±8.77% of control, $p<0.001$) which was inhibited by pre-treatment with compound C (106.2±5.59% of control, $p>0.05$) (Figure 13). RE significantly increased glucose uptake (208±8.11% of control, $p<0.001$) and this effect was significantly reduced by pre-treatment with compound C (142±2.40% of control, $p<0.05$ respectively). These results indicate that AMPK is involved in the regulation of glucose uptake by RE.

3.6 Effects of rosemary extract (RE) on AMPK

Next, we examined whether RE phosphorylates and activates AMPK. Myotubes were treated with 2 mM metformin (2 hours), 2 mM AICAR (2 hours), 100 μM resveratrol (2 hours), 100 nM insulin (15 minutes) or 5 μg/ml and 10 μg/ml RE for 4 hours. Western blot analysis revealed that RE significantly increased AMPK phosphorylation to levels similar to those seen with AICAR (Figure 14). We also examined whether the activation of AMPK by RE is time-dependent. Myotubes were treated with 5 μg/ml of RE for 15 minutes, 30 minutes, 1 hour, 2 hours, and 4 hours. A significant increase in AMPK phosphorylation was observed at 2 hours (157.3±11.3%, $p<0.05$) of RE treatment and remained elevated at 4 hours (190.3±17.6%, $p<0.05$) (Figure 15). Metformin, AICAR and resveratrol significantly increased AMPK phosphorylation (196±27.5%, 238±28.4% and 212±29.3%), while insulin treatment did not have any effects (67±11.2%, $p>0.05$) (Figure 15). Total AMPK levels were not changed by any treatment (Figure 14 & 15). Together, these results (Figure 12-14) suggest that RE stimulates glucose uptake through AMPK activation.

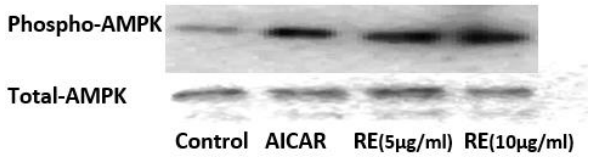

Figure 14: Effect of rosemary extract on AMPK phosphorylation. L6 myotubes were serum-deprived for 2 hours followed by treatment with 2 mM AICAR for 2 hours, 5 µg/ml or 10 µg/ml of RE for 4 hours. Whole cell lysates were prepared, resolved by SDS-PAGE and immunoblotted for phospho-AMPK (Thr172) and total AMPK.

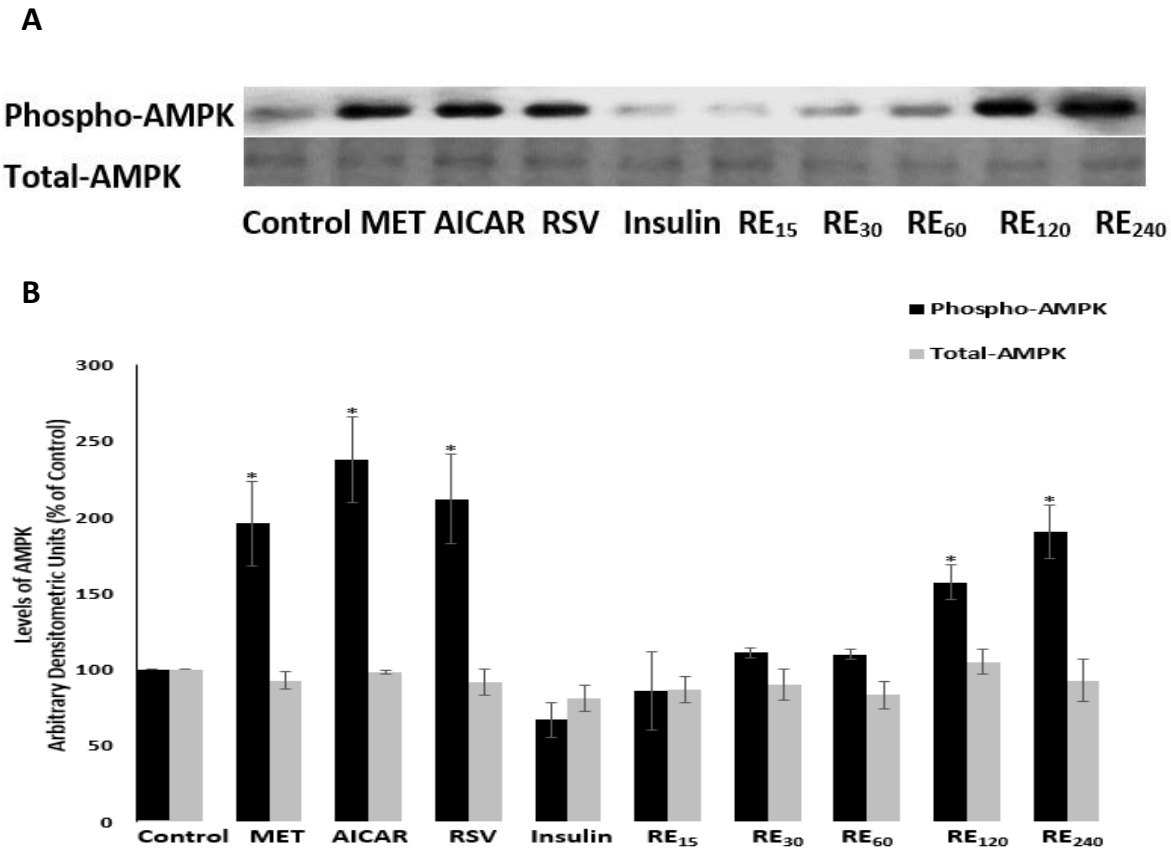

Figure 15: Effect of rosemary extract (RE) on AMPK phosphorylation: Time-Course. L6 myotubes were serum-deprived for 2 hours followed by treatment with 2 mM metformin (MET) (120 min.), 2 mM AICAR (120 min.), 100 µM resveratrol (RSV) (120 min.), or 5 µg/ml of RE for the indicated times. Whole cell lysates were prepared, resolved by SDS-PAGE and immunoblotted for total and phospho-AMPK (Thr172). (A) Representative immunoblots. (B) Immunoblots were scanned to quantitate the density of the bands. Values are arbitrary densitometric units compared to control. Data are the mean ± SE of 3-4 experiments. *$p<0.05$.

3.7 High performance liquid chromatography (HPLC) analysis of rosemary extract (RE)

Previous studies have shown that the major polyphenols in rosemary extract are carnosic acid (CA), and rosmarinic acid (RA) (177,182). Therefore, we wished to investigate whether the rosemary extract (RE) prepared in our lab and used in the experiments up to now (Figure 6-15) contained CA and RA and determine its relative quantity in the extract. To this end, high performance liquid chromatography analysis (HPLC) was performed. RE, and standards of CA and RA were prepared at a concentration of 2 mg/ml to be used in HPLC. The standards of CA and RA were run in HPLC machine followed by RE. The retention time of the peak corresponding to CA from the standard (CA) was used to determine the presence of CA in the extract (Figure 16). The area under the peak corresponding to CA in the extract was used to quantify the relative amount of CA found in the extract (Figure 16). Similar analytical methods were used for RA (Figure 16).

HPLC analysis revealed that the RE contained 2.12±0.22% CA and 13.39±0.23% of RA (Table 6). These concentrations of CA and RA are well within the range of previously reported concentrations and are in agreement with previous studies (178,179,184-186,206). Based on these values and the molecular weight of CA and RA (CA MW: 332.42 g/mol, RA MW: 360.31 g/mol) 5 µg/ml of RE (maximum stimulation of glucose uptake) corresponds to 0.3 µM CA and 2.0 µM RA (Table 6). Therefore, we wished to examine whether 0.3 µM CA and 2.0 µM RA would have an effect on glucose uptake. However, because the major polyphenolic content of rosemary extract varies depending

on soil, climate, geographical location, extraction method and storage (refer to section 1.10), in order to account for this variability and based on previous reports, we decided to use additional CA (0.1 μM, 2.0 μM) and RA (5.0 μM) concentrations and examine their effect on glucose uptake.

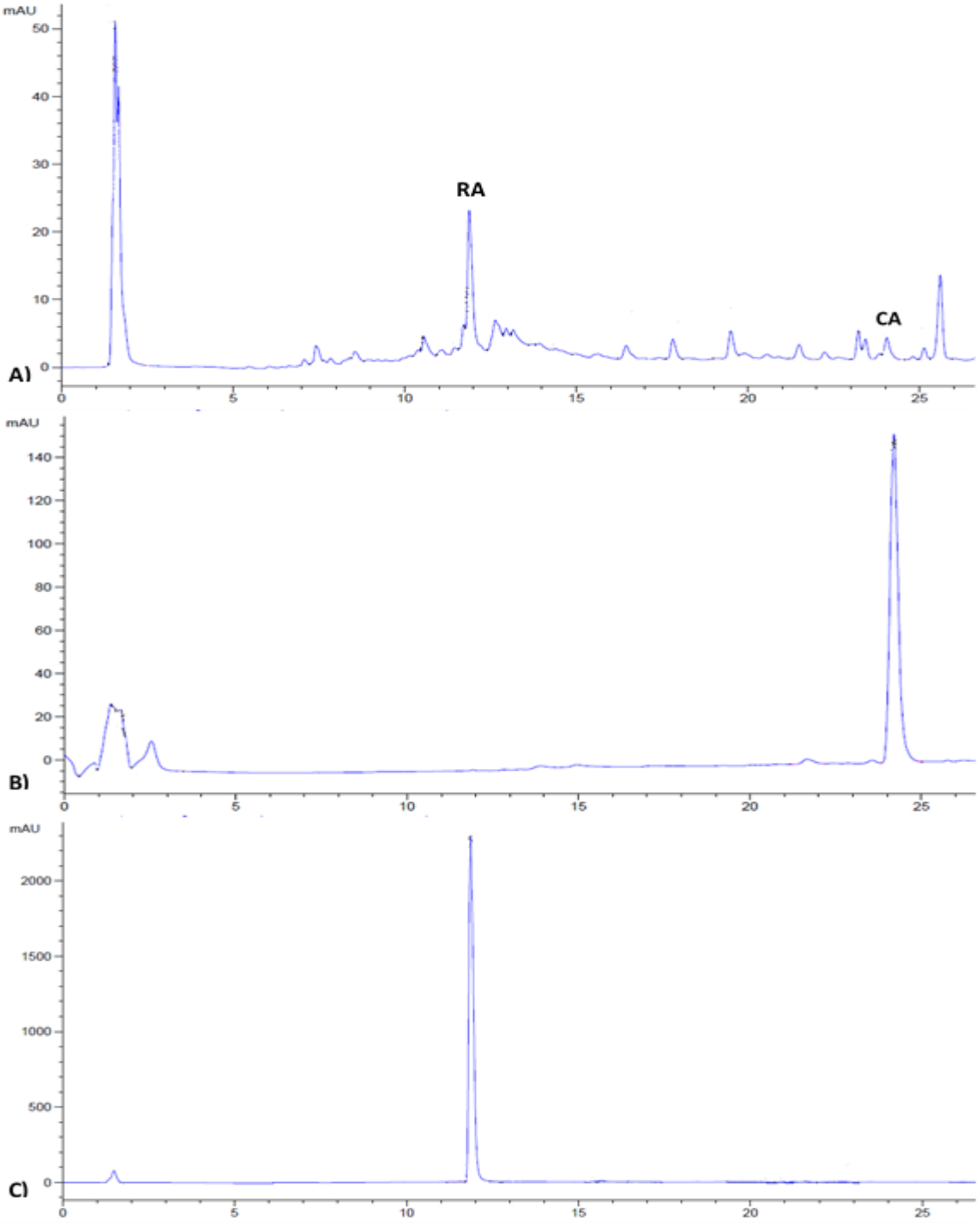

Figure 16: High performance liquid chromatography (HPLC) analysis of rosemary extract (RE). HPLC of RE and standards (carnosic acid & rosmarinic acid) were performed and the quantification of carnosic acid (CA) and rosmarinic acid (RA) in RE was determined by the retention times. A) Chromatograph of RE. B) Chromatograph of CA. C) Chromatograph of RA.

Table 6: Relative concentrations of carnosic acid (CA) and rosmarinic acid (RA) identified in rosemary extract (RE)

Compound	MW (g/mol)	Retention Time (min)	Relative Mean Quantity in RE (%)	Concentration (µg/mg RE)	Concentration in 5 µg/ml of RE (µM)*
Carnosic acid (CA)	332.42	24.197	2.12±0.22	21.2±2.2	0.3±0.031
Rosmarinic acid (RA)	360.13	11.859	13.39±0.23	133.9±2.3	2.0±0.034

*In 5 µg/ml of RE which elicited maximum increase in glucose uptake in myotubes, the corresponding concentrations of CA and RA were measured/calculated.

3.8 Effects of rosemary extract (RE)'s major polyphenolic compounds carnosic acid (CA) and rosmarinic acid (RA) on glucose uptake.

The effects of carnosic acid (CA) and rosmarinic acid (RA) were evaluated on glucose uptake in myotubes. Myotubes were incubated with indicated concentrations of CA and RA for 4 hours (Figure 17). CA at 0.1 µM did not significantly increase glucose uptake (128±4.33% of control, $p>0.05$ respectively). However, CA at 0.3 and 2.0 µM significantly increased glucose uptake (147± 7.72%, and 226±9.62% of control, $p<0.01$ and $p<0.001$ respectively) (Figure 17). RA at 2.0 µM did not significantly increase glucose uptake (121±5.04% of control, $p>0.05$ respectively), while RA at 5.0 µM also increased glucose uptake (180±8.00% of control, $p<0.001$). The degree of glucose uptake in myotubes elicited by RE treatment (184±5.07% of control) was greater than CA (0.3 µM) or RA (2.0 µM) alone indicating that the two compounds (CA, RA) may act synergistically. This could be tested by examining the combined effects of CA and RA at concentrations found in RE on glucose uptake and determine whether the level of glucose uptake seen with RE is comparable to that of combined CA and RA.

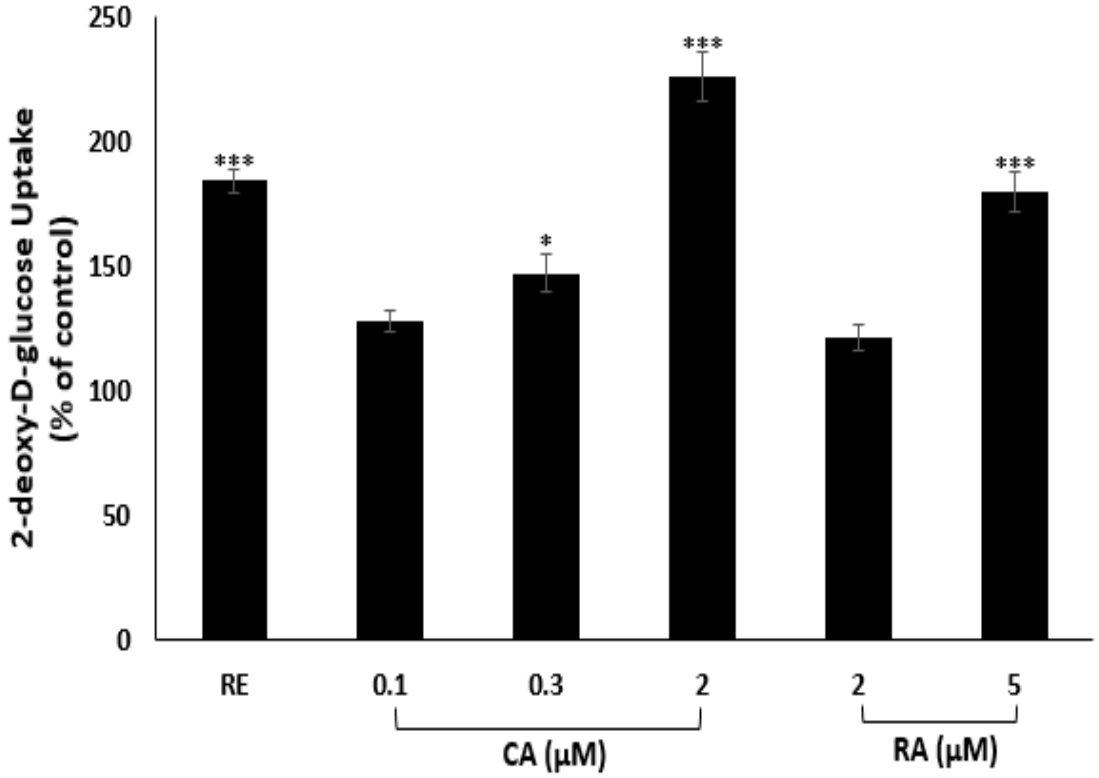

Figure 17: Effects of carnosic acid (CA) and rosmarinic acid (RA) on glucose uptake. Serum deprived L6 myotubes were incubated with 5 µg/ml RE, carnosic acid (CA) or rosmarinic acid (RA) at the indicated concentrations for 4 hours. 2-deoxy-D-glucose uptake was measured according to the methods. Data are expressed as percentage of control. Results are the mean ± SE of three to four independent experiments. *P<0.05, ***P<0.001 vs. control.

3.9 Effects of carnosic acid (CA) and rosmarinic acid (RA) on insulin-stimulated glucose uptake.

Next we investigated whether CA and RA affects insulin-stimulated glucose uptake. Myotubes were treated with or without 2.0 µM CA and 5.0 µM RA (4 hours) followed by treatment with the indicated concentrations of insulin for the last 30 minutes (Figure 18). Glucose uptake measurements were performed following treatments.

Insulin dose-dependently increased glucose uptake (157±9.29%, 161±7.92%, 188±11.45%, 203±9.5% of control, p<0.001) (Figure 18). RA significantly increased

insulin-stimulated glucose uptake at 3 nM insulin concentration (214±11.68% of control, p<0.01). RA did not increase insulin-stimulated glucose uptake at insulin concentrations of 1 nM, 10 nM, and 100 nM (179±2.33%, 210±12.86% and 203±10.17% of control, p>0.05). CA significantly increased insulin-stimulated glucose uptake at submaximal insulin concentrations (1 nM, 3 nM, 10 nM) (249±24.31%, 252±26.83%, 286±23.79% of control, p<0.001, p<0.05, p<0.05) (Figure 18) without a significant effect on the maximal insulin (100 nM) response (272±29.57% of control, p>0.05). These results indicate a potential of CA and RA to affect insulin-stimulated glucose uptake.

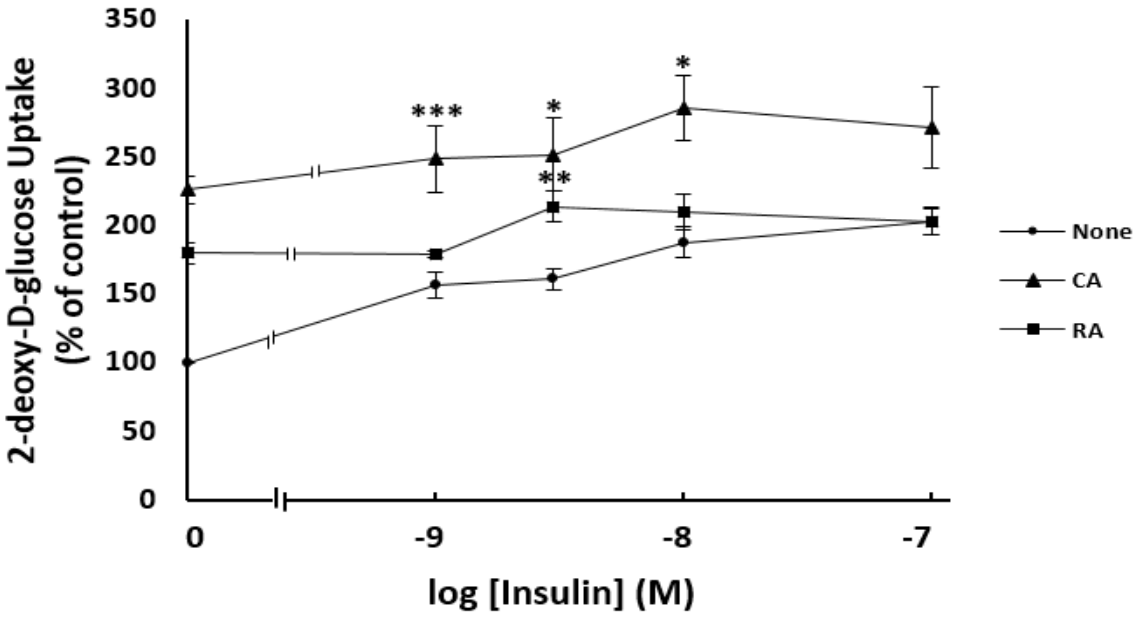

Figure 18: Effect of carnosic acid (CA) and rosmarinic acid (RA) on insulin-stimulated glucose uptake. Serum deprived L6 myotubes were incubated with 2.0 µM CA or 5.0 µM RA for 4 hours and then exposed to different insulin concentrations for the last 30 minutes followed by glucose uptake measurements. Data are expressed as percentage of control. Results are the mean ± SE of three to five independent experiments. *P<0.05, ** P<0.01, ***P<0.001 vs. insulin treatments alone.

3.10 Effects of wortmannin, the PI3K inhibitor, on carnosic acid (CA)- and rosmarinic acid (RA)-induced glucose uptake.

We investigated whether PI3K may be a mediator of CA-, and RA-stimulated glucose uptake by using the PI3K inhibitor, wortmannin. Myotubes were pre-treated with 100 nM of wortmannin for 15 minutes followed by treatment with or without 2.0 µM CA and 5.0 µM RA (4 hours) or 100 nM insulin (30 minutes). After treatments, glucose uptake measurements were performed.

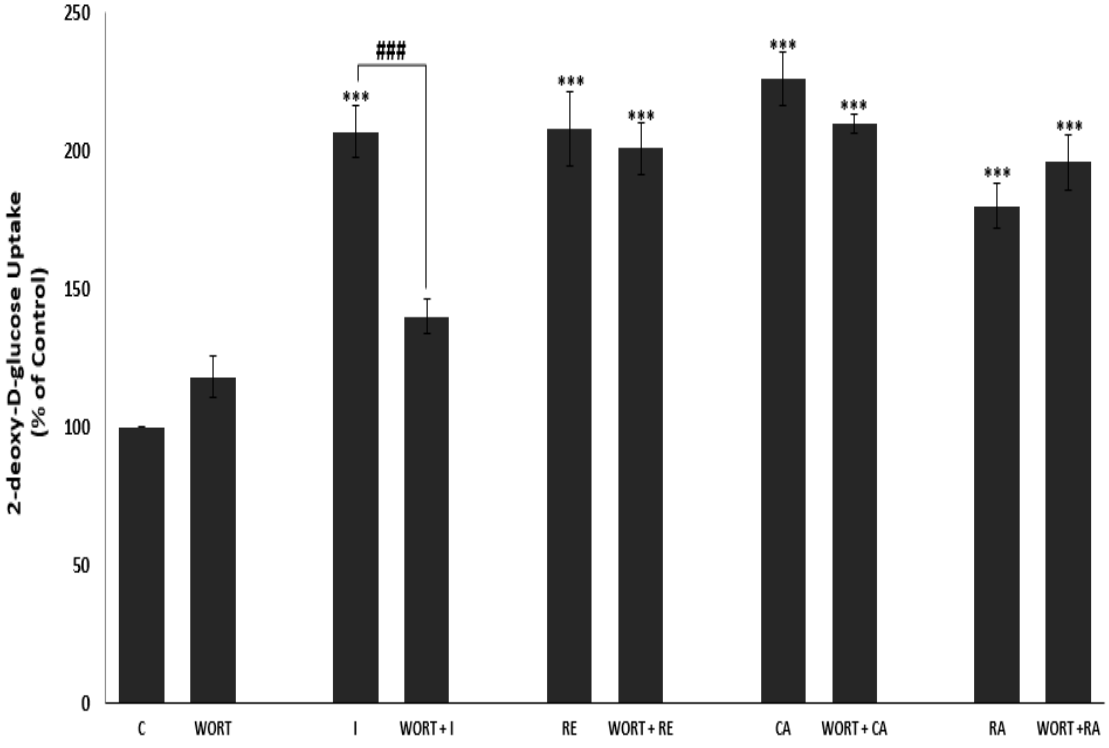

Figure 19: Effect of wortmannin on carnosic acid (CA) and rosmarinic acid (RA)-induced glucose transport. Cells were incubated in the absence or presence of 100 nM wortmannin (WORT) for 15 minutes followed by the addition of 100nM insulin for 30 minutes, 2.0 µM CA, or 5.0 µM RA for 4 hours. 2-deoxy-D-glucose uptake was measured according to the methods. Data are expressed as percentage of control. Results are the mean ± SE of six to seven independent experiments. ***P<0.001 vs. control. ###P<0.001 vs. treatments alone (without inhibitors).

In agreement with our data presented in figure 10, insulin significantly increased glucose uptake (210±9.47% of control, $p<0.001$), and this effect was significantly reduced by wortmannin pre-treatment (140±6.08% of control, $p<0.001$) (Figure 19). Similar to figure 10, RE significantly increased glucose uptake (208±13.62% of control, $p<0.001$) but this was not affected by wortmannin pretreatment (201±9.32% of control, $p>0.05$) (Figure 19). Furthermore, both CA (180±8.00% of control, $p<0.001$) and RA significantly increased glucose uptake (180±8.00% of control, $p<0.001$) and this effect was not altered by wortmannin (210±3.27%, 196±9.99% of control, $p>0.05$). These results suggest that PI3K is not involved in CA- and RA-induced glucose uptake.

3.11 Effects of carnosic acid (CA) and rosmarinic acid (RA) on Akt phosphorylation.

Next, we also examined the effects of CA and RA on Akt. As shown in figure 11 and 12, insulin treatment (100 nM for 15 minutes) strongly stimulated phosphorylation of Ser473 residue of Akt (260±11.5%, $p<0.05$) (Figure 20). However, CA and RA did not have effects on Akt phosphorylation (Figure 20). Metformin, AICAR, resveratrol and RE did not affect Akt phosphorylation (Figure 20). Total Akt levels were not changed by any treatment (Figure 20). These results indicate that the effect of CA and RA on glucose uptake is Akt-independent.

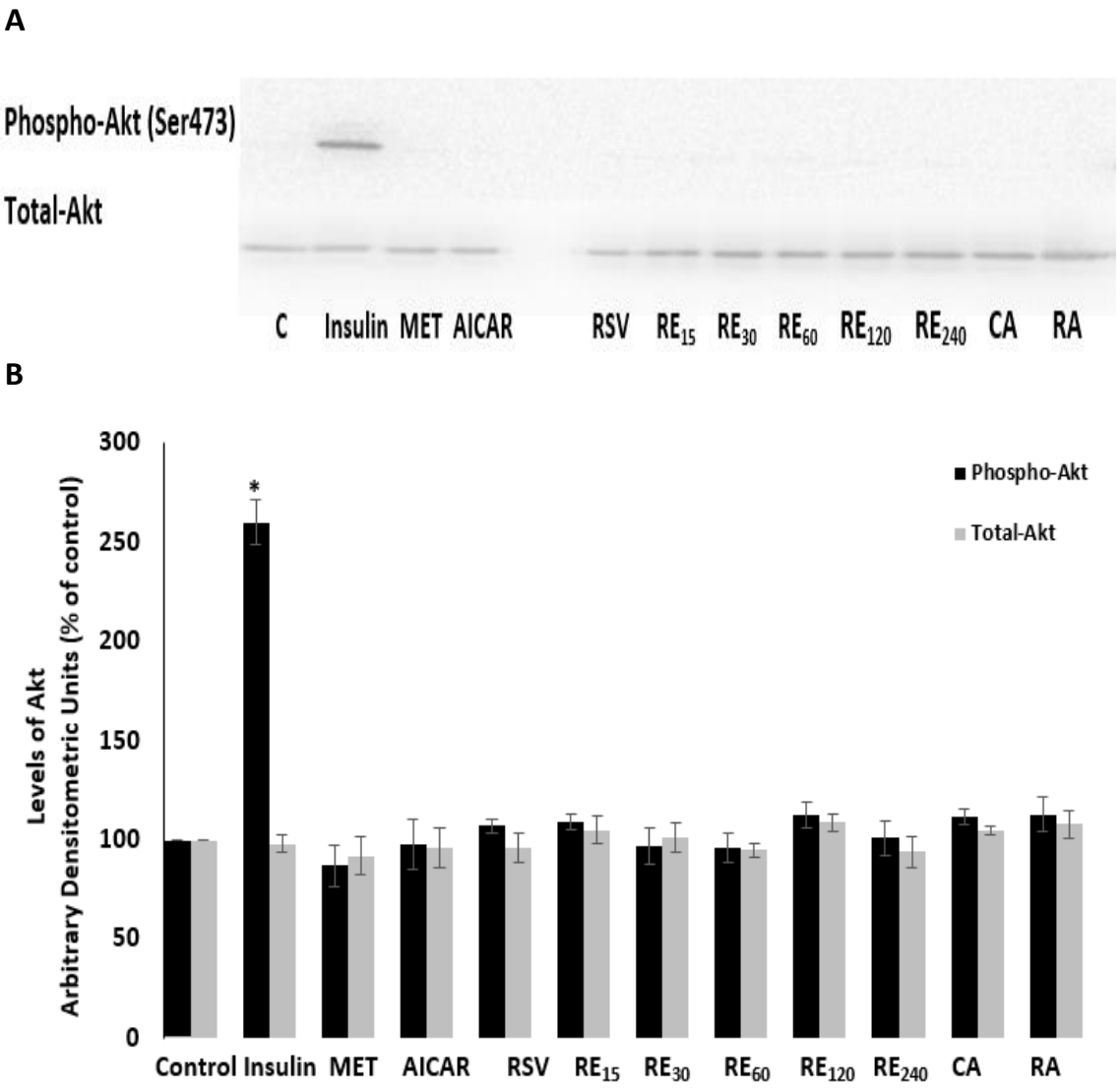

Figure 20: Effect of carnosic acid (CA) and rosmarinic acid (RA) on Akt phosphorylation. L6 myotubes were serum-deprived for 2 hours followed by treatement with 100 nM insulin (15 minutes), 2 mM metformin (MET) (120 minutes), 2mM AICAR (120 minutes), 100 µM resveratrol (RSV) (120 minutes), 5 µg/ml of RE (2 hours), 2.0 µM CA (2 hours) or 5.0 µM RA (2 hours). Whole cell lysates were prepared, resolved by SDS-PAGE and immunoblotted for specific antibodies that recognize total and phospho-Akt (Ser473) (A). Representative immunoblots. (B) Immunoblots were scanned to quantitate the density of the bands. Values are arbitrary densitometric units compared to control. Data are the mean ± SE of 3-4 experiments. *$p<0.05$ compared to untreated control.

3.12 Effects of compound C (CC), the AMPK inhibitor, on carnosic acid (CA) and rosmarinic acid (RA)-induced glucose uptake.

Metformin significantly increased glucose uptake (216±8.77% of control, p<0.001) and this effect was significantly reduced by pre-treatment with compound C (106±5.59% of control, p>0.05) (Figure 21) in agreement with our data in figure 13. CA significantly increased glucose uptake (226±9.62%, p<0.001) which was significantly inhibited by pre-treatment with compound C (160±10.0% of control, p<0.05, p<0.01 respectively). However, RA-stimulated increase in glucose uptake (180±8.0% of control, p<0.001) was not altered by compound C (158±3.32% of control, p>0.05). These results indicate that AMPK is involved in the regulation of glucose uptake by CA but not RA.

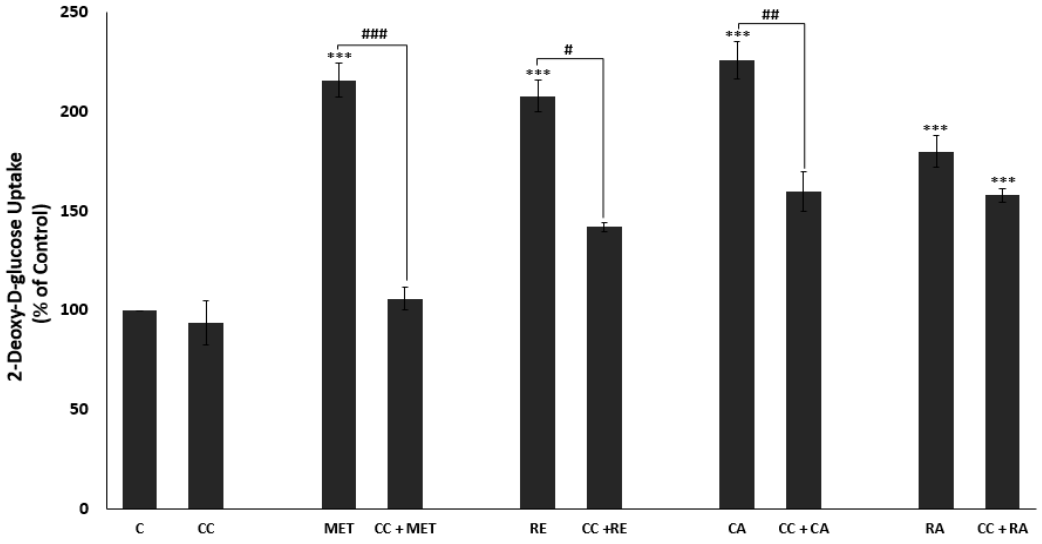

Figure 21: Effect of compound C (CC) on carnosic acid (CA) and rosmarinic acid (RA)-induced glucose transport. Cells were incubated in the absence or presence of 25 µM compound C (CC) for 30 minutes followed by the addition of 2mM metformin (2 hours), 2.0 µM CA, and 5.0 µM RA for 4 hours. 2-deoxy-D-glucose uptake was measured over a 10-minute period, using liquid scintillation counter. Readings are expressed as percentage increase of control. Results are the mean ± SE of six to seven independent experiments. ***P<0.001 vs. control. $^{###}$P<0.001 vs. treatments alone (without inhibitors).

3.13 Effects of carnosic acid (CA) and rosmarinic acid (RA) on AMPK phosphorylation

The effect of CA and RA on AMPK phosphorylation was examined. Metformin, AICAR and resveratrol significantly increased AMPK phosphorylation (196±27.5%, 238±28.4% and 212±29.3% of control, $p<0.05$) while insulin treatment did not have any effects (67±11.2% of control, $p>0.05$). RE treatment significantly increased AMPK phosphorylation (Figure 22). CA and RA treatment for 2 hours increased AMPK phosphorylation (164.0±12.7%, and 166.3±27.6% of control, $p<0.05$).

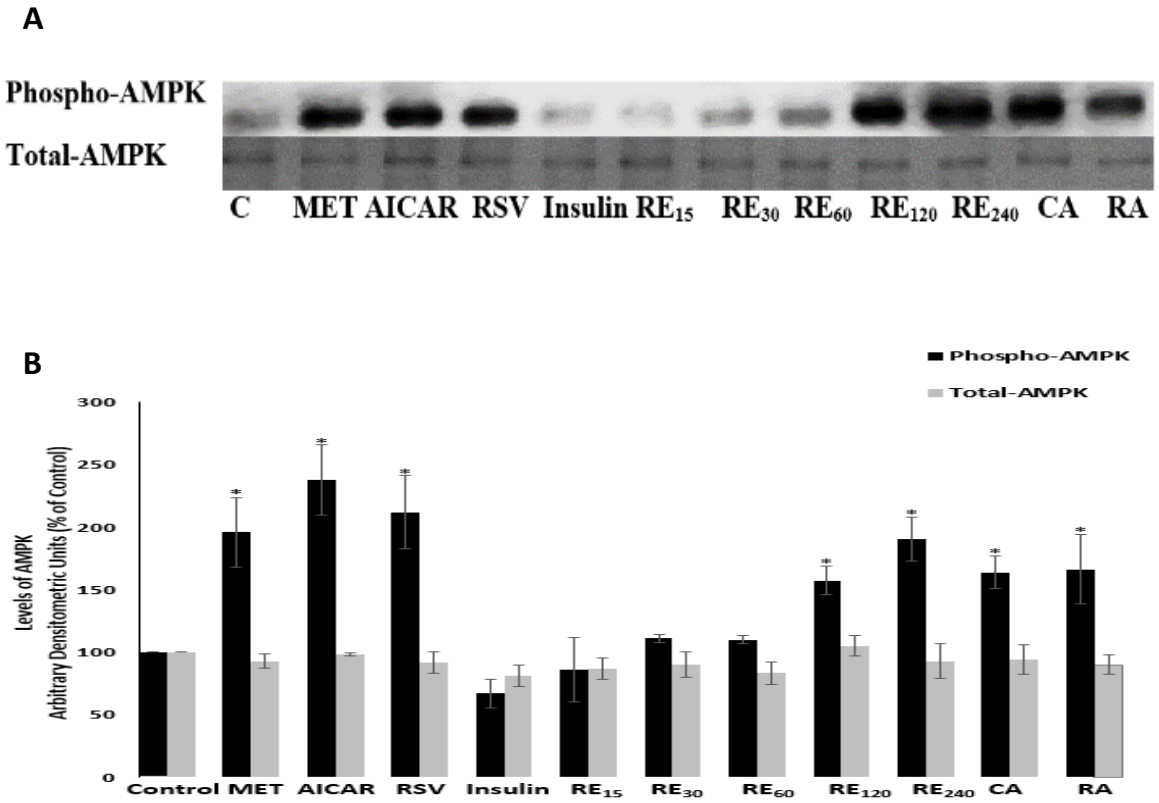

Figure 22: Effect of carnosic acid (CA) and rosmarinic acid (RA) on AMPK phosphorylation. L6 myotubes were treated with 2 mM metformin (MET) (120 minutes), 2 mM AICAR (2 hours), 100 µM resveratrol (RSV) (120 minutes), 5 µg/ml of RE, 2.0 µM CA and 5.0 µM RA (2 hours). (A) Representative immunoblots. (B).Densitometry. Results are the mean± SE of 3-4 independent experiments *$p<0.05$ versus control.

3.14 Effects of RE and its polyphenolic constituents CA, and RA on GLUT4 translocation

Insulin-stimulated glucose transport requires GLUT4 translocation. To elucidate the mechanism by which RE and its polyphenolic constiuents CA and RA altered glucose uptake, we measured surface GLUT1 and GLUT4 levels under the various treatments. L6 GLUT1myc and GLUT4myc cells stably express GLUT1 or GLUT4 tagged with an exofacial c-myc epitope. GLUT1myc and GLUT4myc segregate, cycle and respond to insulin in a manner similar to endogenous GLUT4 (71). The amount of GLUT1myc and GLUT4myc incorporated into the plasma membrane was quantitated by immunologically labelling the myc epitope at the surface of intact cells.

Acute maximal insulin treatment stimulated GLUT4 translocation to 217±11.26% of untreated control cells ($p<0.001$) (Figure 23). Additionally, metformin (1 mM, 6 hours) treatment caused a significant increase in GLUT4myc number on the plasma membrane (175±7.18%, $p<0.001$). However, unlike insulin and metformin, RE treatment did not cause a significant increase in recruitment of GLUT4myc to the plasma membrane (106±3.71% of control, $p>0.05$) (Figure 23). These results suggest that RE-stimulated glucose uptake is not due to GLUT4 translocation. Although RE did not significantly affect GLUT4 recruitment to the plasma membrane, we wished to examine the effects of RE's major polyphenols, CA and RA on these parameters. Neither CA nor RA caused a significant increase in GLUT4 (113±3.53%, 115±2.86% of control, $p>0.05$) (Figure 23)

recruitment to the plasma membrane. These results indicate that RE-, CA- and RA-stimulated glucose uptake is not due to GLUT4 translocation.

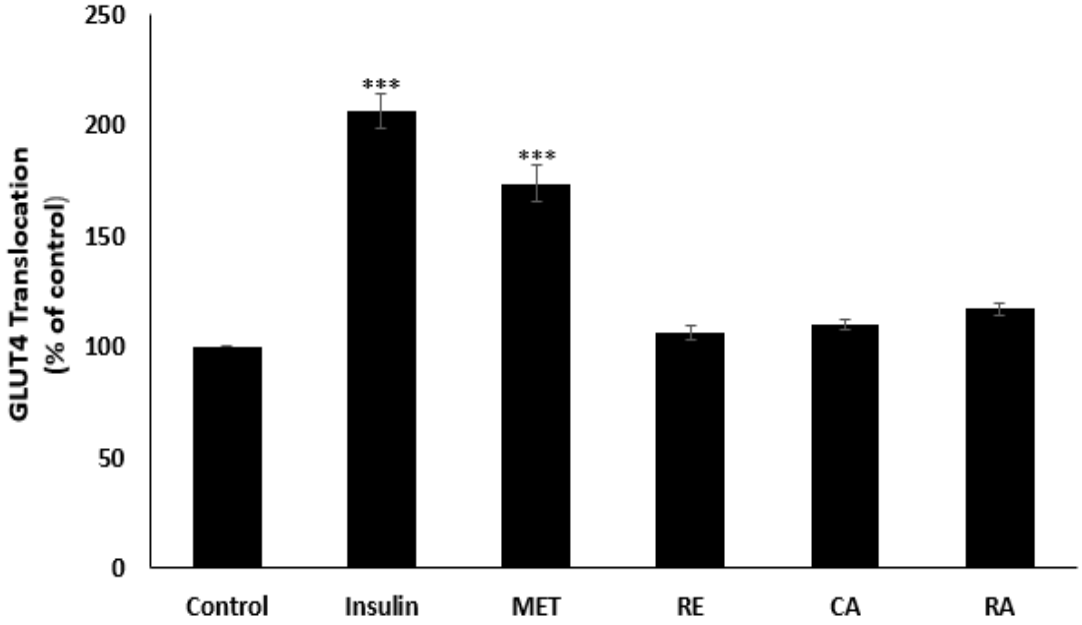

Figure 23: Effect of RE, CA, or RA on plasma membrane GLUT4 levels in GLUT4*myc* overexpressing myotubes. L6 GLUT4*myc* cells were treated with insulin (100 nM, 20 minutes), metformin (1 mM, 6 hours), RE (5µg/ml, 4 hours), CA (2.0 µM, 4 hours) or RA (5.0 µM, 4 hours) followed by GLUT4 transporter translocation measurements. Results are mean±SE of 6-8 independent experiments performed in triplicate and expressed as percentage of control. ***p<0.001 vs control.

3.15 Effects of RE and its polyphenolic constituents CA and RA on GLUT1 translocation

Skeletal muscle cells also express the basal glucose transporter isoform, GLUT1. Since RE and its polyphenolic constituents CA and RA did not affect the translocation of the insulin-sensitive glucose transporter, GLUT4, we wished to examine the effects of these treatments on GLUT1 translocation.

Acute maximal insulin (10^{-7} M, 20 minutes) stimulation alone significantly increased the amount of GLUT1myc epitope at the surface of intact cells to 139±1.44% of

untreated control cells ($p<0.001$) (Figure 24). Metformin (1 mM, 6 hours) treatment also caused a significant increase in GLUT1 recruitment to the plasma membrane (134±7.8% of control, $p<0.001$). However, unlike that of insulin, RE (5 µg/ml, 4 hours) did not cause a significant increase in recruitment of GLUT1myc to the plasma membrane (113±5.52% of control, $p>0.05$) (Figure 24). Furthermore, neither CA nor RA caused a significant increase in GLUT1 (114±4.14%, 116±2.51% of control, $p>0.05$) (Figure 24) recruitment to the plasma membrane. These results indicate that RE-, CA- and RA-stimulated glucose uptake is not due to GLUT1 translocation.

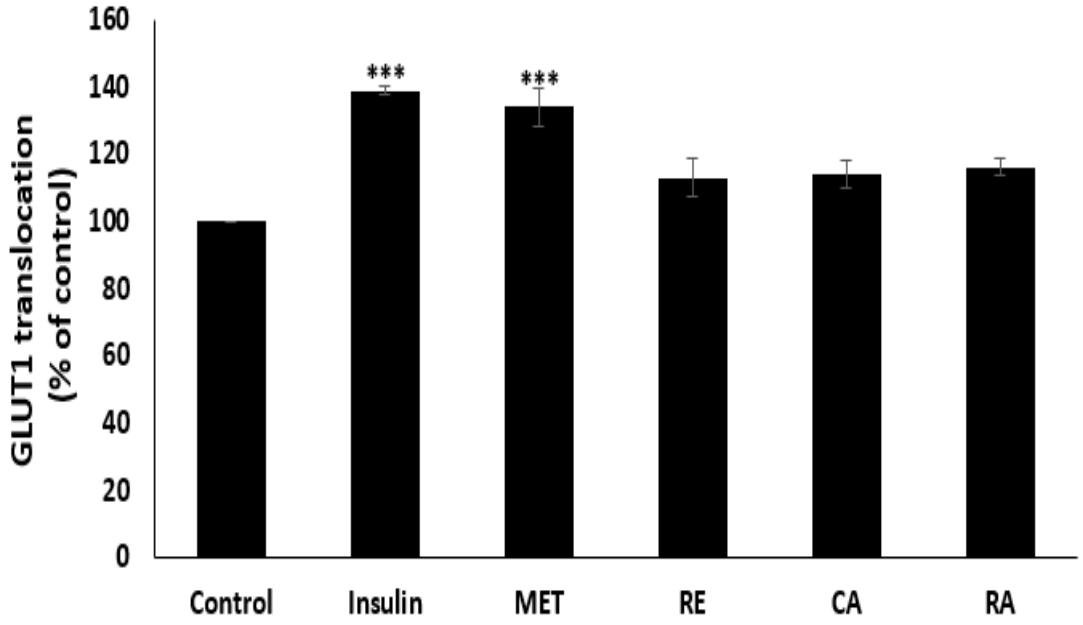

Figure 24: Effect of RE, CA and RA on plasma membrane GLUT1 in GLUT1*myc* overexpressing myotubes. L6 GLUT1*myc* cells were treated with insulin (100 nM, 20 minutes), metformin (1 mM, 6 hours), RE (5µg/ml, 4 hours), CA (2.0 µM, 4 hours) or RA (5.0 µM, 4 hours) followed by GLUT1 transporter translocation measurements. Results are mean±SE of 6-8 independent experiments, ***$p<0.001$ vs. control.

3.16 Effect of RE and its polyphenolic constituents CA and RA on glucose uptake in GLUT4myc overexpressing cells.

Since RE-, CA- and RA-stimulated glucose transport was observed in parental L6 cells and GLUT4 translocation was examined in GLUT4myc overexpressing cells, it was critical to examine whether RE, CA and RA also stimulated glucose uptake in a similar fashion in the GLUT4myc tagged cell line. We measured insulin-, metformin-, RE-, CA- and RA-stimulated glucose transport in overexpressing GLUT4myc tagged cells.

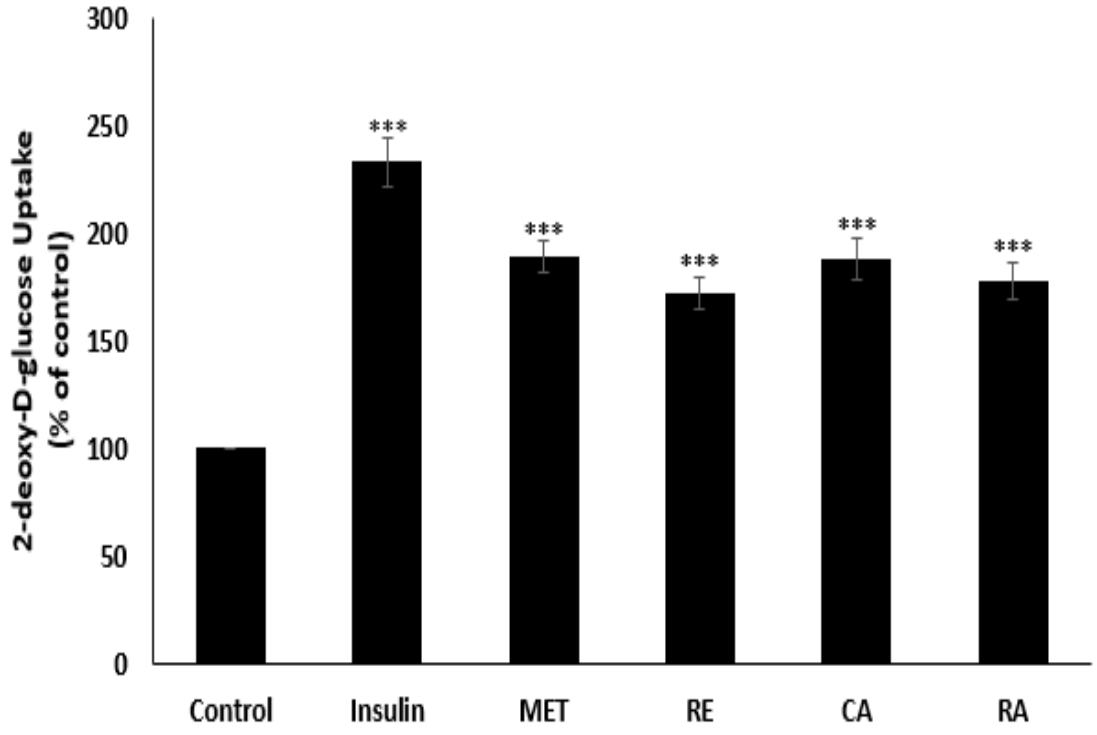

Figure 25: Effects of rosemary extract (RE), carnosic acid (CA), and rosmarinic acid (RA) on glucose uptake in L6 GLUT4myc tagged myotubes. GLUT4myc overexpressing myotubes were incubated with insulin (100 nM, 30 minutes), metformin (2 mM, 2 hours), RE (5 µg/ml, 4 hours), CA (2.0 µM, 4 hours) or RA (5.0 µM, 4 hours) 2-deoxy-D-glucose uptake was measured according to the methods. Results are the mean ±SE of 3-4 independent experiments. ***p<0.001 versus control.

As previously seen in the parental L6 cell line, insulin (10^{-7}M, 30 min) induced a 2-fold increase in glucose transport (233 ± 11.7% of control, p<0.001) in GLUT4myc overexpressing L6 cells (Figure 25). Additionally, metformin significantly increased glucose transport (189±7.36% of control, p<0.001). Treatment with RE (5 µg/ml, 4 hours) did result in a significant increase in glucose uptake (172±7.19% of control, p<0.001) (Figure 25). Additionally, both CA and RA significantly stimulated glucose transport in GLUT4myc (188±10.0%, 178±8.62% of control, p<0.001). Take together, these results (Figure 23 & 25) indicate that RE and its polyphenolic constituents CA and RA significantly stimulate glucose uptake in L6 GLUT4myc cells by a mechanism that is independent of GLUT4 translocation.

3.17 Effect of RE and its polyphenolic constituents CA and RA on glucose uptake in GLUT1myc overexpressing cells

Similarly, since RE-, CA- and RA-stimulated glucose transport was observed in parental L6 cells and GLUT1 translocation was examined in GLUT1myc overexpressing cells, it was critical to examine whether RE, CA and RA also stimulated glucose uptake in a similar fashion in the GLUT1myc tagged cell line. We measured insulin-, metformin-, RE, CA, and RA-stimulated glucose transport in overexpressing GLUT1myc tagged cells.

As previously seen in the parental L6 cell line, insulin (10^{-7}M, 30 min) induced a nearly 2- fold increase in glucose transport (194± 14.2% of control, p<0.001) (Figure 26) in GLUT1myc overexpressing L6 cells which was comparable to the level seen in parental cells (207±5.26% of control, p<0.001) (Figure 8). Additionally, metformin significantly increased glucose transport (183±21.6% of control, p<0.001) (Figure 26). Treatment with

RE (5 µg/ml, 4 hours) did result in a significant increase in glucose uptake (167±8.82% of control, p<0.001) (Figure 26). Both CA (2.0 µM, 4 hours) and RA (5.0 µM, 4 hours) significantly stimulated glucose transport in GLUT1myc cells (201±9.87%, 154±6.35% of control, p<0.001). Take together, these results (Figure 24 & 26) indicate that RE and its polyphenolic constituents CA and RA significantly stimulate glucose uptake in L6 GLUT1myc cells by a mechanism that is independent of GLUT1 translocation.

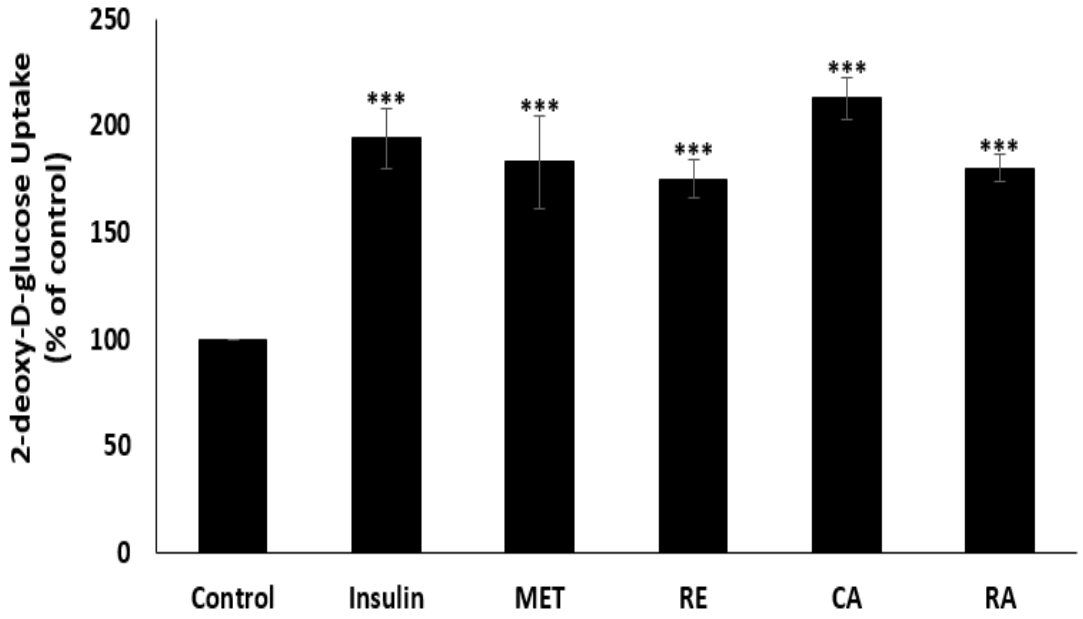

Figure 26: Effects of rosemary extract (RE), carnosic acid (CA) and rosmarinic acid (RA) on glucose uptake in L6 GLUT1*myc* tagged myotubes GLUT1myc overexpressing myotubes were incubated with insulin (100 nM, 30 minutes), metformin (2 mM, 2 hours), RE (5 µg/ml, 4 hours), CA (2.0 µM, 4 hours) or RA (5.0 µM, 4 hours) 2-deoxy-D-glucose uptake was measured according to the methods. Results are the mean ±SE of 3-4 independent experiments. ***p<0.001 versus control.

Chapter 4: Discussion

4.1 Rosemary extract significantly increases skeletal muscle glucose uptake.

Skeletal muscle is responsible for 75-80% of total body glucose uptake and disposal in the postprandial state; therefore, from a quantitative standpoint, it represents a major tissue in glucose homeostasis (13,15,28). Glucose enters skeletal muscle by facilitated transport mediated by the family of plasma membrane proteins, glucose transporters (GLUTs). These GLUTs recycle between intracellular compartments and the plasma membrane (2). Insulin acts on skeletal muscle and increases glucose uptake in this tissue by increasing plasma membrane availability of the specific GLUT isoform, GLUT4. The PI3K-Akt pathway, which is utilized by insulin, is a well-established pathway involved in the regulation of skeletal muscle glucose transport. The failure of skeletal muscle to respond to insulin, termed skeletal muscle insulin resistance (IR), largely contributes to manifestation of chronically elevated plasma glucose levels (hyperglycemia), and type 2 diabetes (T2DM). The underlying cellular mechanism of skeletal muscle IR is an attenuated PI3K-Akt signaling (15). Various anti-diabetogenic stimuli such as exercise, and the oral anti-diabetic drug, metformin increase skeletal muscle glucose uptake by utilizing an insulin-independent (PI3K-Akt independent) pathway. It is well-established that both exercise and metformin-induced increase in skeletal muscle glucose uptake is mediated by the AMPK pathway (86,248). This pathway is known to regulate glucose and lipid metabolism and act as an energy sensor for the cell. Apart from these two factors, certain polyphenols have been demonstrated to increase skeletal muscle

glucose transport. Resveratrol, a polyphenol found in red wine, and naringenin, a polyphenol found in citrus fruits, have been shown to increase skeletal muscle glucose transport *in vitro* (88,247). There are also numerous *in vivo* studies that strongly support the anti-hyperglycemic effects of resveratrol (89,240). Given that skeletal muscle glucose transport is an indispensable process involved in whole body glucose homeostasis and the consequent repercussions (hyperglycemia, T2DM) involved in the failure of this tissue to increase postprandial glucose uptake (insulin resistance), compounds that target this process provide a therapeutic value in this sense. Compeling evidence showing that polyphenols such as resveratrol and narigenin that have been shown to exhibit anti-hyperglycemic benefits, supports the need to explore other food components or herbs that may possess similar properties. Rosemary (*Rosmarinus officinalis*), an herb that is used extensively in the Mediterranean diet, has been reported to have bioactive properties as a potent antioxidant (refer to section 1.10.3) and anti-hyperglycemic agent (refer to section 1.10.6). Therefore, we sought to directly examine the effects of rosemary extract (RE) in skeletal muscle cells as well as explore the mechanisms involved.

In the present study, we used the rat L6 skeletal muscle cell line, which is a well-established model of skeletal muscle extensively used in studies of insulin signaling and glucose transport.

Our findings are the first to show that RE stimulates glucose uptake in L6 skeletal muscle cells and that this effect occurs in a dose- and time-dependent manner. This effect did not require the presence of insulin as the cells were incubated in media

without FBS and therefore without any insulin. Maximum stimulation was seen with 5 µg/ml and 10 µg/ml RE with 4 hours of incubation time. Doses higher than 10 µg/ml (20 µg/ml) did not result in any further increase. Microscopic examination of cells at concentrations ranging from 0.1 to 50 µM of RE tested did not show observable changes in cell morphology or viability indicating a low *in vitro* cytotoxicity profile of RE. Additionally, there were no reported changes in cell morphology in response to longer (6-16 hours) incubation times with 5 µg/ml RE. Although no microscopic evidence of toxicity were observed at RE concentrations of 30-50 µg/ml, the lack of stimulation of glucose uptake may indicate an excessive pharmacological dose with possible associated cytotoxic effects and therefore such high doses are not recommended to be used in future studies. Future studies could employ the lactate dehydrogenase (LDH) assay or the MTT assay to further substantiate the cytotoxicity characteristics of RE and its polyphenols carnosic acid and rosmarinic acid.

RE increased glucose uptake in myotubes in a time-dependent manner. Within 2 hours, RE (5 µg/ml concentration) significantly increased glucose uptake in myotubes which continued to increase at 4 and 6 hours. Longer incubation with RE (16 hours) did not result in any further increase in glucose uptake. Our observation that longer exposure (16 hours) of myotubes to RE resulted in attenuation of glucose uptake compared to a 4 hour time point may be explained by initiation of intracellular negative feedback mechanisms that tend to reduce glucose uptake.

Interestingly, the increase in glucose uptake with RE was similar to that seen with maximum insulin stimulation. Additionally, the extent of RE-induced glucose uptake was

comparable to the oral anti-diabetic drug, metformin. This is the first study to report the novel finding that RE increases glucose uptake in myotubes to levels comparable to insulin and metformin. RE required a longer incubation time to increase glucose uptake to levels comparable to those reached by maximum insulin stimulation. It is possible that this time-dependent action of RE on glucose uptake is due to RE utilizing a different signaling cascade than that of insulin. Interestingly, the effects of RE are similar to metformin, a drug stimulates glucose uptake by activating an insulin-independent signaling cascade and has a kinetically prolonged onset of action in comparison to insulin.

Upon finding that RE enhances basal glucose uptake, the effect of RE on insulin-stimulated glucose uptake was assessed. Interestingly, RE did not lead to significant increases in insulin-stimulated glucose uptake suggesting that RE- and insulin-stimulated pathways may converge at some point.

Previous *in vivo* studies have demonstrated that RE protects against hyperlipidemia and hyperglycemia in genetic, chemically-induced and dietary animal models of obesity and T2DM. Daily administration of RE significantly improved plasma glucose levels in streptozotocin (STZ)-induced diabetic rats (210,223,229); and in alloxan-induced diabetic rats (233) and rabbits (211). In genetically obese mice, carnosic acid, a polyphenolic component of RE protected against fat-induced fasting and non-fasting hyperglycemia and hyperlipidemia (189). Similarly, in a dietary rodent model of obesity, RE significantly protected against high-fat diet (HFD) induced elevations in plasma glucose and total cholesterol levels (190). Collectively, these studies (refer to Table 5)

demonstrate RE's *in vivo* anti-hyperglycemic properties. However, there are currently no studies that delineate the mechanism underlying the reported *in vivo* effects of RE. Our *in vitro* study for the first time shows a direct effect of RE in skeletal muscle and suggest that the *in vivo* anti-hyperglycemic effects of RE may be due to its direct effect on skeletal muscle glucose uptake.

Rosemary contains various subsets of polyphenols including phenolic diterpenes, phenolic triterpenes and flavonoids (178,179,182,183). The major polyphenols found in rosemary are carnosic acid (CA), carnosol (COH) and rosmarinic acid (RA). It has been reported that CA and COH are found at 1.5-5.0% in rosemary (214,249); and RA is found at 0.3-30.0% (184,186). These chemical compounds have been demonstrated to exert antioxidant properties (refer to section 1.10.3). Since rosemary extract (RE) was shown in this study to increase skeletal muscle glucose uptake, we wished to determine whether this effect of RE was attributable to the effects of its major polyphenols on skeletal muscle glucose uptake. Therefore, we sought to determine the relative concentration of CA and RA in the rosemary extract (RE) used in the present study. High performance liquid chromatography analysis of RE indicated that it contained approximately 2.12±0.22% of CA and 13.39±0.23% of RA. These concentrations of CA and RA are well within the range of previously reported concentrations from other studies (178,179,183,206,249,250). CA and RA separately prepared in DMSO were exposed to cells. Both CA and RA significantly increased glucose uptake in skeletal muscle cells at concentrations corresponding to that found in the whole rosemary extract (RE). Higher concentrations of CA and RA had an even greater effect on skeletal

muscle glucose uptake. These novel findings indicate that polyphenolic compounds found in RE increase skeletal muscle glucose uptake and possess anti-hyperglycemic properties. Moreover, it also suggests that the positive effects of RE on skeletal muscle glucose uptake is attributable to its polyphenolic components. Interestingly, the degree of glucose uptake in myotubes elicited by RE treatment was greater than CA and RA alone which suggests that CA and RA may be acting on a mutual signaling pathway which is stimulated more so in the presence of both CA and RA rather than these bioactive compounds alone. Additionally, microscopic examination of cells did not indicate signs of cytotoxicity with all concentrations of CA and RA tested. Notably, an *in vitro* study examining the cytotoxicity of CA in human hepatocytes reported that 50 to 100 µM CA treatment for 24 hours appears to be cytotoxic causing nuclei to be not observed, cytoplasm to become granular and filled with vacuoles, and cause changes in cell morphology (221). The cell viability EC_{50} for CA was determined to be 95 µM with 24 hour incubation in human hepatocytes. Futhermore, Dickman's study also reported that CA at concentrations of ≥ 50 µM to decreased intracellular ATP levels without affecting caspase3/7 activity and lactate dehydrogenase (LDH) release which led authors to conclude that CA may be acting as a mitochondrial toxin (221). These levels (50-100 µM) of CA are much higher than those used in the present study and therefore this is in support of the observation that cell viability was not affected in the present study. On the other hand, an *in vivo* 30-day toxicity study determined that 150-300 mg/kg body weight of CA treatment did not have adverse effects on histopathological and hematological factors in the rat and concluded that CA has a low oral toxicity profile

(216). Furthermore, the acute, median lethal dose (LD_{50}) for CA was determined to be 7100 mg/kg body weight (216).

We also examined the effects of CA and RA on insulin-stimulated glucose uptake. Based on the observation that higher concentrations of CA and RA had a greater effect on basal skeletal muscle glucose uptake compared to concentrations of CA and RA found in RE, we chose to use the former concentrations to determine whether these polyphenolic compounds have an effect on insulin-stimulated glucose uptake. It should be noted that these concentrations of CA and RA have been found in extracts of rosemary by others (176,178,179,182,183,206). This is the first study to report that both CA and RA significantly increased insulin-stimulated glucose uptake. This finding indicates that CA and RA, major polyphenolic components of RE, possess insulin-sensitizing properties and deserve further extensive investigation *in vivo*.

4.2 Elucidating the mechanism of action of RE and its bioactive compounds

Insulin activates the PI3K-Akt pathway in target tissues and the phosphorylation of the proximal enzyme Akt leads to increased GLUT4-containing vesicles translocation which results in greater plasma membrane availability of GLUT4 and increased glucose uptake (15,71). In this study, we examined the potential role of PI3K, a lipid kinase situated upstream of Akt, in mediating the effects of RE and its bioactive compounds CA, and RA. In order to do this, we used wortmannin, which is a microbial secondary metabolite that irreversibly inhibits PI3K (128). Our results indicated that the effect of RE and its bioactive compounds on glucose uptake is PI3K independent since inhibition of PI3K by

wortmannin did not affect RE-, CA- or RA-stimulated glucose uptake while insulin-stimulated glucose uptake was significantly reduced. We further examined the effect of RE and its bioactive compounds on Akt phosphorylation. Full activation of Akt requires phosphorylation of its residues Thr308 and Ser473 and as a result phosphorylation of Akt at either of these residues has been generally accepted as an indication of Akt activation (15). In contrast to insulin, neither RE nor its bioactive compounds, CA and RA, induced Akt phosphorylation. These data indicate that the PI3K-Akt pathway is not involved in RE-, CA- and RA-induced glucose uptake. Studies with resveratrol, another polyphenol, have demonstrated that it increases glucose uptake in L6 myotubes (88) in an Akt-independent manner. Similarly, the polyphenol narigenin was shown to increase glucose uptake in L6 myotubes in an Akt-independent manner (247). Our data indicate that RE and its bioactive compounds CA and RA have similar effects on skeletal muscle glucose uptake to that of resveratrol and narigenin and these effects are achieved in a PI3K-Akt independent manner.

An alternative way of stimulating glucose uptake in skeletal muscle is through activation of AMPK. AMPK is a serine/threonine kinase and activation of this enzyme requires phosphorylation at its Thr172 residue which has been acknowledged as indication of its activation (67). Activators of AMPK include an increase in intracellular AMP: ATP ratio and its upstream kinases LKB1 and CaMKK (38). We report here that RE increased AMPK phosphorylation in a time-dependent manner in skeletal muscle cells. We also found that CA and RA significantly increased AMPK phosphorylation/activation in skeletal muscle cells. Furthermore, inhibition of AMPK with compound C (an ATP-

competitive inhibitor of AMPK) significantly reduced RE- and CA-stimulated skeletal muscle glucose uptake while RA-induced glucose uptake was unaffected. These results indicate that AMPK is involved in RE-stimulated glucose uptake. While, both CA and RA activate AMPK, AMPK appears to be involved in CA-stimulated glucose uptake however, RA does not require AMPK to increase skeletal muscle glucose uptake. Previously, an *in vitro* study demonstrated that RE increased AMPK phosphorylation in hepatocytes (226). Similarly, carnosic acid was shown to activate AMPK in hepatocytes in a time-dependent manner (189). Our present *in vitro* study for the first time shows that RE and its bioactive compounds CA and RA increased AMPK phosphorylation in skeletal muscle. In particular, compound C did not alter RA-stimulated glucose uptake indicating that AMPK may not be involved in its action on the glucose transport in skeletal muscle cells. The role of AMPK in RE, CA and RA stimulated glucose uptake could be strengthened by small interference RNA (siRNA) knockdown and/or dominant negative AMPK mutants in order to confirm or rule out its involvement. Furthermore, RA may affect other well-established signalling molecules that regulate glucose uptake such as protein kinase C (PKC), the CAP/Cbl pathway, or p38 mitogen activated protein kinase (p38 MAPK) which has been shown to regulate GLUT4 activation in L6 myotubes and 3T3-L1 adipocytes (251,252). Future studies could investigate the effects of RE and its major polyphenols on the abovementioned signaling molecules with the western blotting technique.

Given that AMPK activation can occur by increased AMP: ATP ratio, and upstream kinases including LKB1 and CaMKK, it will be important to determine whether the bioactive compounds found in RE affect any of these mechanisms in leading to

increased activity of AMPK. Currently, there are no reported studies examining the effects of RE's or its bioactive compounds on the mechanism of AMPK activation. RE or its bioactive compounds CA and RA may allosterically modulate AMPK activity, increase the activity of upstream kinases (LKB1 and CaMKK) (41), or alternatively cause an increase in the AMP: ATP ratio secondary to inhibition of the mitochondrial complex 1 (78,86,253). Indeed, metformin, an anti-diabetic drug, has been demonstrated to activate AMPK by inhibiting the mitochondrial complex 1 (85,254).

As mentioned before, skeletal muscle glucose uptake is mediated by the glucose transporters (GLUTs). During basal conditions, GLUT1 is predominantly responsible for transporting glucose in skeletal muscle (2). On the other hand, GLUT4 becomes the major glucose transporter in skeletal muscle in response to insulin (2,76). The degree of skeletal muscle glucose uptake dictated by the GLUTs is determined by a combination of regulatory mechanism including GLUTs intrinsic activity, translocation and stability (half-life) (3). Since we report that RE and its bioactive compounds CA and RA increase skeletal muscle glucose uptake, we sought to determine their effects on GLUT1 and GLUT4 translocation. These transporters are expressed in L6 myotubes and have been shown to be affected by insulin and metformin. We measured surface GLUT1 and GLUT4 levels with L6 GLUT1myc and GLUT4myc cells that stably express GLUT1 or GLUT4 respectively, tagged with an exofacial myc epitope. The amount of GLUT1myc and GLUT4myc incorporated into the plasma membrane was quantitated by immunologically labelling the myc epitope at the surface of intact cells.

To date, the study of GLUTs translocation has been performed using subcellular fractionation, immunodetection by light and electron microscopy or GLUT photolabelling (255). These methodological approaches however are limited in providing an accurate quantification of GLUT translocation due to low yield of plasma membrane of treated cells and incomplete separation of the individual membrane compartments. Furthermore, fractionation does not distinguish between GLUT vesicles incorporated into the plasma membrane from those docked but unfused or occluded (256). These shortcomings are circumvented with the use of the L6 cell line expressing GLUTs harboring a myc epitope in the exofacial loop of the transporter at the cell surface of intact cells which can be detected using immunofluorescent and immunochemical labelling techniques of the myc epitope. To note, the intracellular distribution, recycling, exocytotic and endocytotic rates and insulin-response of GLUTmyc are identical to those of GLUT (255). Furthermore, this system enables the direct comparision of the fold GLUTs translocation with the fold stimulation of glucose uptake in response to insulin and as a result facilitate predictions about the intrinsic activity of GLUTs (255,256).

First of all, insulin treatment stimulated GLUT1 and GLUT4 glucose transporter translocation in agreement with other studies in L6 myotubes (257-260), and human primary myotubes (261,262). RE and its major polyphenolic constituents CA and RA did not cause significant increases in GLUT1 and GLUT4 translocation despite significant increases in glucose transport by these treatements in GLUT1 and GLUT4 overexpressing cells. These findings indicate that RE-, CA- and RA-stimulated glucose uptake is not due

to GLUT1 or GLUT4 translocation. The dissociation of glucose transport and glucose transporter (GLUTs) translocation could suggest that RE and its polyphenolic constituents CA, and RA may have a sole or combined effect on 1) the intrinsic activity of the GLUT1 and GLUT4 transporters, 2) the intrinsic activity of other glucose transporters expressed in the L6 cell line (GLUT3), 3) the translocation of GLUT3 4) the stability/half life of the glucose transporters (GLUTs -1,-3, -4).

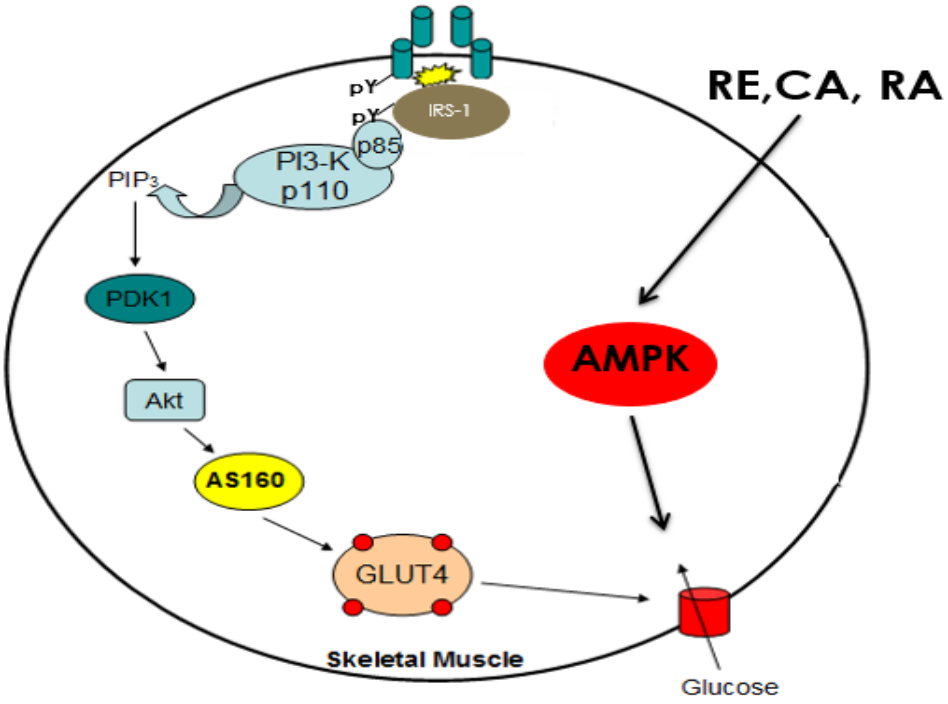

Figure 27: Schematic representation of the proposed *in vitro* mechanism of action of rosemary extract (RE) and its polyphenolic constituents, carnosic acid (CA) & rosmarinic acid (RA), on skeletal muscle glucose uptake. Akt (PKB), protein kinase B; AMPK, AMP-activated Kinase (heterotrimer αβγ subunits); AS160, Akt substrate of 160 kDa; GLUT4, glucose transporter; IRS, Insulin receptor substrate; PDK; phosphoinositide-dependent kinase-1; PI3K, phosphatidylinositol-3-kinase; PIP_3, phosphatidylinositol (3,4,5)-trisphosphate.

It is possible that RE and its polyphenolic constituents may affect the intrinsic activity of GLUTs (GLUT1, GLUT3, GLUT4) that are already present at the plasma membrane.

Alternatively, RE and its polyphenolic constituents may prolong the half-life of glucose transporters (GLUT1, GLUT3, GLUT4) by reducing the degradation rate and stabilizing GLUTs at the plasma membrane.

The increase in glucose uptake seen by RE, CA and RA in the present study may involve changes in hexokinase activity, a rate-limiting enzyme responsible for the initial phosphorylation of glucose and subsequent trapping of glucose inside the cell. This mechanism was reported to be utilized in myotubes which displayed increased glucose uptake in response to troglitazone, an antidiabetic drug belonging to the thiazolidediones class of drugs, whereby this drug caused activation of AMPK, secondary to alterations to the mitochondrial membrane potential, which was associated with increased glycolytic flux and increased hexokinase activity (245). It is possible that RE and its polyphenolic constituents CA and RA have an effect similar to troglitazone.

The bioavability of CA and RA have been reported in a limited number of studies. This information is relevant because these *in vivo* studies demonstrate that RE's major polyphenols, CA and RA, have significant *in vivo* bioavailibity as well as being detectable in tissues; and provide strong evidence for the *in vitro* findings that these polyphenols have significant effects on skeletal muscle cell glucose uptake. Intragastric administration of 90 mg/kg of CA in rats was determined to result in a bioavailability of 65% with a slow absorption (T_{max}=125.6 min), and maximum plasma concentration of 42 mg/L (263). The plasma half-life of CA was longer with intragastric (961 min) versus intravenous administration (68 min) (263). Another study showed a bioavailability of 40% in rats with intragastric administration of 65 mg/kg of CA with a maximum time

(T_{max}) of 137 min and maximum concentration (C_{max}) of 35 mg/L (264) which is in agreement with the previous study. CA was also detected in small intestines, as well as in liver and muscle tissue in trace amounts 24 hours post-administration (264). Furthermore, CA was predominantly found in free form in plasma and excreted in feces verus urine of animals (264). Furthermore, a recent *in vivo* study showed that oral administration of RE rich in CA at doses of 80-120 mg (29-49 mg CA) in the rat provides bioactive concentrations of CA and carnosol in the small and large intestines (up to several hundred μg/g), in the liver (1-15 μg/g) and in plasma (2-30 μM) (265). According to the European Food Safety Authority, the predicted maximal exposure to CA as a food additive is approximately 0.2 mg/kg body weight/day (266). Based on average body weight, total plasma volume, and 65% bioavailability, maximal plasma concentrations are calculated to approximately reach 3 nM (221). Therefore, the doses reported by Vaquero et al. (265) in rats, equivalent to a human dose of 50-100 mg of RE or 20-40 mg of CA/kg body weight per day, can only be attained through the consumption of nutraceuticals or supplements rich in these compounds. These doses are within the range of those established by the European Food Safety Authority as nonobserved adverse effect levels on 90 day feeding studies in rats (266).

In rats, oral administration of 50 mg/kg body weight of RA reaches maximum plasma concentration of 4.63 μM post 30 minutes and is found in free, methylated and conjugated forms of RA as well as its metabolites including caffeic acid, ferulic acid, and *m*-courmaric acid and are excreted in urine (267). Similarly, RA reached maximum serum concentration of 1.36 μM (0.5 mg/L) post 10 minutes in rats administered 100 μmol/kg

(36 mg/kg) body weight (268). In healthy men, single intake of perilla extract containing 200 mg of RA, RA was detected in plasma 30 minutes post-intake with total RA reaching maximum plasma concentrations of 0.87-1.43 μM (267). Furthermore, metabolites of RA including caffeic acid, ferulic acid, and coumaric acid were detected in plasma and the main method of excretion was through the urinary route, (268). The relative potency of RA's metabolic derivatives as compared to RA itself remains to be determined.

The mechanism behind how CA and RA enter cells has not yet been directly examined. Nonetheless, extrapolations can be made from the chemical nature of these polyphenols. Since CA is a lipid-soluble molecule (177), it is possible that it may diffuse through the cell membrane and accumulate in the cytosol in this manner. In contrast, RA is a water-soluble molecule (250) and therefore, it may require a protein channel or transporter to enter the cell. Previous studies have indicated that RA is hydrolyzed neither chemically under the conditions of the gastrointestinal tract (GI) model nor by secreted enzymatic activity (lipase and pancreatic enzymes) but rather is degraded into its metabolic derivatives *m*-coumaric and hydroxylated phenylphropionic acids by gut microflora before absorption and metabolization (268,269). RA's metabolic derivatives were demonstrated to be absorbed and distributed within the body through the monocarboxylic acid transporter (MCT) (268,269). Additionally, it has been suggested that RA is absorbed in human intestinal Caco-2 cells through paracellular diffusion (270).

Based on the available data that RE and its bioactive compounds CA and RA both have a low toxicity profile and significant bioavailability, it would be important to study

the anti-hyperglycemic effects of these RE bioactive compounds *in vivo*. Although previous animal studies have shown that RE has anti-hyperglycemic effects, its mechanism of action was not determined. In the present study, we found that RE and its bioavailable polyphenolic compounds CA and RA increase skeletal muscle glucose uptake in a dose- and time-dependent manner. The reported improvements in plasma glucose levels of animals treated with RE could in fact be a result of RE's direct effects on skeletal muscle glucose uptake. Furthermore, we report that RE, CA and RA activate AMPK in skeletal muscle. RE and CA-stimulated glucose uptake requires AMPK activity which requires further investigation. It remains to be determined how RE's bioactive compounds lead to activation of AMPK.

4.3 Limitations and Future Directions

A limitation of the study is that RE contains various polyphenols which may be acting additively or synergistically to exert their effects and their identification and specific effects was not possible. Although, the effects of the major polyphenols found in RE, CA and RA, were tested on skeletal muscle glucose uptake, their combined effects were not assessed to determine whether they are acting additively or synergistically to exert their effects. Another limitation is that this study was done in an *in vitro* model of rat skeletal muscle which has limited applicability and generalizability to human skeletal muscle. Nonetheless, this particular skeletal muscle cell line is a well-established and extensively used *in vitro* model of skeletal muscle (41,44,241,271) and provides an appropriate, preliminary *in vitro* model for studying novel compounds with insulin-like effects.

It will be pertinent to examine the direct effects of RE, CA and RA in human skeletal muscle both *in vitro* and *in vivo*. Furthermore, the effects of RE, CA and RA could be evaluated in animals *in vivo* using tracer methods to examine if skeletal muscle glucose uptake is affected in response to these treatments.

Based on microscopic analysis, RE and its polyphenolic constituents CA and RA did not have adverse effects on cell morphology or viability. Future studies should assess the cytotoxicity effects of RE and its polyphenols CA and RA using the lactate dehydrogenase (LDH) assay or the [3-(4,5-Dimethylthiazol-2-yl)-2,5-Diphenyltetrazolium bromide (MTT) assay.

It was found that RE and its polyphenolic constituents CA and RA require AMPK in order to increase skeletal muscle glucose uptake which needs to be further confirmed with a small interference RNA (siRNA) approach. In addition, their effects on skeletal muscle glucose uptake could be assessed in cells deficient in AMPK (91). Neither RE nor its polyphenolic constituents (CA, RA) affected GLUT1 or GLUT4 plasma membrane translocation suggesting that they may be modulating these glucose transporters' intrinsic activity which needs to be examined. This potential effect could be determined by pretreating cells with indinavir, a chemical inhibitor of GLUT4, and determining the extent of glucose uptake in response to the various treatments compared to the control group (88,272). Cells would be pretreated with indinavir which would result in inhibiting glucose uptake through GLUT4 and this approach would enable the determination of the contributory roles of the different GLUT isoforms expressed in L6 cells (GLUT1, GLUT3, GLUT4) in increasing skeletal muscle cell glucose uptake in response to RE, CA

and RA. Additionally, studies examining the effects of RE, CA and RA on GLUT half-life could be performed in the future by using [35^{S}]-methionine labelling and glucose transporter immunoprecipitation (273). Furthermore, the effect of RE, CA and RA on GLUT3 translocation could be examined in the future using subcellular fractionation studies and an antibody specific for GLUT3. An alternative approach will be to create GLUT3myc overexpressing cells and employ enzyme-linked immunosorbent assay using anti-myc antibody to quantify cell surface GLUT3. In addition, GLUT1, GLUT3 and/or GLUT4 protein total membrane content should be measured using membrane fractionation and immunoblotting technique to determine whether RE and it's polyphenols CA and RA have effects on total protein expression of these glucose transporters.

It is important to note that the possibility exists that by having used [^{3}H]-2-deoxy-D-glucose, a non-metabolizable analogue of glucose, that can still be phosphorylated by hexokinase, the increases in glucose uptake in response to the various treatments may not solely be representative of glucose transport but glucose phosphorylation as well. The use of 3-*O*-methylglucose, which is a non-metabolizable glucose analogue that cannot be phosphorylated by hexokinase, in the future could provide a better insight in this matter. If an increase in 3-*O*-methylglucose uptake was observed, it would be solely attributable to glucose transport.

4.4 Summary/Conclusion

Skeletal muscle is important in glucose homeostasis and it is quantitatively the most important insulin-target tissue. Impaired insulin action in this tissue leads to insulin resistance and type 2 diabetes mellitus. In recent years, activation of the energy sensor, 5' AMP-activated kinase (AMPK), has been viewed as a targeted approach to counteract insulin resistance. Chemicals found in plant extracts such as polyphenols have attracted attention for their potential use for treating IR. Recent *in-vitro* and *in-vivo* studies indicate that rosemary extract (RE) has anti-diabetic properties, although its effects on muscle and exact mechanisms involved are not known.

In the present thesis, we examined the effects of RE and the mechanism of regulation of glucose uptake in skeletal muscle cells. RE stimulated glucose uptake in L6 myotubes in a dose- and time-dependent manner. Maximum stimulation was seen with 5 µg/ml of RE for 4 h (184±5.07% of control, $p<0.001$), a response comparable to maximum insulin stimulation (191±5.26% of control, $p<0.001$). Furthermore, carnosic acid (CA) and rosmarinic acid (RA), major polyphenols found in RE, increased glucose uptake indicating that these compounds may be responsible for the RE effects. RE along with CA, and RA did not affect Akt phosphorylation while significantly increasing AMPK phosphorylation. Furthermore, RE-, and CA-induced glucose uptake was significantly reduced by the AMPK inhibitor, compound C while remaining unchanged by the PI3K inhibitor, wortmannin. RE, CA and RA did not affect GLUT4 and GLUT1 plasma membrane translocation in L6 GLUT4myc and GLUT1myc overexpressing myotubes while glucose uptake in these cells was similar to the parental L6 cells signifying that

these treatments may be affecting the intrinsic activity of these glucose transporters, which will require further examination. Our study is the first to show a direct effect of RE and it polyphenolic constituents CA and RA on skeletal muscle glucose by a mechanism that involves AMPK activation. Our findings are very important and suggest a potential use of RE to regulate glucose homeostasis and counteract insulin resistance.

References

(1) Huang S, Czech MP. The GLUT4 glucose transporter. Cell metabolism 2007;5(4):237-252.

(2) Zhao FQ, Keating AF. Functional properties and genomics of glucose transporters. Curr Genomics 2007 Apr;8(2):113-128.

(3) Epstein FH, Shepherd PR, Kahn BB. Glucose transporters and insulin action—implications for insulin resistance and diabetes mellitus. N Engl J Med 1999;341(4):248-257.

(4) Bjorbaek C, Echwald SM, Hubricht P, Vestergaard H, Hansen T, Zierath J, et al. Genetic variants in promoters and coding regions of the muscle glycogen synthase and the insulin-responsive GLUT4 genes in NIDDM. Diabetes 1994 Aug;43(8):976-983.

(5) Buse JB, Yasuda K, Lay TP, Seo TS, Olson AL, Pessin JE, et al. Human GLUT4/muscle-fat glucose-transporter gene. Characterization and genetic variation. Diabetes 1992 Nov;41(11):1436-1445.

(6) Rea S, James DE. Moving GLUT4: the biogenesis and trafficking of GLUT4 storage vesicles. Diabetes 1997 Nov;46(11):1667-1677.

(7) Li J, Houseknecht KL, Stenbit AE, Katz EB, Charron MJ. Reduced glucose uptake precedes insulin signaling defects in adipocytes from heterozygous GLUT4 knockout mice. FASEB J 2000 Jun;14(9):1117-1125.

(8) Tsao TS, Stenbit AE, Factor SM, Chen W, Rossetti L, Charron MJ. Prevention of insulin resistance and diabetes in mice heterozygous for GLUT4 ablation by transgenic complementation of GLUT4 in skeletal muscle. Diabetes 1999 Apr;48(4):775-782.

(9) Zisman A, Peroni OD, Abel ED, Michael MD, Mauvais-Jarvis F, Lowell BB, et al. Targeted disruption of the glucose transporter 4 selectively in muscle causes insulin resistance and glucose intolerance. Nat Med 2000;6(8):924-928.

(10) Abel ED, Peroni O, Kim JK, Kim YB, Boss O, Hadro E, et al. Adipose selective targeting of the GLUT4 gene impairs insulin action in muscle and liver. Nature 2001;729:729-733.

(11) Ryder JW, Yang J, Galuska D, Rincon J, Bjornholm M, Krook A, et al. Use of a novel impermeable biotinylated photolabeling reagent to assess insulin- and hypoxia-stimulated cell surface GLUT4 content in skeletal muscle from type 2 diabetic patients. Diabetes 2000 Apr;49(4):647-654.

(12) Butler AE, Janson J, Bonner-Weir S, Ritzel R, Rizza RA, Butler PC. ß-Cell Deficit and Increased ß-Cell Apoptosis in Humans With Type 2 Diabetes. Diabetes 2003 January 01;52(1):102-110.

(13) Tripathy D, Chavez AO. Defects in insulin secretion and action in the pathogenesis of type 2 diabetes mellitus. Current diabetes reports 2010;10(3):184-191.

(14) White BA, Porterfield SP. Endocrine and Reproductive Physiology, Mosby Physiology Monograph Series (with Student Consult Online Access), 4: Endocrine and Reproductive Physiology. : Elsevier Health Sciences; 2013.

(15) Saltiel AR. New perspectives into the molecular pathogenesis and treatment of type 2 diabetes. Cell 2001;104(4):517-529.

(16) Leahy JL. Pathogenesis of type 2 diabetes mellitus. Arch Med Res 2005;36(3):197-209.

(17) Lencioni C, Lupi R, Del Prato S. β-cell failure in type 2 diabetes mellitus. Current diabetes reports 2008;8(3):179-184.

(18) Ferrannini E, Gastaldelli A, Miyazaki Y, Matsuda M, Mari A, DeFronzo RA. β-Cell function in subjects spanning the range from normal glucose tolerance to overt diabetes: a new analysis. The Journal of Clinical Endocrinology & Metabolism 2005;90(1):493-500.

(19) Kolterman OG, Gray RS, Griffin J, Burstein P, Insel J, Scarlett JA, et al. Receptor and postreceptor defects contribute to the insulin resistance in noninsulin-dependent diabetes mellitus. J Clin Invest 1981 Oct;68(4):957-969.

(20) Reaven G, Hollenbeck C, Chen Y. Relationship between glucose tolerance, insulin secretion, and insulin action in non-obese individuals with varying degrees of glucose tolerance. Diabetologia 1989;32(1):52-55.

(21) Pendergrass M, Bertoldo A, Bonadonna R, Nucci G, Mandarino L, Cobelli C, et al. Muscle glucose transport and phosphorylation in type 2 diabetic, obese nondiabetic, and genetically predisposed individuals. Am J Physiol Endocrinol Metab 2007 Jan;292(1):E92-100.

(22) Petersen KF, Shulman GI. Etiology of Insulin Resistance. Am J Med 2006 5;119(5, Supplement 1):S10-S16.

(23) DeFronzo RA. Pathogenesis of type 2 diabetes: metabolic and molecular implications for identifying diabetes genes. Diabetes reviews 1997;5(3):177-269.

(24) Bogardus C, Lillioja S, Stone K, Mott D. Correlation between muscle glycogen synthase activity and in vivo insulin action in man. J Clin Invest 1984 Apr;73(4):1185-1190.

(25) Shulman GI, Rothman DL, Jue T, Stein P, DeFronzo RA, Shulman RG. Quantitation of muscle glycogen synthesis in normal subjects and subjects with non-insulin-dependent diabetes by 13C nuclear magnetic resonance spectroscopy. N Engl J Med 1990;322(4):223-228.

(26) Cross DA, Alessi DR, Cohen P, Andjelkovich M, Hemmings BA. Inhibition of glycogen synthase kinase-3 by insulin mediated by protein kinase B. Nature 1995;378(6559):785-789.

(27) Brady MJ, Nairn AC, Saltiel AR. The regulation of glycogen synthase by protein phosphatase 1 in 3T3-L1 adipocytes. Evidence for a potential role for DARPP-32 in insulin action. J Biol Chem 1997 Nov 21;272(47):29698-29703.

(28) DeFronzo RA. Banting Lecture. From the triumvirate to the ominous octet: a new paradigm for the treatment of type 2 diabetes mellitus. Diabetes 2009 Apr;58(4):773-795.

(29) Bays HE, González-Campoy JM, Bray GA, Kitabchi AE, Bergman DA, Schorr AB, et al. Pathogenic potential of adipose tissue and metabolic consequences of adipocyte hypertrophy and increased visceral adiposity. 2008.

(30) Bonadonna RC, DeFronzo RA. Glucose metabolism in obesity and type 2 diabetes. Diabete Metab 1991 May;17(1 Pt 2):112-135.

(31) DeFronzo R. Dysfunctional fat cells, lipotoxicity and type 2 diabetes. Int J Clin Pract 2004;58(s143):9-21.

(32) Boden G. Role of Fatty Acids in the Pathogenesis of Insulin Resistance and NIDDM. Diabetes 1997 January 01;46(1):3-10.

(33) Saloranta C, Groop L. Interactions between glucose and FFA metabolism in man. Diabetes Metab 1996;12(1):15-36.

(34) Gastaldelli A, Baldi S, Pettiti M, Toschi E, Camastra S, Natali A, et al. Influence of obesity and type 2 diabetes on gluconeogenesis and glucose output in humans: a quantitative study. Diabetes 2000 August 01;49(8):1367-1373.

(35) McGarry JD. Banting Lecture 2001: Dysregulation of Fatty Acid Metabolism in the Etiology of Type 2 Diabetes. Diabetes 2002 January 01;51(1):7-18.

(36) Wellen KE, Hotamisligil GS. Inflammation, stress, and diabetes. J Clin Invest 2005 May;115(5):1111-1119.

(37) Marte BM, Downward J. PKB/Akt: connecting phosphoinositide 3-kinase to cell survival and beyond. Trends Biochem Sci 1997 9;22(9):355-358.

(38) Manning BD, Cantley LC. AKT/PKB Signaling: Navigating Downstream. Cell 2007 6/29;129(7):1261-1274.

(39) Vasudevan KM, Garraway LA. AKT signaling in physiology and disease. Phosphoinositide 3-kinase in Health and Disease: Springer; 2011. p. 105-133.

(40) Sakamoto K, Holman GD. Emerging role for AS160/TBC1D4 and TBC1D1 in the regulation of GLUT4 traffic. Am J Physiol Endocrinol Metab 2008 Jul;295(1):E29-37.

(41) Kramer HF, Witczak CA, Fujii N, Jessen N, Taylor EB, Arnolds DE, et al. Distinct Signals Regulate AS160 Phosphorylation in Response to Insulin, AICAR, and Contraction in Mouse Skeletal Muscle. Diabetes 2006 July 01;55(7):2067-2076.

(42) Matthaei S, Stumvoll M, Kellerer M, Haring H. Pathophysiology and Pharmacological Treatment of Insulin Resistance 1. Endocr Rev 2000;21(6):585-618.

(43) Hribal ML, Federici M, Porzio O, Lauro D, Borboni P, Accili D, et al. The Gly→ Arg972 Amino Acid Polymorphism in Insulin Receptor Substrate-1 Affects Glucose Metabolism in Skeletal Muscle Cells 1. The Journal of Clinical Endocrinology & Metabolism 2000;85(5):2004-2013.

(44) Huang C, Thirone ACP, Huang X, Klip A. Differential Contribution of Insulin Receptor Substrates 1 Versus 2 to Insulin Signaling and Glucose Uptake in L6 Myotubes. Journal of Biological Chemistry 2005 May 13;280(19):19426-19435.

(45) Vollenweider P, Ménard B, Nicod P. Insulin Resistance, Defective Insulin Receptor Substrate 2—Associated Phosphatidylinositol-3’ Kinase Activation, and Impaired Atypical Protein Kinase C (ζ/λ) Activation in Myotubes From Obese Patients With Impaired Glucose Tolerance. Diabetes 2002 April 01;51(4):1052-1059.

(46) Krook A, Björnholm M, Galuska D, Jiang XJ, Fahlman R, Myers MG, et al. Characterization of signal transduction and glucose transport in skeletal muscle from type 2 diabetic patients. Diabetes 2000 February 01;49(2):284-292.

(47) Withers DJ, Gutierrez JS, Towery H, Burks DJ, Ren J, Previs S, et al. Disruption of IRS-2 causes type 2 diabetes in mice. Nature 1998;391(6670):900-904.

(48) Kido Y, Burks DJ, Withers D, Bruning JC, Kahn CR, White MF, et al. Tissue-specific insulin resistance in mice with mutations in the insulin receptor, IRS-1, and IRS-2. J Clin Invest 2000 Jan;105(2):199-205.

(49) Goodyear LJ, Giorgino F, Sherman LA, Carey J, Smith RJ, Dohm GL. Insulin receptor phosphorylation, insulin receptor substrate-1 phosphorylation, and phosphatidylinositol 3-kinase activity are decreased in intact skeletal muscle strips from obese subjects. J Clin Invest 1995 May;95(5):2195-2204.

(50) Björnholm M, Kawano Y, Lehtihet M, Zierath JR. Insulin Receptor Substrate-1 Phosphorylation and Phosphatidylinositol 3-Kinase Activity in Skeletal Muscle From NIDDM Subjects After In Vivo Insulin Stimulation. Diabetes 1997 March 01;46(3):524-527.

(51) Pratipanawatr W, Pratipanawatr T, Cusi K, Berria R, Adams JM, Jenkinson CP, et al. Skeletal Muscle Insulin Resistance in Normoglycemic Subjects With a Strong Family History of Type 2 Diabetes Is Associated With Decreased Insulin-Stimulated Insulin Receptor Substrate-1 Tyrosine Phosphorylation. Diabetes 2001 November 01;50(11):2572-2578.

(52) Cheatham B, Vlahos CJ, Cheatham L, Wang L, Blenis J, Kahn CR. Phosphatidylinositol 3-kinase activation is required for insulin stimulation of pp70 S6 kinase, DNA synthesis, and glucose transporter translocation. Molecular and Cellular Biology 1994 July 01;14(7):4902-4911.

(53) Okada T, Kawano Y, Sakakibara T, Hazeki O, Ui M. Essential role of phosphatidylinositol 3-kinase in insulin-induced glucose transport and antilipolysis in rat adipocytes. Studies with a selective inhibitor wortmannin. Journal of Biological Chemistry 1994 February 04;269(5):3568-3573.

(54) Kahn SE. The importance of the β-cell in the pathogenesis of type 2 diabetes mellitus. Am J Med 2000 4/17;108(6, Supplement 1):2-8.

(55) Martin SS, Haruta T, Morris AJ, Klippel A, Williams LT, Olefsky JM. Activated Phosphatidylinositol 3-Kinase Is Sufficient to Mediate Actin Rearrangement and GLUT4 Translocation in 3T3-L1 Adipocytes. Journal of Biological Chemistry 1996 July 26;271(30):17605-17608.

(56) Katagiri H, Asano T, Ishihara H, Inukai K, Shibasaki Y, Kikuchi M, et al. Overexpression of catalytic subunit p110alpha of phosphatidylinositol 3-kinase increases glucose transport activity with translocation of glucose transporters in 3T3-L1 adipocytes. J Biol Chem 1996 Jul 19;271(29):16987-16990.

(57) Brachmann SM, Ueki K, Engelman JA, Kahn RC, Cantley LC. Phosphoinositide 3-Kinase Catalytic Subunit Deletion and Regulatory Subunit Deletion Have Opposite Effects on Insulin Sensitivity in Mice. Molecular and Cellular Biology 2005 March 01;25(5):1596-1607.

(58) Luo J, Sobkiw CL, Hirshman MF, Logsdon MN, Li TQ, Goodyear LJ, et al. Loss of class IA PI3K signaling in muscle leads to impaired muscle growth, insulin response, and hyperlipidemia. Cell Metabolism 2006 5;3(5):355-366.

(59) Bouzakri K, Roques M, Gual P, Espinosa S, Guebre-Egziabher F, Riou JP, et al. Reduced activation of phosphatidylinositol-3 kinase and increased serine 636 phosphorylation of insulin receptor substrate-1 in primary culture of skeletal muscle cells from patients with type 2 diabetes. Diabetes 2003 Jun;52(6):1319-1325.

(60) Kohn AD, Summers SA, Birnbaum MJ, Roth RA. Expression of a Constitutively Active Akt Ser/Thr Kinase in 3T3-L1 Adipocytes Stimulates Glucose Uptake and Glucose Transporter 4 Translocation. Journal of Biological Chemistry 1996 December 06;271(49):31372-31378.

(61) Katome T, Obata T, Matsushima R, Masuyama N, Cantley LC, Gotoh Y, et al. Use of RNA Interference-mediated Gene Silencing and Adenoviral Overexpression to Elucidate the Roles of AKT/Protein Kinase B Isoforms in Insulin Actions. Journal of Biological Chemistry 2003 July 25;278(30):28312-28323.

(62) Bae SS, Cho H, Mu J, Birnbaum MJ. Isoform-specific Regulation of Insulin-dependent Glucose Uptake by Akt/Protein Kinase B. Journal of Biological Chemistry 2003 December 05;278(49):49530-49536.

(63) Cho H, Mu J, Kim JK, Thorvaldsen JL, Chu Q, Crenshaw EB, et al. Insulin Resistance and a Diabetes Mellitus-Like Syndrome in Mice Lacking the Protein Kinase Akt2 (PKBß). Science 2001 June 01;292(5522):1728-1731.

(64) Garofalo RS, Orena SJ, Rafidi K, Torchia AJ, Stock JL, Hildebrandt AL, et al. Severe diabetes, age-dependent loss of adipose tissue, and mild growth deficiency in mice lacking Akt2/PKB beta. J Clin Invest 2003 Jul;112(2):197-208.

(65) Rondinone C, Carvalho E, Wesslau C, Smith U. Impaired glucose transport and protein kinase B activation by insulin, but not okadaic acid, in adipocytes from subjects with Type II diabetes mellitus. Diabetologia 1999;42(7):819-825.

(66) George S, Rochford JJ, Wolfrum C, Gray SL, Schinner S, Wilson JC, et al. A family with severe insulin resistance and diabetes due to a mutation in AKT2. Science 2004 May 28;304(5675):1325-1328.

(67) Hardie DG, Carling D. The AMP-Activated Protein Kinase. European Journal of Biochemistry 1997;246(2):259-273.

(68) Winder W, Hardie D. Inactivation of acetyl-CoA carboxylase and activation of AMP-activated protein kinase in muscle during exercise. American Journal of Physiology-Endocrinology And Metabolism 1996;33(2):E299.

(69) Sriwijitkamol A, Coletta DK, Wajcberg E, Balbontin GB, Reyna SM, Barrientes J, et al. Effect of Acute Exercise on AMPK Signaling in Skeletal Muscle of Subjects With Type 2 Diabetes: A Time-Course and Dose-Response Study. Diabetes 2007 March 01;56(3):836-848.

(70) Kane S, Sano H, Liu SCH, Asara JM, Lane WS, Garner CC, et al. A Method to Identify Serine Kinase Substrates: Akt PHOSPHORYLATES A NOVEL ADIPOCYTE PROTEIN WITH A Rab GTPASE-ACTIVATING PROTEIN (GAP) DOMAIN. Journal of Biological Chemistry 2002 June 21;277(25):22115-22118.

(71) Thong FSL, Dugani CB, Klip A. Turning Signals On and Off: GLUT4 Traffic in the Insulin-Signaling Highway. Physiology 2005 August 01;20(4):271-284.

(72) Treebak JT, Glund S, Deshmukh A, Klein DK, Long YC, Jensen TE, et al. AMPK-Mediated AS160 Phosphorylation in Skeletal Muscle Is Dependent on AMPK Catalytic and Regulatory Subunits. Diabetes 2006 July 01;55(7):2051-2058.

(73) Deshmukh A, Coffey VG, Zhong Z, Chibalin AV, Hawley JA, Zierath JR. Exercise-Induced Phosphorylation of the Novel Akt Substrates AS160 and Filamin A in Human Skeletal Muscle. Diabetes 2006 June 01;55(6):1776-1782.

(74) Bruss MD, Arias EB, Lienhard GE, Cartee GD. Increased Phosphorylation of Akt Substrate of 160 kDa (AS160) in Rat Skeletal Muscle in Response to Insulin or Contractile Activity. Diabetes 2005 January 01;54(1):41-50.

(75) Smith JL, Patil PB, Fisher JS. AICAR and hyperosmotic stress increase insulin-stimulated glucose transport. Journal of Applied Physiology 2005 September 01;99(3):877-883.

(76) Thong FS, Bilan PJ, Klip A. The Rab GTPase-activating protein AS160 integrates Akt, protein kinase C, and AMP-activated protein kinase signals regulating GLUT4 traffic. Diabetes 2007 Feb;56(2):414-423.

(77) Merrill GF, Kurth EJ, Hardie DG, Winder WW. AICA riboside increases AMP-activated protein kinase, fatty acid oxidation, and glucose uptake in rat muscle. Am J Physiol 1997 Dec;273(6 Pt 1):E1107-12.

(78) Hayashi T, Hirshman MF, Kurth EJ, Winder WW, Goodyear LJ. Evidence for 5'AMP-Activated Protein Kinase Mediation of the Effect of Muscle Contraction on Glucose Transport. Diabetes 1998 August 01;47(8):1369-1373.

(79) Hawley J, Lessard S. Exercise training-induced improvements in insulin action. Acta physiologica 2008;192(1):127-135.

(80) Sigal RJ, Kenny GP, Wasserman DH, Castaneda-Sceppa C. Physical activity/exercise and type 2 diabetes. Diabetes Care 2004 Oct;27(10):2518-2539.

(81) Vavvas D, Apazidis A, Saha AK, Gamble J, Patel A, Kemp BE, et al. Contraction-induced Changes in Acetyl-CoA Carboxylase and 5'-AMP-activated Kinase in Skeletal Muscle. Journal of Biological Chemistry 1997 May 16;272(20):13255-13261.

(82) Bergeron R, Previs SF, Cline GW, Perret P, Russell RR, Young LH, et al. Effect of 5-aminoimidazole-4-carboxamide-1-beta-D-ribofuranoside infusion on in vivo glucose and lipid metabolism in lean and obese Zucker rats. Diabetes 2001;50(5):1076-1082.

(83) Song X, Fiedler M, Galuska D, Ryder J, Fernström M, Chibalin A, et al. 5-Aminoimidazole-4-carboxamide ribonucleoside treatment improves glucose homeostasis in insulin-resistant diabetic (ob/ob) mice. Diabetologia 2002;45(1):56-65.

(84) Fujii N, Ho RC, Manabe Y, Jessen N, Toyoda T, Holland WL, et al. Ablation of AMP-Activated Protein Kinase a2 Activity Exacerbates Insulin Resistance Induced by High-Fat Feeding of Mice. Diabetes 2008 November 01;57(11):2958-2966.

(85) Zhou G, Myers R, Li Y, Chen Y, Shen X, Fenyk-Melody J, et al. Role of AMP-activated protein kinase in mechanism of metformin action. J Clin Invest 2001 Oct;108(8):1167-1174.

(86) Musi N, Hirshman MF, Nygren J, Svanfeldt M, Bavenholm P, Rooyackers O, et al. Metformin Increases AMP-Activated Protein Kinase Activity in Skeletal Muscle of Subjects With Type 2 Diabetes. Diabetes 2002 July 01;51(7):2074-2081.

(87) Zang M, Xu S, Maitland-Toolan KA, Zuccollo A, Hou X, Jiang B, et al. Polyphenols Stimulate AMP-Activated Protein Kinase, Lower Lipids, and Inhibit Accelerated Atherosclerosis in Diabetic LDL Receptor–Deficient Mice. Diabetes 2006 August 01;55(8):2180-2191.

(88) Breen DM, Sanli T, Giacca A, Tsiani E. Stimulation of muscle cell glucose uptake by resveratrol through sirtuins and AMPK. Biochem Biophys Res Commun 2008 9/12;374(1):117-122.

(89) Fröjdö S, Durand C, Molin L, Carey AL, El-Osta A, Kingwell BA, et al. Phosphoinositide 3-kinase as a novel functional target for the regulation of the insulin signaling pathway by SIRT1. Mol Cell Endocrinol 2011 3/30;335(2):166-176.

(90) Baur JA, Pearson KJ, Price NL, Jamieson HA, Lerin C, Kalra A, et al. Resveratrol improves health and survival of mice on a high-calorie diet. Nature 2006;444(7117):337-342.

(91) Um J, Park S, Kang H, Yang S, Foretz M, McBurney MW, et al. AMP-Activated Protein Kinase–Deficient Mice Are Resistant to the Metabolic Effects of Resveratrol. Diabetes 2010 March 01;59(3):554-563.

(92) Timmers S, Konings E, Bilet L, Houtkooper RH, van de Weijer T, Goossens GH, et al. Calorie restriction-like effects of 30 days of resveratrol supplementation on energy metabolism and metabolic profile in obese humans. Cell metabolism 2011;14(5):612-622.

(93) Scheen AJ. From obesity to diabetes: why, when and who? Acta Clin Belg 2000 Jan-Feb;55(1):9-15.

(94) CARO JF. CLINICAL REVIEW 26 Insulin Resistance in Obese and Nonobese Man. The Journal of Clinical Endocrinology & Metabolism 1991;73(4):691-695.

(95) Boden G, Lebed B, Schatz M, Homko C, Lemieux S. Effects of Acute Changes of Plasma Free Fatty Acids on Intramyocellular Fat Content and Insulin Resistance in Healthy Subjects. Diabetes 2001 July 01;50(7):1612-1617.

(96) Knowler WC, Pettitt DJ, Saad MF, Bennett PH. Diabetes mellitus in the Pima Indians: incidence, risk factors and pathogenesis. Diabetes Metab 1990;6(1):1-27.

(97) Reaven GM, Chang H, Ho H, Jeng C, Hoffman BB. Lowering of plasma glucose in diabetic rats by antilipolytic agents. Am J Physiol 1988;254(1 Pt 1):E23-E30.

(98) Kim JK, Gavrilova O, Chen Y, Reitman ML, Shulman GI. Mechanism of Insulin Resistance in A-ZIP/F-1 Fatless Mice. Journal of Biological Chemistry 2000 March 24;275(12):8456-8460.

(99) Kim JK, Fillmore JJ, Sunshine MJ, Chen Y, Zong H, Littman DR, et al. Transgenic mice with inactivation of PKC-Θ are protected from lipid-induced defects in insulin action and signaling in skeletal muscle. Diabetes 2001;50(Suppl 2):A58-A65.

(100) Santomauro AT, Boden G, Silva ME, Rocha DM, Santos RF, Ursich MJ, et al. Overnight lowering of free fatty acids with Acipimox improves insulin resistance and

glucose tolerance in obese diabetic and nondiabetic subjects. Diabetes 1999 September 01;48(9):1836-1841.

(101) Perseghin G, Ghosh S, Gerow K, Shulman GI. Metabolic defects in lean nondiabetic offspring of NIDDM parents: a cross-sectional study. Diabetes 1997 Jun;46(6):1001-1009.

(102) Prentki M, Corkey BE. Are the ß-Cell Signaling Molecules Malonyl-CoA and Cystolic Long-Chain Acyl-CoA Implicated in Multiple Tissue Defects of Obesity and NIDDM? Diabetes 1996 March 01;45(3):273-283.

(103) Griffin ME, Marcucci MJ, Cline GW, Bell K, Barucci N, Lee D, et al. Free fatty acid-induced insulin resistance is associated with activation of protein kinase C theta and alterations in the insulin signaling cascade. Diabetes 1999 June 01;48(6):1270-1274.

(104) Kim YB, Peroni OD, Franke TF, Kahn BB. Divergent regulation of Akt1 and Akt2 isoforms in insulin target tissues of obese Zucker rats. Diabetes 2000 May 01;49(5):847-856.

(105) Kim YB, Nikoulina SE, Ciaraldi TP, Henry RR, Kahn BB. Normal insulin-dependent activation of Akt/protein kinase B, with diminished activation of phosphoinositide 3-kinase, in muscle in type 2 diabetes. J Clin Invest 1999 Sep;104(6):733-741.

(106) Dresner A, Laurent D, Marcucci M, Griffin ME, Dufour S, Cline GW, et al. Effects of free fatty acids on glucose transport and IRS-1-associated phosphatidylinositol 3-kinase activity. J Clin Invest 1999 Jan;103(2):253-259.

(107) Thompson AL, Cooney GJ. Acyl-CoA inhibition of hexokinase in rat and human skeletal muscle is a potential mechanism of lipid-induced insulin resistance. Diabetes 2000 November 01;49(11):1761-1765.

(108) Krssak M, Petersen KF, Dresner A, DiPietro L, Vogel S, Rothman D, et al. Intramyocellular lipid concentrations are correlated with insulin sensitivity in humans: a 1H NMR spectroscopy study. Diabetologia 1999;42(1):113-116.

(109) Jacob S, Machann J, Rett K, Brechtel K, Volk A, Renn W, et al. Association of increased intramyocellular lipid content with insulin resistance in lean nondiabetic offspring of type 2 diabetic subjects. Diabetes 1999 May 01;48(5):1113-1119.

(110) Kelley DE, Mandarino LJ. Fuel selection in human skeletal muscle in insulin resistance: a reexamination. Diabetes 2000 May 01;49(5):677-683.

(111) Itani SI, Ruderman NB, Schmieder F, Boden G. Lipid-Induced Insulin Resistance in Human Muscle Is Associated With Changes in Diacylglycerol, Protein Kinase C, and IκB-α. Diabetes 2002 July 01;51(7):2005-2011.

(112) Ellis BA, Poynten A, Lowy AJ, Furler SM, Chisholm DJ, Kraegen EW, et al. Long-chain acyl-CoA esters as indicators of lipid metabolism and insulin sensitivity in rat and human muscle. Am J Physiol Endocrinol Metab 2000 Sep;279(3):E554-60.

(113) Bahl JJ, Matsuda M, DeFronzo RA, Bressler R. In vitro and in vivo suppression of gluconeogenesis by inhibition of pyruvate carboxylase. Biochem Pharmacol 1997 1/10;53(1):67-74.

(114) Massillon D, Barzilai N, Hawkins M, Prus-Wertheimer D, Rossetti L. Induction of Hepatic Glucose-6-Phosphatase Gene Expression by Lipid Infusion. Diabetes 1997 January 01;46(1):153-157.

(115) Bergman RN, Ader M. Free Fatty Acids and Pathogenesis of Type 2 Diabetes Mellitus. Trends in Endocrinology & Metabolism 2000 11/1;11(9):351-356.

(116) De Fea K, Roth RA. Protein kinase C modulation of insulin receptor substrate-1 tyrosine phosphorylation requires serine 612. Biochemistry (N Y) 1997;36(42):12939-12947.

(117) Ravichandran LV, Esposito DL, Chen J, Quon MJ. Protein Kinase C-ζ Phosphorylates Insulin Receptor Substrate-1 and Impairs Its Ability to Activate Phosphatidylinositol 3-Kinase in Response to Insulin. Journal of Biological Chemistry 2001 February 02;276(5):3543-3549.

(118) Tippett PS, Neet KE. An allosteric model for the inhibition of glucokinase by long chain acyl coenzyme A. J Biol Chem 1982 Nov 10;257(21):12846-12852.

(119) Schmitz-Peiffer C, Browne CL, Oakes ND, Watkinson A, Chisholm DJ, Kraegen EW, et al. Alterations in the Expression and Cellular Localization of Protein Kinase C Isozymes ε and θ Are Associated With Insulin Resistance in Skeletal Muscle of the High-Fat–Fed Rat. Diabetes 1997 February 01;46(2):169-178.

(120) Kim JK, Fillmore JJ, Sunshine MJ, Albrecht B, Higashimori T, Kim DW, et al. PKC-theta knockout mice are protected from fat-induced insulin resistance. J Clin Invest 2004 Sep;114(6):823-827.

(121) Turinsky J, O'Sullivan DM, Bayly BP. 1,2-Diacylglycerol and ceramide levels in insulin-resistant tissues of the rat in vivo. Journal of Biological Chemistry 1990 October 05;265(28):16880-16885.

(122) Adams JM, Pratipanawatr T, Berria R, Wang E, DeFronzo RA, Sullards MC, et al. Ceramide content is increased in skeletal muscle from obese insulin-resistant humans. Diabetes 2004;53:25-31.

(123) Powell D, Turban S, Gray A, Hajduch E, Hundal H. Intracellular ceramide synthesis and protein kinase Czeta activation play an essential role in palmitate-induced insulin resistance in rat L6 skeletal muscle cells. Biochem J 2004;382:619-629.

(124) Previs SF, Withers DJ, Ren JM, White MF, Shulman GI. Contrasting effects of IRS-1 versus IRS-2 gene disruption on carbohydrate and lipid metabolism in vivo. J Biol Chem 2000 Dec 15;275(50):38990-38994.

(125) Samuel VT, Liu Z, Qu X, Elder BD, Bilz S, Befroy D, et al. Mechanism of Hepatic Insulin Resistance in Non-alcoholic Fatty Liver Disease. Journal of Biological Chemistry 2004 July 30;279(31):32345-32353.

(126) Berg CE, Lavan BE, Rondinone CM. Rapamycin partially prevents insulin resistance induced by chronic insulin treatment. Biochem Biophys Res Commun 2002;293(3):1021-1027.

(127) Mordier S, Iynedjian PB. Activation of mammalian target of rapamycin complex 1 and insulin resistance induced by palmitate in hepatocytes. Biochem Biophys Res Commun 2007;362(1):206-211.

(128) Harrington LS, Findlay GM, Gray A, Tolkacheva T, Wigfield S, Rebholz H, et al. The TSC1-2 tumor suppressor controls insulin-PI3K signaling via regulation of IRS proteins. J Cell Biol 2004 Jul 19;166(2):213-223.

(129) Tremblay F, Brule S, Hee Um S, Li Y, Masuda K, Roden M, et al. Identification of IRS-1 Ser-1101 as a target of S6K1 in nutrient- and obesity-induced insulin resistance. Proc Natl Acad Sci U S A 2007 Aug 28;104(35):14056-14061.

(130) Le Bacquer O, Petroulakis E, Paglialunga S, Poulin F, Richard D, Cianflone K, et al. Elevated sensitivity to diet-induced obesity and insulin resistance in mice lacking 4E-BP1 and 4E-BP2. J Clin Invest 2007 Feb;117(2):387-396.

(131) Aguirre V, Uchida T, Yenush L, Davis R, White MF. The c-Jun NH(2)-terminal kinase promotes insulin resistance during association with insulin receptor substrate-1 and phosphorylation of Ser(307). Journal of Biological Chemistry 2002;277:1531-1537.

(132) Gao Z, Zhang X, Zuberi A, Hwang D, Quon MJ, Lefevre M, et al. Inhibition of insulin sensitivity by free fatty acids requires activation of multiple serine kinases in 3T3-L1 adipocytes. Molecular endocrinology 2004;18(8):2024-2034.

(133) Wellen KE, Hotamisligil GS. Inflammation, stress, and diabetes. J Clin Invest 2005 May;115(5):1111-1119.

(134) Hirosumi J, Tuncman G, Chang L, Görgün CZ, Uysal KT, Maeda K, et al. A central role for JNK in obesity and insulin resistance. Nature 2002;420(6913):333-336.

(135) Yin M, Yamamoto Y, Gaynor RB. The anti-inflammatory agents aspirin and salicylate inhibit the activity of IκB kinase-β. Nature 1998;396(6706):77-80.

(136) Hotamisligil GS, Peraldi P, Budavari A, Ellis R, White MF, Spiegelman BM. IRS-1-mediated inhibition of insulin receptor tyrosine kinase activity in TNF-alpha- and obesity-induced insulin resistance. Science 1996 Feb 2;271(5249):665-668.

(137) Paz K, Hemi R, LeRoith D, Karasik A, Elhanany E, Kanety H, et al. A Molecular Basis for Insulin Resistance: ELEVATED SERINE/THREONINE PHOSPHORYLATION OF IRS-1 AND IRS-2 INHIBITS THEIR BINDING TO THE JUXTAMEMBRANE REGION OF THE INSULIN RECEPTOR AND IMPAIRS THEIR ABILITY TO UNDERGO INSULIN-INDUCED TYROSINE PHOSPHORYLATION. Journal of Biological Chemistry 1997 November 21;272(47):29911-29918.

(138) Hotamisligil G, Shargill N, Spiegelman B. Adipose expression of tumor necrosis factor-alpha: direct role in obesity-linked insulin resistance. Science 1993 January 01;259(5091):87-91.

(139) Sethi JK, Hotamisligil GS. The role of TNFα in adipocyte metabolism. Semin Cell Dev Biol 1999 2;10(1):19-29.

(140) Yu C, Chen Y, Cline GW, Zhang D, Zong H, Wang Y, et al. Mechanism by which fatty acids inhibit insulin activation of insulin receptor substrate-1 (IRS-1)-associated phosphatidylinositol 3-kinase activity in muscle. J Biol Chem 2002 Dec 27;277(52):50230-50236.

(141) Hotamisligil GS, Arner P, Caro JF, Atkinson RL, Spiegelman BM. Increased adipose tissue expression of tumor necrosis factor-alpha in human obesity and insulin resistance. J Clin Invest 1995 May;95(5):2409-2415.

(142) Kern PA, Saghizadeh M, Ong JM, Bosch RJ, Deem R, Simsolo RB. The expression of tumor necrosis factor in human adipose tissue. Regulation by obesity, weight loss, and relationship to lipoprotein lipase. J Clin Invest 1995 May;95(5):2111-2119.

(143) Saghizadeh M, Ong JM, Garvey WT, Henry RR, Kern PA. The expression of TNF alpha by human muscle. Relationship to insulin resistance. J Clin Invest 1996 Feb 15;97(4):1111-1116.

(144) Knobler H, Zhornicky T, Sandler A, Haran N, Ashur Y, Schattner A. Tumor necrosis factor–α–induced insulin resistance may mediate the hepatitis C virus–diabetes association. Am J Gastroenterol 2003;98(12):2751-2756.

(145) Greenberg A, McDaniel M. Identifying the links between obesity, insulin resistance and β-cell function: potential role of adipocyte-derived cytokines in the pathogenesis of type 2 diabetes. Eur J Clin Invest 2002;32(s3):24-34.

(146) Zick Y. Insulin resistance: a phosphorylation-based uncoupling of insulin signaling. Trends Cell Biol 2001 11;11, Supplement 1(0):437-441.

(147) Hotamisligil GS, Murray DL, Choy LN, Spiegelman BM. Tumor necrosis factor alpha inhibits signaling from the insulin receptor. Proceedings of the National Academy of Sciences 1994 May 24;91(11):4854-4858.

(148) Uysal KT, Wiesbrock SM, Marino MW, Hotamisligil GS. Protection from obesity-induced insulin resistance in mice lacking TNF-α function. Nature 1997;389(6651):610-614.

(149) Youd JM, Rattigan S, Clark MG. Acute impairment of insulin-mediated capillary recruitment and glucose uptake in rat skeletal muscle in vivo by TNF-alpha. Diabetes 2000 November 01;49(11):1904-1909.

(150) Zinman B, Hanley AJ, Harris SB, Kwan J, Fantus IG. Circulating Tumor Necrosis Factor-α Concentrations in a Native Canadian Population with High Rates of Type 2 Diabetes Mellitus 1. The Journal of Clinical Endocrinology & Metabolism 1999;84(1):272-278.

(151) Kern PA, Ranganathan S, Li C, Wood L, Ranganathan G. Adipose tissue tumor necrosis factor and interleukin-6 expression in human obesity and insulin resistance. Am J Physiol Endocrinol Metab 2001 May;280(5):E745-51.

(152) Gao Z, Hwang D, Bataille F, Lefevre M, York D, Quon MJ, et al. Serine Phosphorylation of Insulin Receptor Substrate 1 by Inhibitor κB Kinase Complex , Journal of Biological Chemistry 2002 December 13;277(50):48115-48121.

(153) Arkan MC, Hevener AL, Greten FR, Maeda S, Li Z, Long JM, et al. IKK-β links inflammation to obesity-induced insulin resistance. Nat Med 2005;11(2):191-198.

(154) Hundal RS, Petersen KF, Mayerson AB, Randhawa PS, Inzucchi S, Shoelson SE, et al. Mechanism by which high-dose aspirin improves glucose metabolism in type 2 diabetes. J Clin Invest 2002 May;109(10):1321-1326.

(155) Fain JN, Madan AK, Hiler ML, Cheema P, Bahouth SW. Comparison of the release of adipokines by adipose tissue, adipose tissue matrix, and adipocytes from visceral and subcutaneous abdominal adipose tissues of obese humans. Endocrinology 2004;145(5):2273-2282.

(156) SANDLER S, BENDTZEN K, Eizirik DL, WELSH M. Interleukin-6 Affects Insulin Secretion and Glucose Metabolism of Rat Pancreatic Islets in Vitro*. Endocrinology 1990;126(2):1288-1294.

(157) Ouchi N, Walsh K. Adiponectin as an anti-inflammatory factor. Clinica Chimica Acta 2007 5/1;380(1–2):24-30.

(158) Hu E, Liang P, Spiegelman BM. AdipoQ Is a Novel Adipose-specific Gene Dysregulated in Obesity. Journal of Biological Chemistry 1996 May 03;271(18):10697-10703.

(159) Nawrocki AR, Rajala MW, Tomas E, Pajvani UB, Saha AK, Trumbauer ME, et al. Mice Lacking Adiponectin Show Decreased Hepatic Insulin Sensitivity and Reduced Responsiveness to Peroxisome Proliferator-activated Receptor γ Agonists. Journal of Biological Chemistry 2006 February 03;281(5):2654-2660.

(160) Berg AH, Combs TP, Du X, Brownlee M, Scherer PE. The adipocyte-secreted protein Acrp30 enhances hepatic insulin action. Nat Med 2001;7(8):947-953.

(161) Arita Y, Kihara S, Ouchi N, Takahashi M, Maeda K, Miyagawa J, et al. Paradoxical decrease of an adipose-specific protein, adiponectin, in obesity. Biochem Biophys Res Commun 1999;257(1):79-83.

(162) Weyer C, Funahashi T, Tanaka S, Hotta K, Matsuzawa Y, Pratley RE, et al. Hypoadiponectinemia in obesity and type 2 diabetes: close association with insulin resistance and hyperinsulinemia. The Journal of Clinical Endocrinology & Metabolism 2001;86(5):1930-1935.

(163) Maeda N, Takahashi M, Funahashi T, Kihara S, Nishizawa H, Kishida K, et al. PPARgamma ligands increase expression and plasma concentrations of adiponectin, an adipose-derived protein. Diabetes 2001 Sep;50(9):2094-2099.

(164) Fasshauer M, Kralisch S, Klier M, Lossner U, Bluher M, Klein J, et al. Adiponectin gene expression and secretion is inhibited by interleukin-6 in 3T3-L1 adipocytes. Biochem Biophys Res Commun 2003 2/21;301(4):1045-1050.

(165) Kappes A, Loffler G. *Influences of ionomycin, dibutyryl-cycloAMP and tumour necrosis factor-alpha on intracellular amount and secretion of apM1 in differentiating primary human preadipocytes*. Hormone & Metabolic Research 2000;32:548-554.

(166) McTernan PG, McTernan CL, Chetty R, Jenner K, Fisher FM, Lauer MN, et al. Increased resistin gene and protein expression in human abdominal adipose tissue. The Journal of Clinical Endocrinology & Metabolism 2002;87(5):2407-2407.

(167) Shimabukuro M, Wang M, Zhou Y, Newgard CB, Unger RH. Protection against lipoapoptosis of ß cells through leptin-dependent maintenance of Bcl-2 expression. Proceedings of the National Academy of Sciences 1998 August 04;95(16):9558-9561.

(168) Smith SR, Bai F, Charbonneau C, Janderova L, Argyropoulos G. A promoter genotype and oxidative stress potentially link resistin to human insulin resistance. Diabetes 2003 Jul;52(7):1611-1618.

(169) Florez JC. The new type 2 diabetes gene TCF7L2. Curr Opin Clin Nutr Metab Care 2007 Jul;10(4):391-396.

(170) Donath MY, Ehses JA, Maedler K, Schumann DM, Ellingsgaard H, Eppler E, et al. Mechanisms of β-Cell Death in Type 2 Diabetes. Diabetes 2005 December 01;54(suppl 2):S108-S113.

(171) LeRoith D. β-cell dysfunction and insulin resistance in type 2 diabetes: role of metabolic and genetic abnormalities. Am J Med 2002 10/28;113(6, Supplement):3-11.

(172) Bent S. Herbal medicine in the United States: review of efficacy, safety, and regulation. Journal of general internal medicine 2008;23(6):854-859.

(173) Kamboj V. Herbal medicine. CURRENT SCIENCE-BANGALORE- 2000;78(1):35-38.

(174) Schwarz K. Phenolic Diterpenes from rosemary and sage. In: Shi L, Mazza G, Le Marguer M, editors. Functional foods: biochemical and processing aspects Boca Raton, Florida: CRC; 2002. p. 188-210.

(175) Ulbricht C, Abrams TR, Brigham A, Ceurvels J, Clubb J, Curtiss W, et al. An evidence-based systematic review of rosemary (Rosmarinus officinalis) by the Natural Standard Research Collaboration. Journal of dietary supplements 2010;7(4):351-413.

(176) CA R. Pharmacology of rosemary (Rosmarinus officinalis Linn.) and its therapeutic potentials. Indian J Exp Biol 1999;37:124-131.

(177) Zhang Y, Smuts JP, Dodbiba E, Rangarajan R, Lang JC, Armstrong DW. Degradation study of carnosic acid, carnosol, rosmarinic acid, and rosemary extract (Rosmarinus officinalis L.) assessed using HPLC. J Agric Food Chem 2012;60(36):9305-9314.

(178) Andersson D, Cheng Y, Duan R. Ursolic acid inhibits the formation of aberrant crypt foci and affects colonic sphingomyelin hydrolyzing enzymes in azoxymethane-treated rats. J Cancer Res Clin Oncol 2008;134(1):101-107.

(179) Ho C, Wang M, Wei G, Huang T, Huang M. Chemistry and antioxidative factors in rosemary and sage. Biofactors 2000;13(1-4):161-166.

(180) Hossain MB, Rai DK, Brunton NP, Martin-Diana AB, Barry-Ryan C. Characterization of phenolic composition in Lamiaceae spices by LC-ESI-MS/MS. J Agric Food Chem 2010;58(19):10576-10581.

(181) Hossain M, Barry-Ryan C, Martin-Diana AB, Brunton N. Optimisation of accelerated solvent extraction of antioxidant compounds from rosemary (< i> Rosmarinus officinalis L.), marjoram (< i> Origanum majorana L.) and oregano (< i> Origanum vulgare L.) using response surface methodology. Food Chem 2011;126(1):339-346.

(182) Costa S, Utan A, Speroni E, Cervellati R, Piva G, Prandini A, et al. Carnosic acid from rosemary extracts: a potential chemoprotective agent against aflatoxin B1. An in vitro study. Journal of Applied Toxicology 2007;27(2):152-159.

(183) Moran AE, Carothers AM, Weyant MJ, Redston M, Bertagnolli MM. Carnosol Inhibits ß-Catenin Tyrosine Phosphorylation and Prevents Adenoma Formation in the C57BL/6J/Min/+ (Min/+) Mouse. Cancer Research 2005 February 01;65(3):1097-1104.

(184) Meziane-Assami D, Tomao V, Ruiz K, Meklati BY, Chemat F. Geographical differentiation of rosemary based on GC/MS and fast HPLC analyses. Food Analytical Methods 2013;6(1):282-288.

(185) Vallverdú-Queralt A, Regueiro J, Martínez-Huélamo M, Rinaldi Alvarenga JF, Leal LN, Lamuela-Raventos RM. A comprehensive study on the phenolic profile of widely used culinary herbs and spices: Rosemary, thyme, oregano, cinnamon, cumin and bay. Food Chem 2014;154:299-307.

(186) Shan B, Cai YZ, Sun M, Corke H. Antioxidant capacity of 26 spice extracts and characterization of their phenolic constituents. J Agric Food Chem 2005;53(20):7749-7759.

(187) Gaya M, Repetto V, Toneatto J, Anesini C, Piwien-Pilipuk G, Moreno S. Antiadipogenic effect of carnosic acid, a natural compound present in< i> Rosmarinus officinalis, is exerted through the C/EBPs and PPARγ pathways at the onset of the differentiation program. Biochimica et Biophysica Acta (BBA)-General Subjects 2013;1830(6):3796-3806.

(188) Romo-Vaquero M, Larrosa M, Yáñez-Gascón MJ, Issaly N, Flanagan J, Roller M, et al. A rosemary extract enriched in carnosic acid improves circulating adipocytokines and modulates key metabolic sensors in lean Zucker rats: Critical and contrasting differences in the obese genotype. Molecular nutrition & food research 2014;58(5):942-953.

(189) Wang T, Takikawa Y, Satoh T, Yoshioka Y, Kosaka K, Tatemichi Y, et al. Carnosic acid prevents obesity and hepatic steatosis in ob/ob mice. Hepatology Research 2011;41(1):87-92.

(190) Ibarra A, Cases J, Roller M, Chiralt-Boix A, Coussaert A, Ripoll C. Carnosic acid-rich rosemary (Rosmarinus officinalis L.) leaf extract limits weight gain and improves cholesterol levels and glycaemia in mice on a high-fat diet. Br J Nutr 2011;106(08):1182-1189.

(191) Posadas SJ, Caz V, Largo C, De la Gándara B, Matallanas B, Reglero G, et al. Protective effect of supercritical fluid rosemary extract, Rosmarinus officinalis, on antioxidants of major organs of aged rats. Exp Gerontol 2009 0;44(6–7):383-389.

(192) Romano CS, Abadi K, Repetto V, Vojnov AA, Moreno S. Synergistic antioxidant and antibacterial activity of rosemary plus butylated derivatives. Food Chem 2009 7/15;115(2):456-461.

(193) Ajila CM, Brar SK. Chapter 16 in Nutrition, Diet and Cancer . In: Shankar S, Srivastava RK, editors. Role of Dietary Antioxidants in Cancer. : Springer Science; 2012. p. 213-221.

(194) Erkan N, Ayranci G, Ayranci E. Antioxidant activities of rosemary (Rosmarinus Officinalis L.) extract, blackseed (Nigella sativa L.) essential oil, carnosic acid, rosmarinic acid and sesamol. Food Chem 2008 9/1;110(1):76-82.

(195) Pérez MB, Calderón NL, Croci CA. Radiation-induced enhancement of antioxidant activity in extracts of rosemary (Rosmarinus officinalis L.). Food Chem 2007;104(2):585-592.

(196) EL-BELTAGI, H., BADAWI,M. Comparison of Antioxidant and Antimicrobial Properties for Ginkgo biloba and Rosemary (Rosmarinus officinalis L.) from Egypt. Notulae Botanicae Horti Agrobotanici Cluj-Napoca 2013;41(1).

(197) Cazzola R, Camerotto C, Cestaro B. Anti-oxidant, anti-glycant, and inhibitory activity against α-amylase and α-glucosidase of selected spices and culinary herbs. Int J Food Sci Nutr 2011;62(02):175-184.

(198) Chen H, Lin Y, Hsieh C. Evaluation of antioxidant activity of aqueous extract of some selected nutraceutical herbs. Food Chem 2007;104(4):1418-1424.

(199) Cuvelier M, Richard H, Berset C. Antioxidative activity and phenolic composition of pilot-plant and commercial extracts of sage and rosemary. J Am Oil Chem Soc 1996;73(5):645-652.

(200) Masuda T, Inaba Y, Takeda Y. Antioxidant mechanism of carnosic acid: structural identification of two oxidation products. J Agric Food Chem 2001;49(11):5560-5565.

(201) Cheung S, Tai J. Anti-proliferative and antioxidant properties of rosemary Rosmarinus officinalis. Oncol Rep 2007;17(6):1525-1532.

(202) Vicente G, Molina S, González-Vallinas M, García-Risco MR, Fornari T, Reglero G, et al. Supercritical rosemary extracts, their antioxidant activity and effect on hepatic tumor progression. The Journal of Supercritical Fluids 2013 7;79(0):101-108.

(203) Đilas S, Knez Ž, Četojević-Simin D, Tumbas V, Škerget M, Čanadanović-Brunet J, et al. In vitro antioxidant and antiproliferative activity of three rosemary (Rosmarinus officinalis L.) extract formulations. Int J Food Sci Tech 2012;47(10):2052-2062.

(204) Lo A, Liang Y, Lin-Shiau S, Ho C, Lin J. Carnosol, an antioxidant in rosemary, suppresses inducible nitric oxide synthase through down-regulating nuclear factor-κB in mouse macrophages. Carcinogenesis 2002 June 01;23(6):983-991.

(205) Park JB. Identification and quantification of a major anti-oxidant and anti-inflammatory phenolic compound found in basil, lemon thyme, mint, oregano, rosemary, sage, and thyme. Int J Food Sci Nutr 2011;62(6):577-584.

(206) Moreno S, Scheyer T, Romano CS, Vojnov AA. Antioxidant and antimicrobial activities of rosemary extracts linked to their polyphenol composition. Free Radic Res 2006;40(2):223-231.

(207) Bubonja-Sonje M, Giacometti J, Abram M. Antioxidant and antilisterial activity of olive oil, cocoa and rosemary extract polyphenols. Food Chem 2011 8/15;127(4):1821-1827.

(208) Asai A, Nakagawa K, Miyazawa T. Antioxidative effects of turmeric, rosemary and capsicum extracts on membrane phospholipid peroxidation and liver lipid metabolism in mice. Biosci Biotechnol Biochem 1999;63(12):2118-2122.

(209) Eman MA. Comparative evaluation of antidiabetic activity of Rosmarinus officinalis L. and Chamomile recutita in streptozotocin induced diabetic rats. Agriculture and Biology Journal of North American 2012;3(6):247-252.

(210) Khalil OA, Ramadan KS, Danial EN, Alnahdi HS, Ayaz NO. Antidiabetic activity of Rosmarinus officinalis and its relationship with the antioxidant property. African Journal of Pharmacy and Pharmacology 2012;6(14):1031-1036.

(211) Bakırel T, Bakırel U, Keleş OÜ, Ülgen SG, Yardibi H. In vivo assessment of antidiabetic and antioxidant activities of rosemary (Rosmarinus officinalis) in alloxan-diabetic rabbits. J Ethnopharmacol 2008 2/28;116(1):64-73.

(212) Sinkovic A, Suran D, Lokar L, Fliser E, Skerget M, Novak Z, et al. Rosemary extracts improve flow-mediated dilatation of the brachial artery and plasma PAI-1 activity in healthy young volunteers. Phytotherapy Research 2011;25(3):402-407.

(213) Lukaczer D, Darland G, Tripp M, Liska DA, Lerman RH, Schiltz B, et al. A Pilot trial evaluating meta050, a proprietary combination of reduced iso-alpha acids, rosemary extract and oleanolic acid in patients with arthritis and fibromyalgia. Phytotherapy Research 2005;19(10):864-869.

(214) Yun YS, Noda S, Shigemori G, Kuriyama R, Takahashi S, Umemura M, et al. Phenolic Diterpenes from Rosemary Suppress cAMP Responsiveness of Gluconeogenic Gene Promoters. Phytotherapy Research 2013;27(6):906-910.

(215) Tu Z, Moss-Pierce T, Ford P, Jiang TA. Rosemary (Rosmarinus officinalis L.) extract regulates glucose and lipid metabolism by activating AMPK and PPAR pathways in HepG2 cells. J Agric Food Chem 2013;61(11):2803-2810.

(216) Wang QL, Li H, Li XX, Cui CY, Wang R, Yu NX, et al. Acute and 30-day oral toxicity studies of administered carnosic acid. Food and Chemical Toxicology 2012;50(12):4348-4355.

(217) Christensen KB, Minet A, Svenstrup H, Grevsen K, Zhang H, Schrader E, et al. Identification of plant extracts with potential antidiabetic properties: effect on human peroxisome proliferator-activated receptor (PPAR), adipocyte differentiation and insulin-stimulated glucose uptake. Phytotherapy research 2009;23(9):1316-1325.

(218) Rau O, Wurglics M, Dingermann T, Abdel-Tawab M, Schubert-Zsilavecz M. Screening of herbal extracts for activation of the human peroxisome proliferator-activated receptor. Die Pharmazie-An International Journal of Pharmaceutical Sciences 2006;61(11):952-956.

(219) Renzulli C, Galvano F, Pierdomenico L, Speroni E, Guerra M. Effects of rosmarinic acid against aflatoxin B1 and ochratoxin-A-induced cell damage in a human hepatoma cell line (Hep G2). Journal of Applied Toxicology 2004;24(4):289-296.

(220) Qiao S, Li W, Tsubouchi R, Haneda M, Murakami K, Takeuchi F, et al. Rosmarinic acid inhibits the formation of reactive oxygen and nitrogen species in RAW264. 7 macrophages. Free Radic Res 2005;39(9):995-1003.

(221) Dickmann LJ, VandenBrink BM, Lin YS. In vitro hepatotoxicity and cytochrome P450 induction and inhibition characteristics of carnosic acid, a dietary supplement with antiadipogenic properties. Drug Metab Dispos 2012 Jul;40(7):1263-1267.

(222) Funke I, Melzig MF. Traditionally used plants in diabetes therapy: phytotherapeutics as inhibitors of alpha-amylase activity. Revista Brasileira de Farmacognosia 2006;16(1):1-5.

(223) Koga K, Shibata H, Yoshino K, Nomoto K. Effects of 50% Ethanol Extract from Rosemary (Rosmarinus officinalis) on α-Glucosidase Inhibitory Activity and the Elevation of Plasma Glucose Level in Rats, and Its Active Compound. J Food Sci 2006;71(7):S507-S512.

(224) McCue PP, Shetty K. Inhibitory effects of rosmarinic acid extracts on porcine pancreatic amylase in vitro. Asia Pac J Clin Nutr 2004;13(1):101-106.

(225) Bustanji Y, Issa A, Mohammad M, Hudaib M, Tawah K, Alkhatib H, et al. Inhibition of hormone sensitive lipase and pancreatic lipase by Rosmarinus officinalis extract and selected phenolic constituents. J Med Plants Res 2010;4:2235-2242.

(226) Tu Z, Moss-Pierce T, Ford P, Jiang TA. Rosemary (Rosmarinus officinalis L.) extract regulates glucose and lipid metabolism by activating AMPK and PPAR pathways in HepG2 cells. J Agric Food Chem 2013;61(11):2803-2810.

(227) McCue PP, Shetty K. Inhibitory effects of rosmarinic acid extracts on porcine pancreatic amylase in vitro. Asia Pac J Clin Nutr 2004;13(1):101-106.

(228) Erenmemisoglu A, Saraymen R, Ustun H. Effect of Rosmarinus officinalis leaves extract on plasma glucose levels in normoglycaemic and diabetic mice. Pharmazie 1997;52:645-646.

(229) Aljamal AR, Alqadi T. Effects of rosemary on lipid profile in diabetic rats. Jordan Journal of Biological Sciences 2011;4(4):199-204.

(230) Alnahdi HS. Effect of Rosmarinus Officinalis extract on some cardiac enzymes of streptozotocin-induced diabetic rats. Journal of Health Sciences 2012;2(4):33-37.

(231) Ramadan KS, Khalil OA, Danial EN, Alnahdi HS, Ayaz NO. Hypoglycemic and hepatoprotective activity of Rosmarinus officinalis extract in diabetic rats. J Physiol Biochem 2013;69(4):779-783.

(232) Aleih G, Arash K, Laya F, AmirAfshin K, Mehdi M, Hamidreza AA, et al. Effect of rosmarinic acid on estrogen, FSH and LH in female diabetic rats. African Journal of Pharmacy and Pharmacology 2011;5(11):1427-1431.

(233) Kensara OA, ElSawy NA, Altaf FM, Header EA. Hypoglycemic and Hepato-protective Effects of Rosmarinus officinalis in Experimental Diabetic Rats.

(234) Tavafi M, Ahmadvand H, TAMJIDIPOOR A. Rosmarinic acid ameliorates diabetic nephropathy in uninephrectomized diabetic rats. Iranian Journal of Basic Medical Sciences 2011.

(235) Al-Sheyab FM, Abuharfeil N, Salloum L, Hani RB, Awad DS. The effect of rosemary plant extracts on immune response and lipid profile in mice. Journal of Biology and Life Science 2012;3(1):31-58.

(236) Vanithadevi B, Anuradha CV. Effect of rosmarinic acid on insulin sensitivity, glyoxalase system and oxidative events in liver of fructose-fed mice. International Journal of Diabetes and Metabolism 2008;16:35-44.

(237) Vaquero MR, Yáñez-Gascón M, Villalba RG, Larrosa M, Fromentin E, Ibarra A, et al. Inhibition of gastric lipase as a mechanism for body weight and plasma lipids reduction in Zucker rats fed a rosemary extract rich in Carnosic acid. PloS one 2012;7(6):e39773.

(238) Afonso MS, de O Silvia AM, Carvalho EBT, Rivelli DP, Barros SBM, Rogero MM, et al. Phenolic compounds from Rosemary (Rosmarinus officinalis L.) attenuate oxidative stress and reduce blood cholesterol concentrations in diet-induced hypercholesterolemic rats. Nutrition & Metabolism 2013;10(19):1-9.

(239) Hauner H. The mode of action of thiazolidinediones. Diabetes Metab Res 2002;18(S2):S10-S15.

(240) Timmers S, Konings E, Bilet L, Houtkooper RH, van de Weijer T, Goossens GH, et al. Calorie restriction-like effects of 30 days of resveratrol supplementation on energy metabolism and metabolic profile in obese humans. Cell metabolism 2011;14(5):612-622.

(241) Klip A, Paquet MR. Glucose transport and glucose transporters in muscle and their metabolic regulation. Diabetes Care 1990 Mar;13(3):228-243.

(242) Mitsumoto Y, Burdett E, Grant A, Klip A. Differential expression of the GLUT1 and GLUT4 glucose transporters during differentiation of L6 muscle cells. Biochem Biophys Res Commun 1991 3/15;175(2):652-659.

(243) Ishiki M, Klip A. Minireview: recent developments in the regulation of glucose transporter-4 traffic: new signals, locations, and partners. Endocrinology 2005;146(12):5071-5078.

(244) Klip A. The many ways to regulate glucose transporter 4 This paper is one of a selection of papers published in this Special Issue, entitled 14th International Biochemistry of Exercise Conference-Muscles as Molecular and Metabolic Machines, and has undergone the Journal's usual peer review process. Applied Physiology, Nutrition, and Metabolism 2009;34(3):481-487.

(245) Konrad D, Rudich A, Bilan PJ, Patel N, Richardson C, Witters LA, et al. Troglitazone causes acute mitochondrial membrane depolarisation and an AMPK-mediated increase in glucose phosphorylation in muscle cells. Diabetologia 2005;48(5):954-966.

(246) Saltiel AR, Kahn CR. Insulin signalling and the regulation of glucose and lipid metabolism. Nature 2001;414(6865):799-806.

(247) Zygmunt K, Faubert B, MacNeil J, Tsiani E. Naringenin, a citrus flavonoid, increases muscle cell glucose uptake via AMPK. Biochem Biophys Res Commun 2010 7/23;398(2):178-183.

(248) Fujii N, Ho RC, Manabe Y, Jessen N, Toyoda T, Holland WL, et al. Ablation of AMP-Activated Protein Kinase a2 Activity Exacerbates Insulin Resistance Induced by High-Fat Feeding of Mice. Diabetes 2008 November 01;57(11):2958-2966.

(249) Yu Y, Lin H, Chang W. Carnosic acid prevents the migration of human aortic smooth muscle cells by inhibiting the activation and expression of matrix metalloproteinase-9. Br J Nutr 2008;100(04):731-738.

(250) Baba S, Osakabe N, Natsume M, Yasuda A, Muto Y, Hiyoshi T, et al. Absorption, metabolism, degradation and urinary excretion of rosmarinic acid after intake of Perilla frutescens extract in humans. Eur J Nutr 2005;44(1):1-9.

(251) Fazakerley DJ, Holman GD, Marley A, James DE, Stöckli J, Coster ACF. Kinetic Evidence for Unique Regulation of GLUT4 Trafficking by Insulin and AMP-activated Protein Kinase Activators in L6 Myotubes. Journal of Biological Chemistry 2010 January 15;285(3):1653-1660.

(252) Owen M, DORAN E, Halestrap A. Evidence that metformin exerts its anti-diabetic effects through inhibition of complex 1 of the mitochondrial respiratory chain. Biochem J 2000;348:607-614.

(253) Konrad D, Bilan PJ, Nawaz Z, Sweeney G, Niu W, Liu Z, et al. Need for GLUT4 activation to reach maximum effect of insulin-mediated glucose uptake in brown

adipocytes isolated from GLUT4myc-expressing mice. Diabetes 2002 Sep;51(9):2719-2726.

(254) Li D, Randhawa VK, Patel N, Hayashi M, Klip A. Hyperosmolarity reduces GLUT4 endocytosis and increases its exocytosis from a VAMP2-independent pool in l6 muscle cells. J Biol Chem 2001 Jun 22;276(25):22883-22891.

(255) Ishikura S, Bilan PJ, Klip A. Rabs 8A and 14 are targets of the insulin-regulated Rab-GAP AS160 regulating GLUT4 traffic in muscle cells. Biochem Biophys Res Commun 2007;353(4):1074-1079.

(256) Wang Q, Khayat Z, Kishi K, Ebina Y, Klip A. GLUT4 translocation by insulin in intact muscle cells: detection by a fast and quantitative assay. FEBS Lett 1998;427(2):193-197.

(257) Wang Q, Somwar R, Bilan PJ, Liu Z, Jin J, Woodgett JR, et al. Protein kinase B/Akt participates in GLUT4 translocation by insulin in L6 myoblasts. Mol Cell Biol 1999 Jun;19(6):4008-4018.

(258) Khayat ZA, Tong P, Yaworsky K, Bloch RJ, Klip A. Insulin-induced actin filament remodeling colocalizes actin with phosphatidylinositol 3-kinase and GLUT4 in L6 myotubes. J Cell Sci 2000 Jan;113 Pt 2:279-290.

(259) Al-Khalili L, Chibalin A, Kannisto K, Zhang B, Permert J, Holman G, et al. Insulin action in cultured human skeletal muscle cells during differentiation: assessment of cell surface GLUT4 and GLUT1 content. Cellular and Molecular Life Sciences CMLS 2003;60(5):991-998.

(260) Ploug T, van Deurs B, Ai H, Cushman SW, Ralston E. Analysis of GLUT4 distribution in whole skeletal muscle fibers: identification of distinct storage compartments that are recruited by insulin and muscle contractions. J Cell Biol 1998 Sep 21;142(6):1429-1446.

(261) Yan H, Wang L, Li X, Yu C, Zhang K, Jiang Y, et al. High-performance liquid chromatography method for determination of carnosic acid in rat plasma and its application to pharmacokinetic study. Biomedical Chromatography 2009;23(7):776-781.

(262) Doolaege EH, Raes K, De Vos F, Verhé R, De Smet S. Absorption, distribution and elimination of carnosic acid, a natural antioxidant from Rosmarinus officinalis, in rats. Plant foods for human nutrition 2011;66(2):196-202.

(263) Romo Vaquero M, García Villalba R, Larrosa M, Yáñez-Gascón MJ, Fromentin E, Flanagan J, et al. Bioavailability of the major bioactive diterpenoids in a rosemary extract: metabolic profile in the intestine, liver, plasma, and brain of Zucker rats. Molecular nutrition & food research 2013;57(10):1834-1846.

(264) Aguilar F, Autrup H, Barlow S, Castle L, Crebelli R, Dekant W, et al. Use of rosemary extracts as a food additive . The European Food Safety Authority Journal 2008;721:1-29.

(265) Baba S, Osakabe N, Natsume M, Terao J. Orally administered rosmarinic acid is present as the conjugated and/or methylated forms in plasma, and is degraded and metabolized to conjugated forms of caffeic acid, ferulic acid and< i> m-coumaric acid. Life Sci 2004;75(2):165-178.

(266) Konishi Y, Hitomi Y, Yoshida M, Yoshioka E. Pharmacokinetic study of caffeic and rosmarinic acids in rats after oral administration. J Agric Food Chem 2005;53(12):4740-4746.

(267) Bel-Rhlid R, Crespy V, Page-Zoerkler N, Nagy K, Raab T, Hansen C. Hydrolysis of rosmarinic acid from rosemary extract with esterases and Lactobacillus johnsonii in vitro and in a gastrointestinal model. J Agric Food Chem 2009;57(17):7700-7705.

(268) Konishi Y, Kobayashi S. Transepithelial transport of rosmarinic acid in intestinal Caco-2 cell monolayers. Biosci Biotechnol Biochem 2005;69(3):583-591.

(269) Mitsumoto Y, Burdett E, Grant A, Klip A. Differential expression of the GLUT1 and GLUT4 glucose transporters during differentiation of L6 muscle cells. Biochem Biophys Res Commun 1991 3/15;175(2):652-659.

(270) Rudich A, Konrad D, Török D, Ben-Romano R, Huang C, Niu W, et al. Indinavir uncovers different contributions of GLUT4 and GLUT1 towards glucose uptake in muscle and fat cells and tissues. Diabetologia 2003;46(5):649-658.

(271) Khayat Z, McCall A, Klip A. Unique mechanism of GLUT3 glucose transporter regulation by prolonged energy demand: increased protein half-life. Biochem J 1998;333:713-718.